

**5th Conference on Nonlinear Vibrations, Localization and Energy Transfer -
NV2014**

July 2-4 2014, Istanbul, Turkey

Book of Abstracts



5th Conference on Nonlinear Vibrations, Localization and Energy Transfer
Istanbul, July 2–4, 2014

CONFERENCE ORGANIZATION

Conference Chairman

Cetin Cetinkaya
Photo-Acoustics Research Laboratory, Nanomechanics/Nanomaterials Laboratory
Dept. of Mechanical and Aeronautical Engineering
Wallace H. Coulter School of Engineering, Center for Advanced Materials Processing
Clarkson University
8 Clarkson Ave. Potsdam, NY 13699-5725, USA
cetin@clarkson.edu

Scientific Committee

C. Cetinkaya, Chairman (Clarkson University, USA/
Abdullah Gül University (Sabbatical), Turkey)
L. Bergman (University of Illinois, USA)
C. Daraio (ETH Zurich, Switzerland)
M. Eriten, Co-chairman (University of Wisconsin, USA)
O. Gendelman (Technion – Israel Institute of Technology)
C. Lamarque (Ecole Nationale des Travaux Publics de l'Etat, France)
D. Quinn (University of Akron, USA)
G. Rezazadeh (Urmia University, Iran)
S. Shaw (Michigan State University, USA)
P. Marzocca (Clarkson University, USA)
A. Vakakis (University of Illinois, USA)
M. Younis (KAUST, Saudi Arabia)
R. Rand (Cornell University, USA)
H. Dankowicz (University of Illinois, USA)
F. Vestroni (University of Rome 'La Sapienza')

Local Organizing Committee

Ibrahim Ozkol (Istanbul Technical University, Turkey)
Vedat Ziya Dogan (Istanbul Technical University, Turkey)
Elmas Atabay (Istanbul Technical University, Turkey)
Aytac Arikoglu (Istanbul Technical University, Turkey)

Secreteriat

Elmas Atabay, Istanbul Technical University, anli@itu.edu.tr

Support Services Manager

Mehmet Kurt (University of Illinois, USA)

Website Developer

Zeki Çelikbaş, Istanbul Technical University

5th Conference on Nonlinear Vibrations, Localization and Energy Transfer
Istanbul, July 2–4, 2014

KEYNOTE SPEECHES

Engineering Extreme Materials with Defects and Nonlinearity

Chiara Daraio

We study the fundamental dynamic response of discrete nonlinear systems and study the effects of defects in the energy localization and propagation. We exploit this understanding to create experimentally novel materials and devices at different scales (for example, for application in energy absorption, acoustic imaging and energy harvesting). We use granular systems as a basic platform for testing, and control the constitutive behavior of the new materials selecting the particles' geometry, their arrangement and materials properties. Ordered arrangements of particles exhibit a highly nonlinear dynamic response, which has opened the door to exciting fundamental physical observations (i.e., compact solitary waves, energy trapping phenomena, and acoustic rectification). This talk will focus on energy localization and redirection in one- and two-dimensional systems.

Normal Modes of Nonlinear Systems: Numerical Computation and Experimental Identification

Gaetan Kershen, University of Liege

Today, the demand to utilize nonlinear (or even strongly nonlinear) structural components is increasingly present in engineering applications. In this context, a rigorous nonlinear analog of modal analysis would help engineers address the challenges associated with nonlinear designs. During the past couple of decades, the theory of nonlinear normal modes (NNMs) has been developed for this purpose. In this presentation I will first focus on the direct problem, i.e., the computation of NNMs from mathematical models, and demonstrate that the nonlinear dynamics exhibited by large-scale structures can be interpreted thanks to NNMs. The inverse problem, i.e., how NNMs can be identified from data measured on the structure subjected to harmonic or broadband forcing, will then be described. Both undamped and damped NNMs will be discussed.

5th Conference on Nonlinear Vibrations, Localization and Energy Transfer
Istanbul, July 2–4, 2014

CONFERENCE PROGRAM

July 2, 2014

15:00-16:45 Registration
16:45-17:00 Opening Remarks (Prof. Cetinkaya)
17:00-19:00 Welcome Reception (drinks + hors d'oeuvres)

July 3, 2014

07:30-08:30 Registration (Drinks and Refreshments)
08:30-09:20 Keynote 1 (Prof. Daraio)
09:20-10:50 Oral Presentation Session 1
10:50-11:20 Refreshment break
11:20-12:35 Oral Presentation Session 2
12:35-14:00 Lunch break
14:00-16:00 Oral Presentation Session 3
16:00 Social Program (TBA)

July 4, 2014

08:00-08:30 Registration (Drinks and Refreshments)
08:30-09:20 Keynote 2 (Prof. Kerschen)
09:20-10:50 Oral Presentation Session 4
10:50-11:20 Refreshment break
11:20-12:35 Oral Presentation Session 5
12:35-14:00 Lunch break
14:00-15:15 Oral Presentation Session 6
15:15-15:45 Refreshment break
15:45-17:00 Oral Presentation Session 7
17:00-17:10 Closing Remarks
17:10-18:00 Closing Reception

ORAL PRESENTATION SESSIONS

July 3, 2014	
	Session 1 Chair: Oleg Gendelman, Technion-Israel Institute of Technology
9:20-9:35	<i>Unified Nonlinear and Dissipative Electroelastic Dynamics of Piezoelectric Structures for Energy Harvesting, Sensing, and Actuation</i> , S. Leadenham, A. Ertürk
9:35-9:50	<i>Energy Pumping Between a Main Oscillator and a Nonsmooth Nonlinear Energy Sink with Time-Dependent Masses</i> , A.T. Savadkoohi, C.H. Lamarque
9:50-10:05	<i>Effects of Quasi-Periodic Excitation on an Acoustic System Coupled to a Nonlinear Damper</i> , R. C'ote, S. Bellizzi, M. Pachebat
10:05-10:20	<i>Tuned Pendulum as Nonlinear Energy Sink for Broad Energy Range</i> , M. Farid, O. Gendelman
10:20-10:35	<i>The Effect of Nonlinear Damping on Energy Harvesting Performance</i> , D. Dane Quinn, Kevin Remick, D. Michael McFarland, Larry Bergman, Alex Vakakis
10:35-10:50	<i>The Nonlinear Tuned Vibration Absorber, Part I: Design and Performance Analysis</i> , G. Habib, T. Detroux, G. Kerschen
	Session 2 Chair: Dane Quinn, University of Akron
11:20-11:35	<i>The Nonlinear Tuned Vibration Absorber, Part II: Robustness and Sensitivity Analysis</i> , T. Detroux, G. Habib, L. Masset, G. Kerschen
11:35-11:50	<i>Nonlinear Transverse Vibrations of Axially Moving Beams with Clamped Ends and One Intermediate Simple Support</i> , F. Köstekçi
11:50-12:05	<i>Nonlinear Behavior of a Timoshenko Nano-Beam Subjected to a Displacement Dependent Pressure Considering Modified Couple Stress Theory</i> , H. Etemadi, R. Shabani, G. Rezazadeh, V. Sadighi
12:05-12:20	<i>Effects of the Gap Distance on the Dynamics of a Nano-Resonant Beam Subjected to a Nonlinear Electrostatic Pressure</i> , M. Fathalilou, M. Sadeghi, G. Rezazadeh

5th Conference on Nonlinear Vibrations, Localization and Energy Transfer
Istanbul, July 2–4, 2014

12:20-12:35	<i>Flexural–Torsional Vibration and Stability Analysis of Multilayer Beams Subjected to Axial Load and End Moment – A Dynamic Finite Element Formulation</i> , M T Towliat, S M Hashemi
	Session 3 Chair: Alex Vakakis, University of Illinois at Urbana-Champaign Vice Chair: Mehmet Kurt, Stanford University
14:00-14:15	<i>Discrete Breathers in Forced Chains of Oscillators with Cubic Nonlinearities</i> , F. Romeo, M. Veremkroit, O. Gendelman
14:15-14:30	<i>Microscopic Approach to Shear Localization and Plasticity in Amorphous Solids</i> , O.V. Gendelman
14:30-14:45	<i>Discrete Breathers in 2D Chains with Vibro-Impact</i> , I. Grinberg, O.V. Gendelman
14:45-15:00	<i>Equation-Free Computations for Data Driven Studies of Granular Chains</i> , M.O. Williams, D. Pozharskiy, R.W. Holzel, C. Chong, F. Li
15:00-15:15	<i>Basins of attraction of coupled nonlinear resonators in periodic lattices</i> , D. Bitar, N. Kacem, N. Bouhaddi
15:15-15:30	<i>Modal Analysis of Nonlinear Dissipative Systems: Application to Vibration Damping with Shape Memory Materials</i> , M. Krack, L. Panning-von Secheidt, J. Wallaschek
15:30-15:45	<i>Delayed Feedback Control of Nonlinear Surge Response of Multi-point Mooring System under Harmonic Waves</i> , A.K. Banik, R.K. Mitra
15:45-16:00	<i>Experimental Study of Acoustic Bands and Propagating Breathers in Ordered Granular Media Embedded in Matrix</i> , M.A. Hasan, S. Cho, K. Remick, D.M. McFarland, W. Kriven, A.F. Vakakis
July 4, 2014	
	Session 4 Chair: Cetin Cetinkaya, Clarkson University
9:20-9:35	<i>Estimation of Nonlinear Frequency Response for a System with Backlash Nonlinearity Using Multiterm Harmonic Balance Method</i> , O.T. Şen, R. Singh
9:35-9:50	<i>Parameter Identification of a Nonlinear Beam with Hardening Behavior Using Volterra Series</i> , S.B. Shiki, C. Hansen, S. Da Silva

5th Conference on Nonlinear Vibrations, Localization and Energy Transfer
Istanbul, July 2–4, 2014

9:50-10:05	<i>Comparison Between a Finite-Element-Based and a Trajectory-Based Method for Computing Damped Nonlinear Normal Modes</i> , L. Renson, G. Kerschen
10:05-10:20	<i>A Comparison between Two Reduced-Order Approaches in Nonlinear Capacitive Micro-Resonators</i> , M. Fathalilou, G. Rezazadeh, M. Sadeghi, A.M. Abazari
10:20-10:35	<i>Nonlinear Model Updating Based on Global/Local Nonlinear System Identification Approach</i> , M. Kurt, M. Eriten, M. McFarland
	Session 5 Chair: Larry Bergman, University of Illinois at Urbana-Champaign
11:20-11:35	<i>Nonlinear Dynamics of a Capacitive Micro-Resonator Considering Nonlocal Theory</i> , M. Fathalilou, G. Rezazadeh, M. Sadeghi, A.M. Abazari
11:35-11:50	<i>Transversal Vibration of a Micro-beam in Interacting with a Micro-scale Fluid Media Based on Micro-Polar Theory</i> , Mina Ghanbri, Siamak Hossainpour, Ghader Rezazadeh
11:50-12:05	<i>Nonlinear Solutions in BEC for Different Potentials</i> , E. Tosyalı, F. Aydođmuş
12:05-12:20	<i>Detection of Hydrogen Sulphide Agents Using Frequency Shifting of a Doubly Clamped Micro-Beam Based Sensor Considering Couple Stress Effect</i> , M. Safavai, A.M. Abazari, G. Rezazadeh
12:20-12:35	<i>Nonlinear Dynamics of Adhesive Micro-spherical Particles on Vibrating Substrates</i> , Armin Saeedi Vahdat, Saber Azizi, Çetin Çetinkaya
	Session 6 Chair: Melih Eriten, University of Wisconsin-Madison
14:00-14:15	<i>Nonlinear Energy Transmission in a Finite Dissipative Periodic Structure</i> , B. Yousefzadeh, A.S. Phani
14:15-14:30	<i>Viscous Damping Effect in Laterally Vibrating Micro-resonator Considering Slip Boundary Conditions</i> , Sahra Azma, Elnaz Alizadeh Haghighi, Afsoon Vefagi, Ghader Rezazadeh
14:30-14:45	<i>Experimental Evaluation of Multiple Nonlinear Energy Sinks Coupled to a Large Nine-story Frame Structure for Seismic Hazard Mitigation</i> , Nicholas Wierschem, Sean Hubbard, Jie Luo, D. Michael McFarland, Larry Fahnestock, Bill Spencer, Dane Quinn, Alexander Vakakis, Lawrence Bergman

5th Conference on Nonlinear Vibrations, Localization and Energy Transfer
Istanbul, July 2–4, 2014

14:45-15:00	<i>Nonlinear Stiffening and Damping Effects of Non-contact Excitation System in Oberst Test Rig</i> , H. Koruk, M.S. Özer, K.Y. Şanlıtürk
	Session 7 Chair: Elmas Atabay, Istanbul Technical University
15:45-16:00	<i>On a Nonlinear Energy Sink Control (NES) Approach Applied to an Electro Pendulum Arm Like Device</i> , G.F. Alışverişçi, H. Bayıroğlu, J.L.P. Felix, J.M. Balthazar, R.M.L.R. de Fonseca Brazil
16:00-16:15	<i>Vibration Measurement on a 1000 HP Gas Turbine Engine to Test a Newly Designed Cascade Compressor Module</i> , S. Yılmaztürk, S. Aslan, T. Yasa
16:15-16:30	<i>Control of Helicopter Ground Resonance by Means of Passive Non-Linear Energy Sink</i> , B. Bergeot, S. Bellizzi, B. Cochelin
16:30-16:45	<i>Collective Dynamics of Coupled Nonlinear Pendulums under Simultaneous External and Parametric Excitations</i> , A. Jallouli, N. Kacem, N. Bouhaddi
16:45-17:00	<i>Stability of an Inclined Travelling Heavy Cable</i> , A.R. Dehadrai, I. Sharma, S.S. Gupta

5th Conference on Nonlinear Vibrations, Localization and Energy Transfer
Istanbul, July 2–4, 2014

INTERNET ACCESS

Wireless internet access will be available at the conference site through the networks “ITUnetmisafir” and “eduroam”, neither of which requires a password.

LIST OF AUTHORS

Abazari, Amir Musa	am.abazari@gmail.com
Alışverişçi, G. Füsün	afusun@yildiz.edu.tr
Aslan, Samet	samet.aslan@tei.com.tr
Aydođmuş, Fatma	fatmaa@istanbul.edu.tr
Azizi, Saber	
Azma, Sahra	
Balthazar, José M.	jmbaltha@rc.unesp.br
Banik, Atul K.	akbanik@gmail.com
Bayırođlu, Hüseyin	hbayir@yildiz.edu.tr
Bellizzi, S.	bellizzi@lma.cnrs-mrs.fr
Bergeot, Baptiste	baptiste.bergeot@centrale-marseille.fr
Bergman, Larry	lbergman@uiuc.edu
Bitar, Diala	diala.bitar@femto-st.fr
Bouhaddi, Nouredine	nouredine.bouhaddi@univ-fcomte.fr
Cho, Shinhu	
Chong, C.	
Cochelin, B.	bruno.cochelin@centrale-marseille.fr
C'ote, R.	cote@lma.cnrs-mrs.fr
Çetinkaya, Çetin	cetin@clarkson.edu
da Silva, Samuel	samuel@dem.feis.unesp.br
da Fonseca Brasil, Reyolando Manoel Lopes Rebello	
Daraio, Chiara	
Dehadrai, Abhinav R.	abhinavd@iitk.ac.in
Detroux, T.	tdetroux@ulg.ac.be
Dođan, Vedat Ziya	doganve@itu.edu.tr
Eriten, Melih	

5th Conference on Nonlinear Vibrations, Localization and Energy Transfer
Istanbul, July 2–4, 2014

Ertürk, Alper	alper.erturk@me.gatech.edu
Etemadi, Hadi	Hadi_Etemadi2007@yahoo.com
Fahnestock, Larry	
Farid, Maor	maorfarid@hotmail.com
Fathalilou, Mohammad	m.fathalilou@tabrizu.ac.ir
Gençkal, Neslihan	genckal@itu.edu.tr
Gendelman, Oleg	ovgend@tx.technion.ac.il
Ghanbari, Mina	minaghanbari@yahoo.com
Grinberg, Itay	grinbergitay@gmail.com
Gupta, Shakti. S.	
Habib, Giuseppe	giuseppe.habib@ulg.ac.be
Haghighi, Elnaz Alizadeh	elnaz_ah.me20@yahoo.com
Hansen, Cristian	engcristianhansen@gmail.com
Hasan, M. Arif	
Hashemi, S. M.	shashem@ryerson.ca
Hossainpour, Siamak	hossainpour@sut.ac.ir
Hölzel, R.W.	
Hubbard, Sean	
Jallouli, Aymen	jallouli_aymen_enis@yahoo.fr
Kacem, Najib	najib.kacem@femto-st.fr
Kerschen, Gaëtan	g.kerschen@ulg.ac.be
Kevrekidis, Ioannis G.	yannis@arnold.princeton.edu
Kevrekidis, Panayotis G.	kevrekid@gmail.com
Koruk, Hasan	hasan.koruk@mef.edu.tr
Köstekci, Ferid	feridkostekci@hitit.edu.tr
Krack, Malte	krack@ids.uni-hannover.de
Kriven, Waltraud	

5th Conference on Nonlinear Vibrations, Localization and Energy Transfer
Istanbul, July 2–4, 2014

Kurt, Mehmet

Lamarque, Claude-Henri claude.lamarque@entpe.fr

Leadenham, Stephen

Li, F.

Luo, Jie

McFarland, D. Michael

Mitra, R. K.

Özer, Mehmet Sait ozermehmet1@itu.edu.tr

Pachebat, M. pachebat@lma.cnrs-mrs.fr

Palacios Felix, Jorge Luis

Phani, A. Srikantha phani@mech.ubc.ca

Pozharskiy, D.

Quinn, Dane D. quinn@uakron.edu

Remick, Kevin

Renson, Ludovic l.renson@ulg.ac.be

Rezazadeh, Ghader g.rezazadeh@urmia.ac.ir

Romeo, Francesco francesco.romeo@uniroma1.it

Sadeghi, Morteza

Sadighi, V.

Safavai, Mohsen

Savadkoohi, Alireza Ture alireza.turesavadkoohi@entpe.fr

Shabani, R.

Sharma, Ishan

Shiki, Sidney B. sbshiki@gmail.com

Simitçioğlu, Gökay simitcioglu@itu.edu.tr

Singh, Rajendra singh.3@osu.edu

Spencer, Bill

5th Conference on Nonlinear Vibrations, Localization and Energy Transfer
Istanbul, July 2–4, 2014

Şanlıtürk, Kenan Y.	sanliturk@itu.edu.tr
Şen, Osman Taha	senos@itu.edu.tr
Tosyalı, Eren	eren.tosyali@bilgi.edu.tr
Towliat, M.T.	mtowliat@ryerson.ca
Vahdat, Armin Saeedi	saeedia@clarkson.edu
Vakakis, Alexander F.	avakakis@illinois.edu
Vefagi, Afsoon	
Veremkroit, Michael	
von Scheidt, Lars Panning	
Yang, J.	
Yasa, Tolga	tolga.yasa@tei.com.tr
Yilmaztürk, Sefa	sefa.yilmazturk@tei.com.tr
Yousefzadeh, Behrooz	behroozy@alumni.ubc.ca
Wallaschek, Jörg	
Wierschem, Nicholas	
Williams, Matthew O.	mow2@princeton.edu

5th Conference on Nonlinear Vibrations, Localization and Energy Transfer
Istanbul, Turkey, July 2–4, 2014

SESSION 1

Unified nonlinear and dissipative electroelastic dynamics of piezoelectric structures for energy harvesting, sensing, and actuation

Stephen Leadenham and Alper Erturk*
G.W. Woodruff School of Mechanical Engineering
Georgia Institute of Technology
Atlanta, GA 30332
 * alper.erturk@me.gatech.edu

Inherent nonlinearities of piezoelectric materials are pronounced in various engineering applications such as actuation, sensing, their combined implementations in feedback problems such as vibration control, and most recently, in energy harvesting from dynamical systems.^{1,2} The existing literature focusing on the dynamics of electroelastic structures made of piezoelectric materials have explored such nonlinearities in a disconnected way for the separate problems of mechanical and electrical excitation such that nonlinear resonance trends have been attributed to different additional terms in constitutive equations by different researchers. Experimental manifestations of nonlinearities have been attributed to purely elastic nonlinear terms,³ purely electrical nonlinear terms in electric field,⁴ and combination of elastic softening and coupling nonlinearities^{5,6} by various authors. However, a reliable nonlinear constitutive equation pair for a given piezoelectric material is expected to be rather unique and valid regardless of the application, such as energy harvesting, sensing, or actuation. A systematic approach focusing on the two-way coupling can result in a sound mathematical framework. To this end, the present work investigates the nonlinear non-conservative dynamic behavior of a bimorph piezoelectric cantilever under low-to-high mechanical and electrical excitation levels in energy harvesting, sensing, and actuation. A mathematical framework is developed and analyzed by using the method of harmonic balance to identify and validate the nonlinear and dissipative system parameters for energy harvesting (Figure 1a) and dynamic actuation (Figure 1b) based on a set of rigorous experiments (Figure 2).

The nonlinear constitutive equation pair of the piezoelectric laminates employed in this work can be given along with the hysteretic dissipation function as follows:

$$T_1 = c_{11}(1 - \alpha |S_1|)S_1 - e_{31}E_3 + c_{111}S_1^2 + c_{1111}S_1^3 - e_{311}S_1E_3 - e_{3111}S_1^2E_3 \quad (1)$$

$$D_3 = e_{31}S_1 + \epsilon_{33}E_3 + e_{311}S_1E_3 + e_{3111}S_1^2E_3 \quad (2)$$

$$U_{dis} = 4\gamma c_{11} |S_1|^3 / 3 \quad (3)$$

where T_1 is the bending stress, S_1 is the bending strain, D_3 is the electric displacement, E_3 is the electric field, c_{11} is the linear elastic modulus, c_{111} and c_{1111} are the higher order elastic terms, e_{31} is the linear piezoelectric constant, e_{311} and e_{3111} are the higher order piezoelectric constants, and ϵ_{33} is the permittivity constant. Ferroelastic softening is due to α , while the associated hysteretic loss U_{dis} is proportional to γ . This nonlinear and dissipative framework is a synthesis of recent efforts by von Wagner and Hagedorn⁵ and Stanton et al.⁶ (for higher order terms in the Gibbs free energy expansion), and Goldschmidtboeing et al.⁷ (for the ferroelastic hysteresis model). In the existing literature, the former approach^{5,6} excludes hysteretic effects (and attributes the losses to other terms such as air damping⁶), while the latter⁷ accounts for hysteresis only.

In a set of experiments (Figure 2), this model has been validated for a broad range of excitation levels in energy harvesting (e.g. Figure 3 for 1g base excitation) and dynamic actuation (Figure 4). Among other results, the importance of quadratic softening and dissipative nonlinearities (even for a cantilever with symmetric laminates) originating from the hysteresis model is pointed out for moderate excitation levels. Higher-order softening and coupling terms from the Gibbs free energy become effective for high excitation levels.

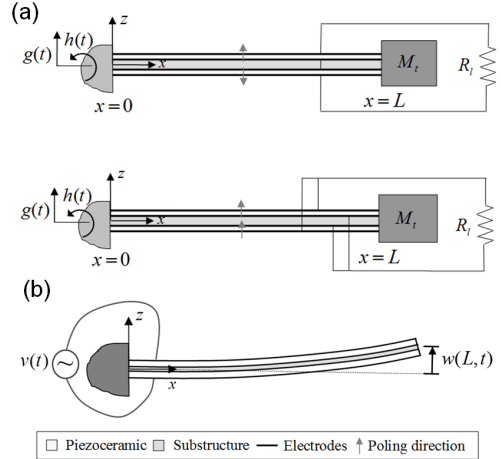


Figure 1: Schematics of bimorph piezoelectric cantilevers used for (a) vibration energy harvesting from base excitation and (b) dynamic actuation.

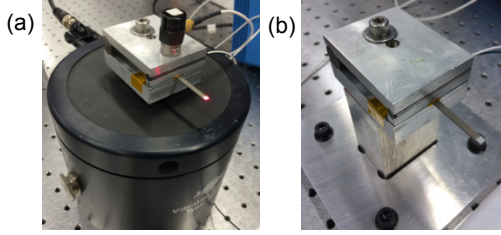


Figure 2: Close-up pictures of the experimental configurations for (a) energy harvesting from base excitation (with a controlled shaker for constant base acceleration frequency sweep tests) for a set of electrical load resistance values ranging from short- to open-circuit conditions and (b) dynamic actuation experiments in fixed-free boundary conditions for a range of actuation voltage levels. Tip velocity of the cantilever in both cases is measured by a laser Doppler vibrometer.

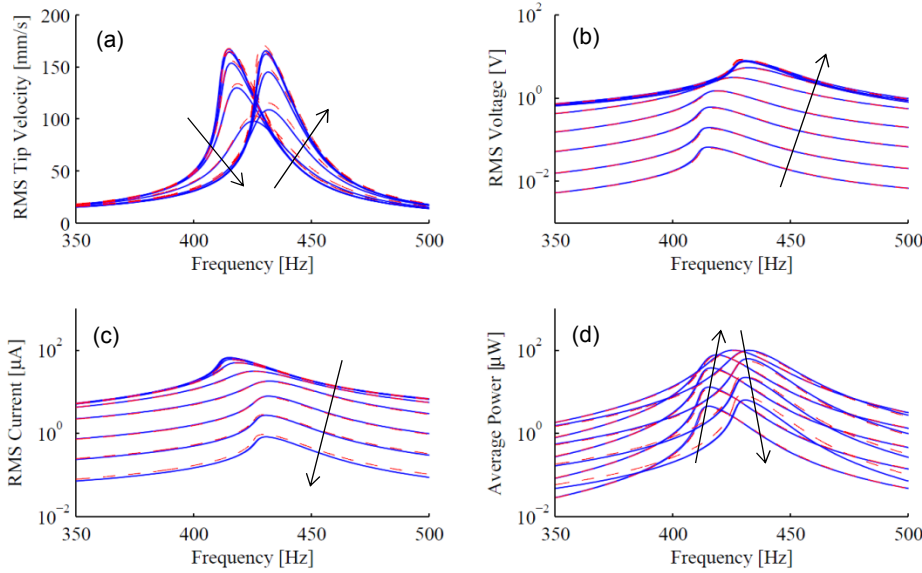


Figure 3: Nonlinear (a) tip velocity, (b) voltage output, (c) current output, and (d) power output frequency response curves for a set of load resistance values (ranging from 1 k Ω to 10 M Ω) under a constant base excitation magnitude of 1g RMS. Solid blue curves are experimental data, and dashed red curves are the nonlinear model predictions with harmonic balance analysis. Arrows indicate the direction of increasing load resistance.

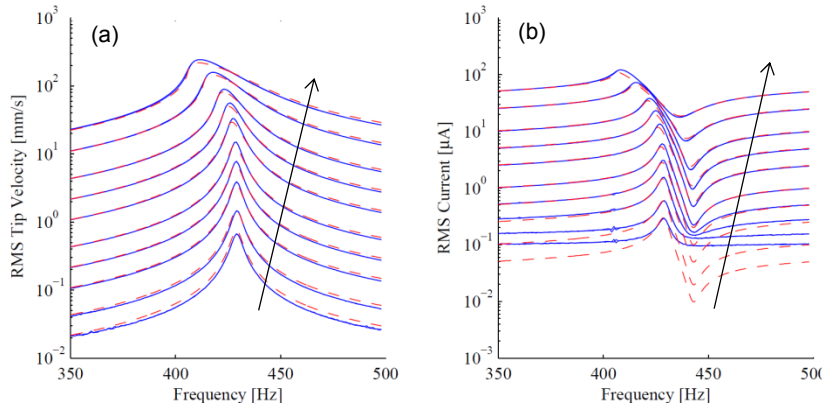


Figure 4: Dynamic actuation frequency response curves for the (a) transverse tip velocity of the cantilever and (b) current drawn by the cantilever (i.e. dynamic admittance multiplied by voltage). Solid blue curves are experimental data, and dashed red curves are the nonlinear model predictions with harmonic balance analysis. Arrows indicate the direction of increasing actuation voltage amplitude (from 10mV to 10V). The mismatch for low voltage level cases is because the current signal level is below the noise floor of the data acquisition system.

Acknowledgments

This work was supported in part by the National Science Foundation under Grant CMMI-1254262.

References

- 1 Erturk, A. & Inman, D. J. *Piezoelectric energy harvesting*. (John Wiley & Sons, 2011).
- 2 Elvin, N. & Erturk, A. *Advances in energy harvesting methods*. (Springer, 2013).
- 3 Wolf, K. & Gottlieb, O. Nonlinear Dynamics of a Cantilever Beam Actuated by Piezoelectric Layers in Symmetric and Asymmetric Configuration. (2001).
- 4 Tiersten, H. Electroelastic equations for electroded thin plates subject to large driving voltages. *J Appl Phys* **74**, 3389-3393 (1993).
- 5 Von Wagner, U. & Hagedorn, P. Piezo-beam systems subjected to weak electric field: experiments and modeling of nonlinearities. *Journal of Sound and Vibration* **256**, 861-872 (2002).
- 6 Stanton, S. C., Erturk, A., Mann, B. P. & Inman, D. J. Nonlinear piezoelectricity in electroelastic energy harvesters: modeling and experimental identification. *J Appl Phys* **108**, 074903 (2010).
- 7 Goldschmidtboeing, F., Eichhorn, C., Wischke, M., Kroener, M. & Woias, P. in *Proceedings of the 11th International Workshop on Micro and Nanotechnology for Power Generation and Energy Conversion Applications*. 114-117.

Energy pumping between a main oscillator and a nonsmooth nonlinear energy sink with time-dependent masses

Alireza TURE SAVADKOOHI*, Claude-Henri LAMARQUE *

*ENTPE, Université de Lyon, LGCB and LTDS UMR CNRS 5513, France.

Summary. Energy exchange between a main oscillator and a nonsmooth nonlinear energy sink (NES) by consideration of two different cases is studied: i) the main structure with time-dependent mass is coupled to a nonsmooth NES with constant mass; ii) the main structure possesses constant mass while the mass of the nonsmooth NES is varying.

Case i: the main structure with time-varying mass and coupled nonsmooth NES

Let us consider an academic model of a 2dof system which consists of a main structure with time-dependent mass (that is a smooth function of time), damping and elastic stiffness as $\tilde{M}(t)$ ($\tilde{M}(t) = M_0(1 + \epsilon M(t))$), C and k_1 which is coupled to a non-smooth NES with the mass m . The mass m can move freely in a clearance of 2δ until it reaches to elastic springs with the stiffness k_2 at two sides. The overall damping of the NES system is supposed to be $\tilde{\lambda}$. If we assume that the mean velocity at which the mass is "leaving or entering" the mass of the main system in the x direction is zero, then governing equations of the system can be summarized as [1]:

$$\begin{aligned} \tilde{M}(t)\ddot{x}_1 + C\dot{x}_1 + k_1x_1 + \tilde{F}(x_1 - x_2) + \tilde{\lambda}(\dot{x}_1 - \dot{x}_2) + \dot{\tilde{M}}(t)\dot{x}_1 &= \Gamma \sin(\Omega t) \\ m\ddot{x}_2 + \tilde{F}(x_2 - x_1) + \tilde{\lambda}(\dot{x}_2 - \dot{x}_1) &= 0 \end{aligned} \quad (1)$$

The non-smooth potential \tilde{F} of the NES is defined as:

$$\tilde{F}(z) = -\frac{\partial V(z)}{\partial z} = -\tilde{F}(-z) = \begin{cases} 0 & -\delta \leq z \leq \delta \\ k_2(z - \delta) & z \geq \delta \\ k_2(z + \delta) & z \leq -\delta \end{cases} \quad (2)$$

ϵ is a small parameter which corresponds to ratio of the mass of NES and initial mass of the main system, i.e. $0 < \epsilon = \frac{m}{M_0} \ll 1$. We assume that $(1 + \epsilon M(t)) \geq 0$ for a time long enough. We would like to re-scale the system with respect to the new time domain T where $T = t\sqrt{\frac{k_1}{M_0}} = t\vartheta$. At the new time domain we use following replacements of variables:

$x_i(t) \rightarrow y_i(T)$. Following change of variables are considered: $\frac{C}{\sqrt{M_0k_1}} = \epsilon\zeta$, $\frac{1}{k_1}\tilde{F} = \epsilon\hat{F}$, $k = \frac{1}{\epsilon}\frac{k_2}{k_1}$, $\frac{\tilde{\lambda}}{\sqrt{M_0k_1}} = \epsilon\lambda$, $\frac{1}{k_1}\Gamma = \epsilon f_0$ and $\frac{\Omega}{\vartheta} = \omega$ and we assume that $k = o(\epsilon^0)$. We transfer the system to the coordinates $v = y_1 + \epsilon y_2$ and $w = y_1 - y_2$ and then we apply complex variables of Manevitch i.e. $\varphi_1 e^{i\omega T} = \dot{v} + i\omega v$ and $\varphi_2 e^{i\omega T} = \dot{w} + i\omega w$ with $i = \sqrt{-1}$. The system is studied around 1 : 1 resonance by imposing $\omega = 1 + \sigma\epsilon$. By using Galerkin's technique and keeping first harmonics and truncating higher ones and also ignoring higher orders of ϵ , system equations read:

$$\begin{aligned} \dot{\varphi}_1 + \frac{i}{2}(1 + \sigma\epsilon)\varphi_1 + \frac{\epsilon}{2(1 + \epsilon)}\zeta\varphi_1 - \frac{i}{2(1 + \epsilon)(1 + \sigma\epsilon)}(\varphi_1 + \epsilon\varphi_2) + \frac{i}{2(1 + \epsilon)(1 + \sigma\epsilon)}(\epsilon m_0\varphi_1 - \epsilon m_2\varphi_1^*) \\ + \frac{1}{2(1 + \epsilon)}(2i(1 + \sigma\epsilon)\epsilon m_2\varphi_1^*) = -\frac{i\epsilon f_0}{2} \\ \dot{\varphi}_2 + \frac{i}{2}(1 + \sigma\epsilon)\varphi_2 + \frac{\epsilon}{2(1 + \epsilon)}\zeta\varphi_1 - \frac{i}{2(1 + \epsilon)(1 + \sigma\epsilon)}(\varphi_1 + \epsilon\varphi_2) + \frac{i}{2(1 + \epsilon)(1 + \sigma\epsilon)}(\epsilon m_0\varphi_1 - \epsilon m_2\varphi_1^*) \\ - \frac{i}{2}(1 + \epsilon)\varphi_2 G(|\varphi_2|^2) + \frac{1 + \epsilon}{2}\lambda\varphi_2 + \frac{1}{2(1 + \epsilon)}(2i(1 + \sigma\epsilon)\epsilon m_2\varphi_1^*) = -\frac{i\epsilon f_0}{2} \end{aligned} \quad (3)$$

$G(\chi)$ is the averaged form of the nonsmooth potential. We would like to study system behavior at fast and slow time scales. To this end, we should analyze the system at different scales of ϵ . The behavior of the system during fast time scale and at its fixed point reveals its invariant manifold as $N_1 = H(N_2)$ where $\varphi_1 = N_1 e^{i\delta_1}$ and $\varphi_2 = N_2 e^{i\delta_2}$. If we analyze system behavior at slow time scale around its invariant manifold, following reduced order of system equations can be obtained:

$$\frac{\partial N_2}{\partial \tau_1} = \frac{\Sigma_1(N_2, \delta_2)}{E(N_2)}, \quad \frac{\partial \delta_2}{\partial \tau_1} = \frac{\Sigma_2(N_2, \delta_2)}{E(N_2)} \quad (4)$$

Ordinary equilibrium points of the system are those who satisfy $E(N_2) \neq 0$ and $\Sigma_1(N_2, \delta_2) = \Sigma_2(N_2, \delta_2) = 0$. In addition to ordinary equilibrium points, the system may possess fold singularities that satisfy $E(N_2) = \Sigma_1(N_2, \delta_2) = \Sigma_2(N_2, \delta_2) = 0$. Let us take a mass profile which is depicted in Fig. 1a and study the system under external forcing term $f_0 = 3.624$. We take direct numerical integration of re-scaled form of the system (1) by assuming following initial conditions $y_1(0) = 1.5$ and $y_2(0) = y_1'(0) = y_2'(0) = 0$. Zeros of the reduced order of system equations at slow time

scale are depicted in Fig. 1b. The system has two equilibrium points namely no. 3 and 6, four fold singularities, namely no. 1, 2, 4 and 5 and another equilibrium point, α , which is in the unstable area of the system. Detailed analysis reveals that points 1 and 2 are saddle and node, points 5 and 6 are saddle and equilibrium points no. 3 and 6 are stable. The invariant manifold of the system and obtained numerical results are illustrated in Fig. 1c. This figure shows that the system repeatedly faces bifurcations between its stable zones. This behavior is named as "strongly modulated response" [2] and it is the result of existence of fold singularities ($E(N_2) = \Sigma_1(N_2, \delta_2) = \Sigma_2(N_2, \delta_2) = 0$).

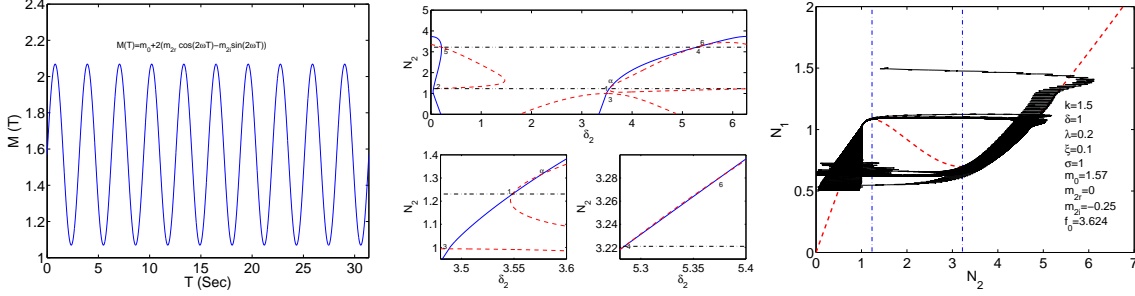


Figure 1: From left to right a) mass profile of the main system; b) zeros of the reduced order of system equations at slow time scale: $\Sigma_1 = 0$ (—), $\Sigma_2 = 0$ (- - -), $E = 0$ (- · - · -); c) invariant manifold and corresponding numerical results.

Case ii: the main structure with constant mass and coupled nonsmooth NES with time-varying mass

The main linear structure with constant mass M is coupled to a nonsmooth NES with the potential which is described in Eq. (2) and with the time-varying mass $\tilde{m}(t) = m_0(1 + \epsilon m(t))$, where $0 < \epsilon = \frac{m_0}{M} \ll 1$. We have:

$$\begin{aligned} M\ddot{x}_1 + C\dot{x}_1 + k_1x_1 + \tilde{F}(x_1 - x_2) + \tilde{\lambda}(\dot{x}_1 - \dot{x}_2) &= \Gamma \sin(\Omega t) \\ \tilde{m}(t)\ddot{x}_2 + \tilde{F}(x_2 - x_1) + \tilde{\lambda}(\dot{x}_2 - \dot{x}_1) + \tilde{m}(t)\dot{x}_2 &= 0 \end{aligned} \quad (5)$$

The same steps of the previous section are adopted: i.e., re-scaling the system, change of system coordinates, applying complex variables of Manevitch, endowing Galerkin's technique and detecting system behaviors at fast and slow time scales. We are able to detect invariant manifold of the system at fast time scale and then to obtain reduced order of system equations at slow time scale in order to highlight equilibrium and singular points of the system. In this section we do not present detailed results and we just present the application of such a system in passive control of main structures. The assumed profile of the mass of the NES is illustrated in Fig. 2a where $m(T) = m_{0r} + 2(m_{1r} \cos(\omega T) - m_{1i} \sin(\omega T)) + 2(m_{2r} \cos(2\omega T) - m_{2i} \sin(2\omega T))$. Histories of the displacements of the main structure without and with coupled nonsmooth NES with time-varying mass which are obtained by direct numerical integrations of system equations are depicted in Fig.2b. This figure shows the capability of the attached nonsmooth NES in passive control of the main structure. Histories of the amplitudes of the main structure and the NES during the passive control which are given in Figs.2c and 2d show that the system present strongly modulated response during passive control process.

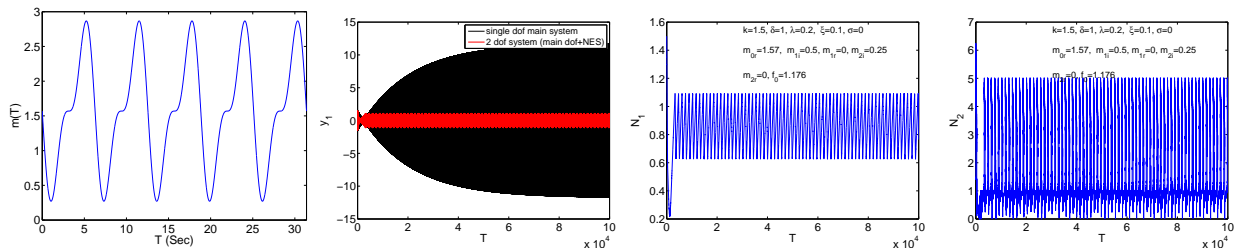


Figure 2: From left to right a) mass profile of the NES: $m_{0r} = 1.57$, $m_{1i} = 0.5$, $m_{1r} = 0$, $m_{2i} = 0.25$ and $m_{2r} = 0$; b) Displacement histories of the main structure; c) Amplitude histories of the main structure; d) Amplitude histories of the NES.

References

- [1] Lamarque C.-H., Ture Savadkoohi A., (2014), "Dynamics of a linear system with time-dependent mass and a coupled light mass with non-smooth potential", *Meccanica*, **49** (1), 135–145.
- [2] Starosvetsky Y, Gendelman O. V.,(2008), "Strongly modulated response in forced 2DOF oscillatory system with essential mass and potential asymmetry", *Physica D*, **237**, 1719–1733.

Effects of quasi-periodic excitation on an acoustic system coupled to a nonlinear damper

R. Côte, S. Bellizzi, M. Pachebat

LMA, CNRS, UPR 7051, Aix-Marseille Univ, Centrale Marseille
F-13420 Marseille Cedex 20, France.

(cote@lma.cnrs-mrs.fr, bellizzi@lma.cnrs-mrs.fr, pachebat@lma.cnrs-mrs.fr)

Introduction: Targeted Energy Transfer (TET) concept based on an additional essentially nonlinear attachment also named Nonlinear Energy Sink (NES) to an existing primary linear system has been extensively studied from theoretical, numerical and experimental point of views. It provided very efficient reduction for vibration and noise. These studies include transient and steady state dynamic analysis. More recently multi-forcing frequencies has been considered in [1] where two excitation frequencies are used, one equal to the resonance frequency of the primary system, the other one situated in its vicinity. Results show strong modification of the response regimes. Two additive sinusoidal components at both resonance frequencies of the primary system were considered in [2] showing that a two one-to-one resonances of the system is possible simultaneously resulting on vibration reduction around the two resonance frequencies. The present work aims at understanding how TET occurs under quasi-periodic external excitation. As in [3], the primary system is an acoustic medium. The main objective of this study is to obtain experimental confirmations of the simultaneous efficiency of a single NES on a linear system under two-frequency excitation with frequencies near the resonance frequencies of the linear system.

The acoustic system and the NES: The system (shown in Fig. 1(a,b)) consists of an acoustic medium coupled to a simple thin circular clamped visco-elastic membrane (the NES) by means of a coupling box. The acoustic medium composed of two pipes of different lengths and section areas opened on both ends. The coupling between the pipes and the membrane is ensured acoustically by the air

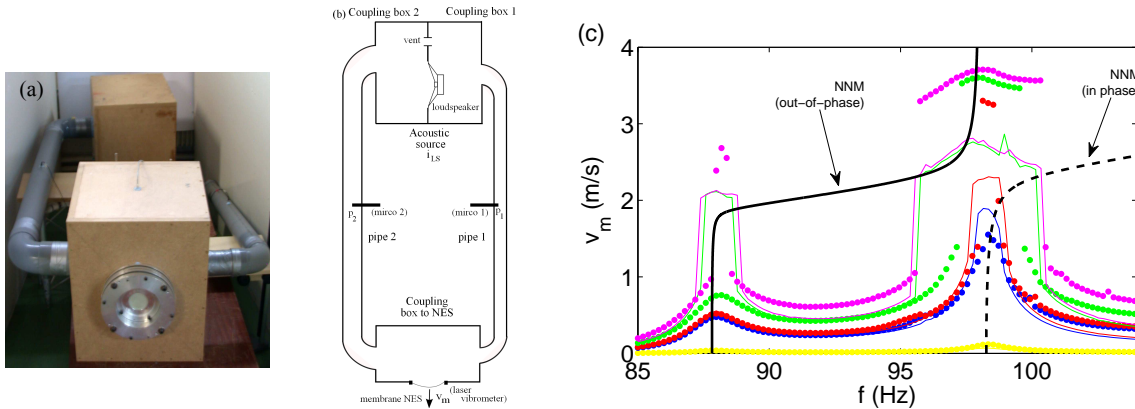


Figure 1: (a) Picture and (b) schema of the set-up. (c) RMS velocity of the NES under one-frequency excitation: comparison of experiment (dotted lines) and model (continuous lines) for several excitation levels. Also shown: Nonlinear Normal Modes (black curves).

in a coupling box, which is sufficiently large to give a weak linear coupling stiffness. An acoustic source consisting of a loudspeaker and a coupling box which is connected to the entrance of both pipes is used. A simple model to predict qualitatively the behavior of the vibroacoustic system was developed as reported in [4]. Experimental and numerical results under one-frequency excitation in the neighborhood of two resonance frequencies ($f_1^0 \simeq 88$ Hz, $f_2^0 \simeq 98.5$ Hz) are reported Fig. 1(c) showing the NES acts separately on around the two resonance frequencies.

Results under two-frequency excitation (f^A and f^B): The quasi-periodic regimes (1:1-1:1) were studied analytically using the complexification method combined to the averaging method. A local stability diagram of the quasi-periodic regimes is reported Fig. 2(1) using the excitation frequencies ($f^A(= \sigma_1\omega_1^{-1})$ in the neighborhood of f_1^0 and $f^B(= \sigma_2\omega_2^{-1})$ in the neighborhood of f_2^0) as control parameters. Zones where no stable quasi-periodic regime occurs are shown in black. The corresponding NES velocity amplitude along the segment line EF (constant f^B and scanning f^A) is reported Fig. 2(2).

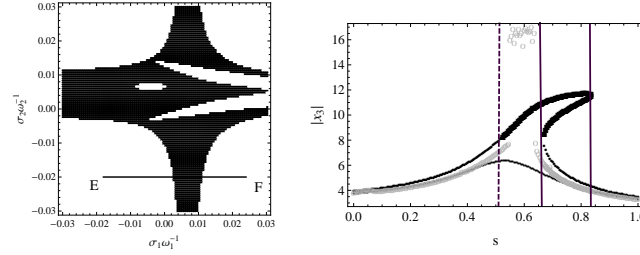


Figure 2: (1) Local stability diagram. (2) NES velocity amplitude along the segment line EF.

An extended experimental dataset of the system response was analyzed under steady state excitation at two frequencies. Thresholds between low and high damping states within the system and associated noise reduction were observed and quantified thanks to frequency conversion and RMS efficiency indicators. It is shown as observed in Test08 corresponding to scanning f^A and constant $f^B = 98.8$ Hz (in line with the segment line EF) that the membrane NES acts (see Fig. 3(1)) simultaneously and efficiently on two acoustic resonances (see Fig. 3(2,3)). In all cases, the introduction of energy at a second excitation frequency appears favorable to lower the frequency conversion threshold and to lower the noise within the linear system. In particular a simultaneous control of two one-to-one resonances by the NES is observed. These results will be discussed.

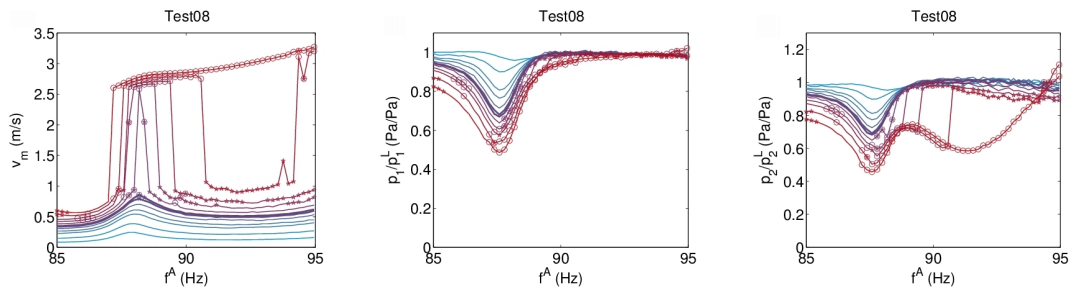


Figure 3: (1) RMS measured velocity of the NES and ratios of the RMS measured sound pressure (with NES) and the sound pressure considering the underlying linear system (without NES) for (2) the pipe 1 and (3) the pipe 2 for several excitation levels.

References:

- [1] Y. Starosvetsky, O. Gendelman, Response regimes in forced system with non-linear energy sink: quasi-periodic and random forcing, *Nonlinear Dynamics* 64 (2011) 177-195.
- [2] T. Pham, C. Lamarque, A. T. Savadkoohi, Multi-resonance capturing in a two-degree-of-freedom system under two different harmonic excitations, *Journal of Vibration and Control* 18 (3) (2012) 451-466.
- [3] R. Bellet, B. Cochelin, P. Herzog, P.-O. Mattei, Experimental study of targeted energy transfer from an acoustic system to a nonlinear membrane absorber, *Journal of Sound and Vibration* 329 (2010) 2768-2791.
- [4] S. Bellizzi, R. Côte, M. Pachebat, Responses of a two degree-of-freedom system coupled to a nonlinear damper under multi-forcing frequencies, *Journal of Sound and Vibration* 332 (2013) 1639-1653.

Tuned Pendulum as Nonlinear Energy Sink for Broad Energy Range

Maor Farid, Oleg Gendelman

Faculty of Mechanical Engineering, Technion – Israel Institute of Technology

Nonlinear Energy Sinks (NES) are widely studied as possible engineering solution for mitigation of steady-state, impulsive, transient and broadband excitations. Current work is devoted to applicability of common pendulum as the NES for mitigation of impulsive excitations. It turns out that if the pendulum is tuned at linear frequency of the primary mass, it can overcome one of main shortcomings of traditional NES designs and efficiently absorb energy in a wide range of energies. The reason is that for small energies the pendulum responds as tuned mass damper; at higher energies the pendulum acts as rotational NES. Thus, relatively broad diapason of energies can be covered.

The model of the eccentric NES is presented in Figure 1.

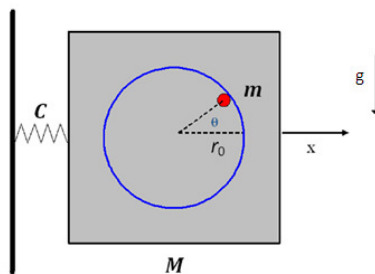


Figure 1- Scheme of primary mass with attached eccentric rotator

We demonstrate numerically that the properly tuned pendulum can be used as the NES and indeed has broader energy range than regular rotational NES. We study analytically and numerically the dynamics of such pendulum NES and explore corrections to a structure of its slow invariant manifold caused by presence of the gravity. Besides, we discuss the relationship between the pendulum NES performance and variation of its initial conditions, as one can see in Figure - the mean time for sufficient energy absorbance and its standard deviation for different values of initial energy, given by different values of initial conditions, with account of the gravity.

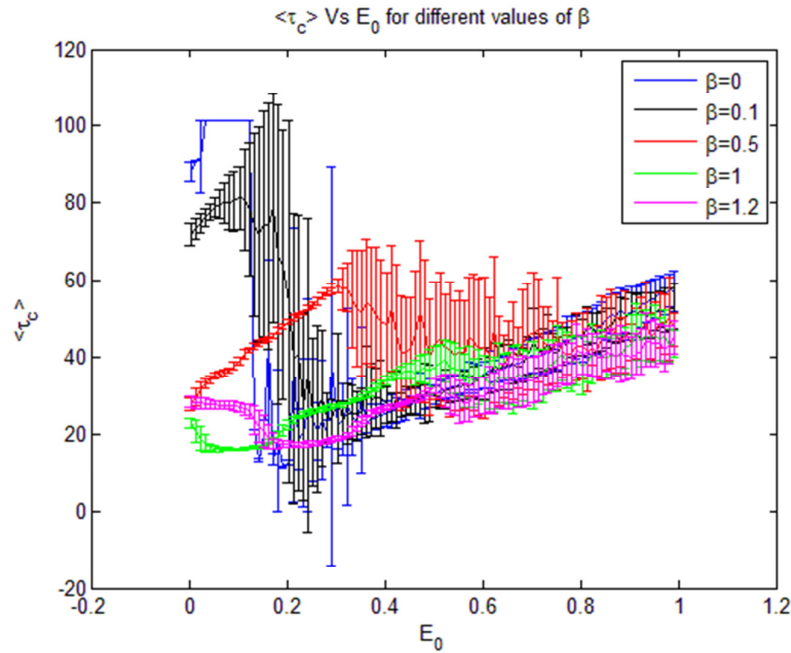


Figure 2 – The average characteristic time of energy dissipation and its standard deviation for different values of initial energy, with account of different values of initial conditions

As one can conclude from Figure , the most efficient design coefficient for energy absorbance, both for low energy values and for higher ones, was found for $\beta \approx 1$. It corresponds to an internal resonance in the NES system, between the natural frequency of the main mass's translations, and the natural frequency of the pendulum oscillations. In rotational regimes, the effect of the gravity on the NES performance turns out to be relatively small.

The Effect of Nonlinear Damping on Energy Harvesting Performance

D. Dane Quinn^{*}, Kevin Remick[†], D. Michael McFarland[†], Larry Bergman[°], Alex Vakakis[†]

^{*}*Department of Mechanical Engineering, The University of Akron, Akron, OH USA
44325-3903*

[†]*Department of Mechanical Science and Engineering, University of Illinois at
Urbana-Champaign, Urbana, IL USA 61801*

[°]*Department of Aerospace Engineering, University of Illinois at Urbana-Champaign, Urbana,
IL USA 61801*

Summary. This work considers the effect of mechanical damping on the performance of vibration-based energy harvesting system. In particular, the time-averaged power harvested is evaluated for two different physically motivated nonlinear mechanical damping models, friction damping and a physically derived cubic nonlinear damping, and compared against the performance of the more commonly used linear mechanical damping. It is shown that for each model of damping the harvested energy decays as the strength of the mechanical damping increases. However, the decay in performance is very different for the three models in question, so that the optimal design of the system depends critically on the form of the mechanical damping present in the system.

Introduction

Vibration-based energy harvesting involves the conversion of mechanical into electrical energy by means of electro-mechanical coupling, such as electromagnetic, piezoelectric, magnetostrictive, or electrostatic transduction. Many common designs incorporate an attached mass to an oscillating source as a mechanism for the mechanical displacement and as a source for the electro-mechanical coupling. The properties of this attachment, including the coupling and electrical component, must then be chosen to maximize the harvested power. For a linear device, the system is typically tuned so that the attachment is in resonance with the underlying mechanical oscillations to maximize the relative displacement of the attachment, thereby maximizing the mechanical energy available to harvest. Then, the electro-mechanical coupling and the electrical load are then tuned to maximize the harvested energy. For simple resistive electrical loads the optimal electro-mechanical coupling and load is tuned to match the existing mechanical damping present in the system [1]. However, these results assume that the mechanical damping is linear in form. The response of the system with other forms of damping has received much less attention. While the mechanical damping in the attachment limits the time-averaged power that can be harvested, the subsequent tuning depends on the form of the mechanical damping.

Model

A simple design of an electromechanical energy harvesting device is proposed and modeled by a single degree-of-freedom system. The displacement of the attached mass is defined as z , the mass of the attachment is m_a , and the corresponding stiffness is k_a . The electro-magnetic coupling and a resistive load, the electro-mechanical coupling is equivalent to viscous damping with coefficient b_e . Finally, the mechanical damping is represented by the force $f_{a,\text{damping}}(z, \dot{z})$, so that the equation of motion for the proposed model is

$$m_a \ddot{z} + f_{a,\text{damping}}(z, \dot{z}) + b_e \dot{z} + k_a z = -m_a \ddot{u}. \quad (1)$$

The system is assumed to be driven by constant amplitude base acceleration, so that $\ddot{u} \equiv A \sin(\omega t)$. The average power over a forcing cycle of $T = 2\pi/\omega$ can then be determined as

$$P_{\text{avg}} = \frac{1}{T} \int_0^T b_e \dot{x}^2 dt \quad (2)$$

The mechanical damping is assumed to take one of three forms

$$f_{a,\text{damping}}(z, \dot{z}) = \lambda \frac{\dot{z}}{|\dot{z}|}, \quad \text{Coulomb friction,} \quad (3a)$$

$$= \lambda \dot{z}, \quad \text{Linear damping,} \quad (3b)$$

$$= \lambda z^2 \dot{z}, \quad \text{Cubic damping} \quad (3c)$$

Note that the form of the cubic damping arises naturally in nonlinear energy harvesters based on essentially nonlinear elements [2].

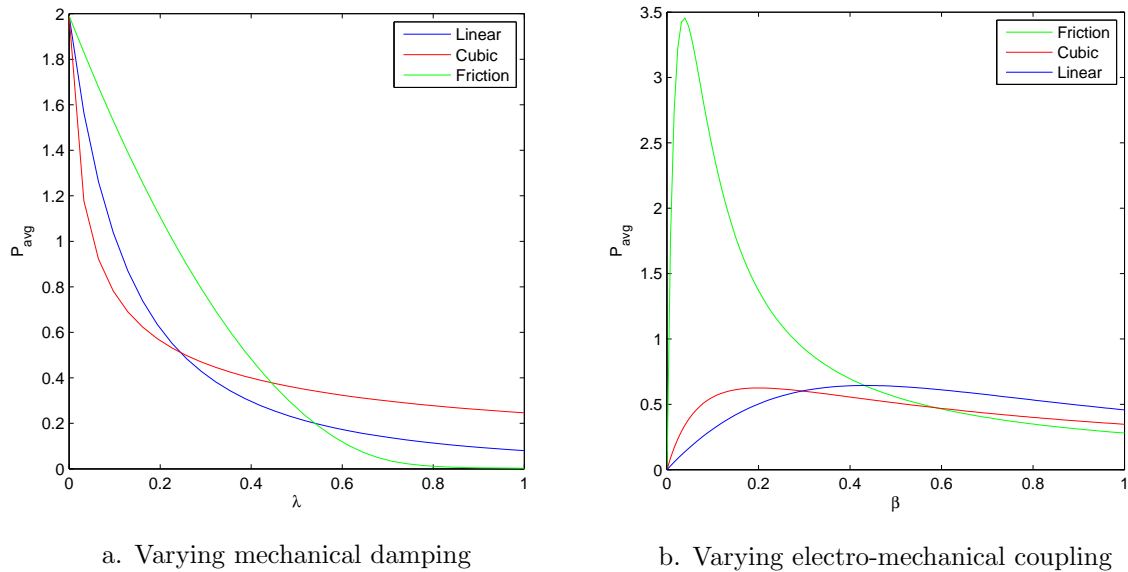


Figure 1: Average harvested power.

Results and Conclusions

The numerical simulations were performed with

$$\omega = 1.00, \quad m_a = 1.00, \quad b_e = 0.25, \quad k = 1.00. \quad (4)$$

Note that the mass and stiffness can be nondimensionalized to these values without loss of generality. In Figure 1a the average harvested power is shown as the mechanical damping parameter λ is varied, with $b_e = 0.25$. While the response of the system with linear damping is well-known, in the presence of friction damping the harvested power decays more slowly for small values of λ but then is reduced as compared to linear damping for larger values of λ . In contrast the behavior for the cubic damping is reversed. It initially decays faster than that for linear damping, but levels off and eventually decays slower than that observed for the system with linear mechanical damping.

In Figure 1b, the average harvested power is shown as the electro-mechanical coupling coefficient b_e varies, with $\lambda = 0.20$. While the systems with cubic and linear damping show similar levels of harvested power, the system with frictional damping is able to harvest significantly more energy, and the optimal coupling coefficient is lower than the other cases. Thus, the maximum harvested power and the optimal design parameters depend critically on the form of the mechanical damping present in the energy harvesting system.

References

- [1] S. Roundy, P. K. Wright, J. Rabaey, A Study of Low Level Vibrations as a Power Source for Wireless Sensor Nodes, *Comp. Comm.* 26 (2003) 1131–1144.
- [2] K. Remick, H. K. Joo, D. M. McFarland, T. P. Sapsis, L. A. Bergman, D. D. Quinn, A. F. Vakakis, Sustained High-frequency Energy Harvesting Through a Strongly Nonlinear Electromechanical System Under Single and Repeated Impulsive Excitations, *J. Sound Vib.* 333 (2014) 3214–3235.

The Nonlinear Tuned Vibration Absorber, Part I: Design and Performance Analysis

G. Habib, T. Detroux and G. Kerschen

Space Structures and System Laboratory
Department of Aerospace and Mechanical Engineering
University of Liège, Liège, Belgium.

Introduction

With continual interest in expanding the performance envelope of engineering systems, nonlinear components are increasingly utilized in real-world applications. Mitigating the resonant vibrations of nonlinear structures is therefore becoming a problem of great practical significance; it is the focus of the present study.

Nonlinear vibration absorbers, including the autoparametric vibration absorber [1], the nonlinear energy sink (NES) [2] and other variants [3, 4], can absorb disturbances in wide ranges of frequencies due to their increased bandwidth. However, the performance of existing nonlinear vibration absorbers is known to exhibit marked sensitivity to motion amplitudes. For instance, there exists a well-defined threshold of input energy below which no significant energy dissipation can be induced in an NES [2].

This paper builds upon previous developments [5] to introduce a new nonlinear vibration absorber for mitigating the vibrations around one problem nonlinear resonance. The absorber is termed the nonlinear tuned vibration absorber (NLTV), because its nonlinear restoring force is determined according to the nonlinear restoring force of the host structure. In other words, we propose to synthesize the absorber's load-deflection characteristic so that the NLTV can mitigate the considered nonlinear resonance in wide ranges of motion amplitudes.

Furthermore, a nonlinear generalization of Den Hartog's equal-peak method for determining the NLTV parameters is developed. The basic idea is to select the nonlinear coefficient of the absorber that ensures equal peaks in the nonlinear receptance function for an as large as possible range of forcing amplitudes. We will show that this is only feasible when the mathematical form of the NLTV's restoring force is carefully chosen, which justifies the proposed synthesis of the absorber's load-deflection curve.

Mathematical Model and Tuning Rule

The dynamics of a Duffing oscillator with an attached NLTV is considered:

$$\begin{aligned} m_1 \ddot{x}_1 + c_1 \dot{x}_1 + k_1 x_1 + k_{nl1} x_1^3 + c_2 (\dot{x}_1 - \dot{x}_2) + g(x_1 - x_2) &= F \cos \omega t \\ m_2 \ddot{x}_2 + c_2 (\dot{x}_2 - \dot{x}_1) - g(x_1 - x_2) &= 0 \end{aligned} \quad (1)$$

where $x_1(t)$ and $x_2(t)$ are the displacements of the primary system and of the NLTV, respectively. The NLTV is assumed to have a generic smooth restoring force $g(x_1 - x_2)$ with $g(0) = 0$. Adimensionalizing the equation of motion, the forcing amplitude F disappears from the linear terms, which confirms that the linear part of the absorber is amplitude independent. Furthermore, expanding $g(x_1 - x_2)$ in Taylor series, it can be noted that F appears in the dimensionless coefficients of the nonlinear term with exponent $k - 1$, where k is the order of the corresponding coefficient. This suggests that, if an optimal set of absorber parameters is chosen for a specific value of F , variations of F will detune the nonlinear absorber, unless the nonlinear coefficients of the primary system and of the absorber undergo a similar variation with F . This can be achieved by selecting the same mathematical function for the absorber as that of the primary system. When coupled to a Duffing oscillator, the NLTV should therefore possess a linear (k_2) and a cubic (k_{nl2}) spring.

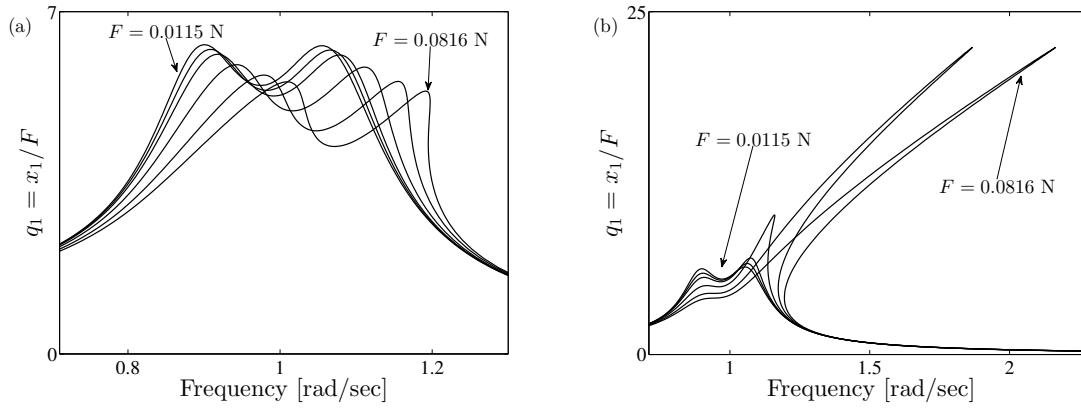


Figure 1: Frequency response of a Duffing oscillator with an attached NLTVA (a) and LTVA (b). For the computation $m_1 = 1$ kg, $c_1 = 0.002$ N.s/m, $k_1 = 1$ N/m, $k_{nl1} = 1$ N/m³ and $\epsilon = 0.05$. For the different curves $F = 0.0115$ N, $F = 0.0258$ N, $F = 0.0365$ N, $F = 0.0577$ N, and $F = 0.0816$ N.

In order to have an optimal behavior of the system at low forcing amplitudes, the well-known Den Hartog's tuning rule [6] for equal peaks, or alternatively the more precise formulas in [7], should be used. Then, based on a numerical procedure, the optimal value of the coefficient of the nonlinear restoring force of the absorber k_{nl2} , which guarantees equal peaks, can be obtained. Performing the optimization procedure for several values of the Duffing term and of the forcing amplitude, it can be observed that the optimal value of k_{nl2} does not depend on the amplitude and it is linear with respect to variations of k_{nl1} . Through a regression of the dimensionless coefficients of the system, we obtain the formula $k_{nl2} = 2\epsilon^2 k_{nl1}/(1 + 4\epsilon)$, where $\epsilon = m_2/m_1$, which approximates with excellent precision the value obtained through a numerical optimization procedure. This formula allows to easily tune the nonlinear spring restoring force and therefore can be considered as a nonlinear extension of Den Hartog's equal peaks rule.

Interestingly, the Duffing oscillator with an attached NLTVA exhibits linear-like dynamics in the investigated range of forcing amplitude. As shown in Fig. 1 (a), the frequency response increases almost linearly with respect to the forcing amplitude, in spite of the frequency shift of the resonant peaks. On the contrary, a linear tuned vibration absorber (LTVA) is rapidly detuned and its performance is strongly dependent on forcing amplitude (Fig. 1 (b)). For any value of the forcing amplitude in the investigated range, an important results is that the NLTVA has always better performance than the LTVA, which confirms the effectiveness of the proposed device and tuning rule.

Acknowledgments

The authors G. Habib, T. Detroux and G. Kerschen would like to acknowledge the financial support of the European Union (ERC Starting Grant NoVib-307265).

References

- [1] S. Oueini, A. Nayfeh, J. Vib. Contr. **6**, (2000) 999-1016.
- [2] A.F. Vakakis, O. Gendelman, L.A. Bergman, D.M. McFarland, G. Kerschen, Y.S. Lee, *Nonlinear Targeted Energy Transfer in Mechanical and Structural Systems* (Springer, 2009).
- [3] J. Shaw, S.W. Shaw, A.G. Haddow, Int. J. Nonlin. Mech **24**, (1989) 281-293.
- [4] N.A. Alexander, F. Schilder, J. Sound Vib. **319**, (2009) 445-462.
- [5] R. Vigiúí, G. Kerschen, J. Sound Vib. **326**, (2009) 780-793.
- [6] J.P. Den Hartog, *Mechanical Vibrations* (McGraw-Hill, New York 1934).
- [7] T. Asami, O. Nishihara, J. Vib. Acoust. **125**, (2003) 398-405.

5th Conference on Nonlinear Vibrations, Localization and Energy Transfer
Istanbul, Turkey, July 2–4, 2014

SESSION 2

The Nonlinear Tuned Vibration Absorber, Part II: Robustness and Sensitivity Analysis

T. Detroux, G. Habib, L. Masset and G. Kerschen

Space Structures and System Laboratory
Department of Aerospace and Mechanical Engineering
University of Liège, Liège, Belgium.

Introduction

Nonlinear vibration absorbers, including the autoparametric vibration absorber [1], the nonlinear energy sink (NES) [2] and other variants [3, 4], can absorb disturbances in wide ranges of frequencies due to their increased bandwidth. However, the performance of existing nonlinear vibration absorbers is known to exhibit marked sensitivity to motion amplitudes. For instance, there exists a well-defined threshold of input energy below which no significant energy dissipation can be induced in an NES [2]. In the companion of the present paper [5], a Nonlinear Tuned Vibration Absorber (NLTVA) is introduced to address these problems by extending Den Hartog's linear tuning rule [6] to the nonlinear domain.

While excellent performance of the NLTVA is observed at low and moderate energy levels, some peculiar phenomena can arise at higher energies, such as the apparition of detached resonance curves (DRCs), and quasiperiodic solutions; this is the focus of the present study.

In order to identify the working range of the NLTVA in the presence of such adverse dynamics, the absorber's robustness has to be assessed. The analysis proposed in this study builds upon numerical methods such as the continuation of codimension-1 bifurcations in parameter space, and the identification of the basins of attraction of the periodic and quasiperiodic solutions. It is shown that some variations of the absorber parameters can improve its robustness without deteriorating the performance significantly.

Computation of the adverse dynamics of the NLTVA

The dynamics of a Duffing oscillator with an attached NLTVA is considered:

$$\begin{aligned} m_1 \ddot{x}_1 + c_1 \dot{x}_1 + k_1 x_1 + k_{n1} x_1^3 + c_2 (\dot{x}_1 - \dot{x}_2) + g(x_1 - x_2) &= F \cos \omega t \\ m_2 \ddot{x}_2 + c_2 (\dot{x}_2 - \dot{x}_1) - g(x_1 - x_2) &= 0 \end{aligned} \quad (1)$$

where $x_1(t)$ and $x_2(t)$ are the displacements of the primary system and of the NLTVA, respectively. The application of the tuning procedure proposed in [5] gives a restoring force for the NLTVA with both linear and cubic stiffness, i.e., $g(x_1 - x_2) = k_2(x_1 - x_2) + k_{n2}(x_1 - x_2)^3$.

The system described in (1) exhibits linear-like dynamics in an important range of forcing amplitudes but, for high values of F , some nonlinear phenomena can arise and possibly alter the performance of the NLTVA. As an illustration of the adverse dynamics, Figure 1(a) depicts the frequency response of the Duffing oscillator for a forcing amplitude $F = 0.15$ N. One first observes that the main frequency response verifies Den Hartog's criterion, with two resonance peaks of same amplitude, which validates the effectiveness of the absorber. In this case, however, one can also detect the presence of pairs of fold and Neimark-Sacker bifurcations, with stable quasiperiodic oscillations emanating from the latter through a combination resonance. This can lead to higher oscillation amplitudes than what was expected from the study of the main frequency response, but a careful investigation shows that they remain acceptable. For higher frequencies, one notices the

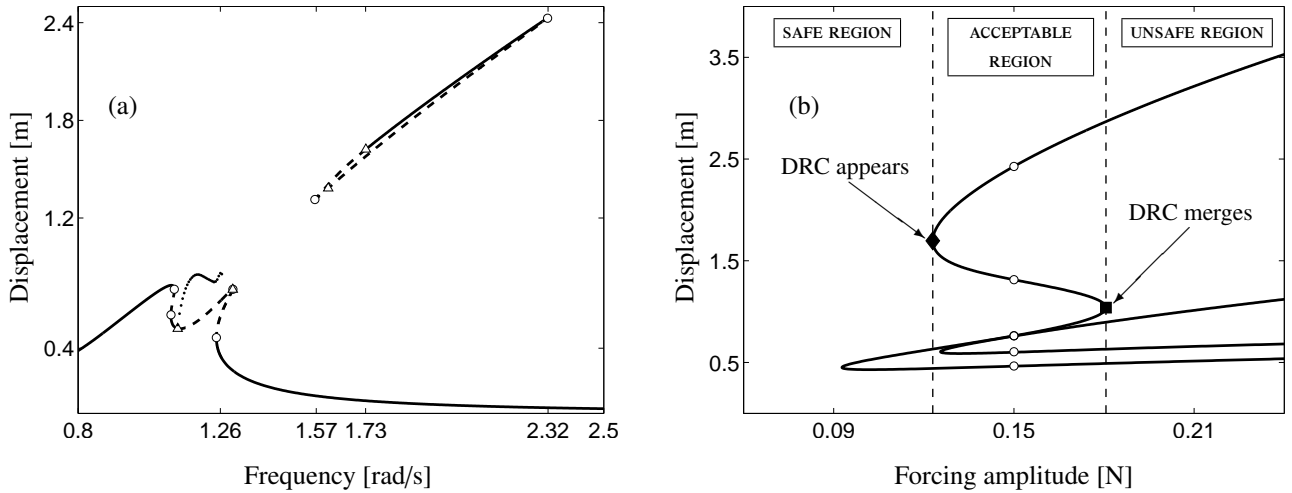


Figure 1: Adverse dynamics and robustness analysis of the NLTVA. (a) Frequency response of the Duffing oscillator with an attached NLTVA for $F = 0.15$ N. The solid and dashed lines represent stable and unstable solutions, respectively. The dots represent the amplitude of stable quasiperiodic oscillations. Fold and Neimark-Sacker bifurcations are depicted with circle and triangle markers, respectively. (b) Projection of the branches of fold bifurcations on the F -displacement plane. The circle markers highlight fold bifurcations at the forcing amplitude of interest.

presence of a DRC with stable parts coexisting with periodic solutions of lower amplitude.

In order to assess the robustness of the NLTVA with respect to these phenomena, one of the methods we propose consists in tracking fold bifurcations against the forcing parameters, F and ω . This is performed in Figure 1(b) which shows the projection of branches of fold bifurcations in the F -displacement plane. Interestingly, together with the bifurcations on the main frequency response, the branches indicate the presence of bifurcations on the DRC, which gives valuable information about this isolated solution. From the upper turning point, one can identify the forcing amplitude at which the DRC appears, one can then quantify its growth, and, from the lower turning point, one can eventually evaluate a forcing amplitude at which it merges with the main frequency response. This forms the basis of the concept of safe, acceptable and unsafe regions, for the performance of the NLTVA (see Figure 1(b)). The present work is based on the study of the evolution of the regions for variations of the NLTVA parameters, and shows the compromises that can be made to enlarge the working range of the NLTVA and enhance its practical applicability.

Acknowledgments

The authors T. Detroux, G. Habib, L. Masset and G. Kerschen would like to acknowledge the financial support of the European Union (ERC Starting Grant NoVib-307265).

References

- [1] S. Oueini, A. Nayfeh, *J. Vib. Contr.* **6**, (2000) 999-1016.
- [2] A.F. Vakakis, O. Gendelman, L.A. Bergman, D.M. McFarland, G. Kerschen, Y.S. Lee, *Nonlinear Targeted Energy Transfer in Mechanical and Structural Systems* (Springer, 2009).
- [3] J. Shaw, S.W. Shaw, A.G. Haddow, *Int. J. Nonlin. Mech.* **24**, (1989) 281-293.
- [4] N.A. Alexander, F. Schilder, *J. Sound Vib.* **319**, (2009) 445-462.
- [5] G. Habib, T. Detroux, G. Kerschen, The Nonlinear Tuned Vibration Absorber, Part I: Design and Performance Analysis, *Proceedings of the 5th Conference on Nonlinear Vibrations, Localization and Energy Transfer*, Istanbul, 2014.
- [6] J.P. Den Hartog, *Mechanical Vibrations* (McGraw-Hill, New York 1934).

Nonlinear Transverse Vibrations of Axially Moving Beams with Clamped Ends and One Intermediate Simple Support

Ferid Köstekci ^{a)}

Department of Mechanical Engineering, Faculty of Engineering, Hitit University, 19030, Corum, Turkey

Abstract: This study deals with the nonlinear response of an axially moving Euler-Bernoulli beam with clamped ends and one intermediate simple support. Examination of the traveling beam problem with these boundary conditions is the main contribution of this search. The support conditions mean that the beam is passing through two frictionless guides and one intermediate simple support placed between two guides. It is assumed that the beam has immovable boundaries at the outer ends. The assumption introduces nonlinearity because of stretching of neutral fibers. It is considered that the beam is axially moving along its length at a harmonically varying velocity about a constant mean value. In this paper variations at the velocities are assumed to be suitably weak. Differential equations governing the motion of the two sides of the beam are derived using variational formulation. A damping term is added into the equations. The method of multiple scales is applied to obtain approximate analytical solutions in this weakly nonlinear system. Natural frequencies are calculated in order to discuss effects of variations in flexural rigidity, mean translating speed and the location of intermediate support. Solvability condition for the case of principal parametric resonance is derived, amplitude-phase curves of steady-state responses and stability conditions are investigated.

INTRODUCTION

Magnetic tapes, power transmission belts, band saw, serpentine belts, robot arms and aerial cable tramways are engineering examples classified as axially moving continuum bodies [1-4]. Paper sheets, chain drives, fiber textiles, oil pipelines, wire and sheet metal processing systems such as straightening are the most common examples of axially moving continua. Transvers vibrations of moving continuous materials cause poor quality and failure. Therefore, the examination of these vibrations is of essential importance in design processes. Traveling bodies are modelled mathematically as either a traveling beam or string. There has been vast research into the vibration of axially moving continua. Wickert and Mote Jr. investigated the transverse vibration of axially moving beams and strings using an eigenfunction method. They also examined the vibrations of an axially moving string loaded suspended mass [5]. Pakdemirli and Öz computed the natural frequencies of axially moving beams with clamped ends in the super critical regime, and found the beam unstable at those velocities [6]. Pakdemirli and Nayfeh showed that the midplane stretching has a great effect on frequency-response and force-response [7]. Bağdatlı et al. [8] investigated the nonlinear vibrations of beams supported at both ends and also had an intermediate support. An Euler-Bernoulli-type axially moving beam on multiple supports (simple support type) was considered [9]. Natural frequencies, modes and critical speeds of axially moving beams on different supports were analysed based on Timoshenko model by Tang et al. [10]. Amplitude and phase modulation relations were presented for different forcing and damping cases and 3:1 internal resonance cases were investigated between different modes of vibration [11]. Numerical examples were carried out to show the effects of variation in flexural rigidity, mean translating speed and the location of intermediate support on natural frequencies [12].

The present paper investigates nonlinear response and stability of an axially moving beam. The Euler-Bernoulli-type beam passing through two frictionless guides is traveling with a slightly varying harmonic velocity and there is one simple support between the guides. The paper is organized as follows. The governing partial differential equations of motion and boundary conditions are derived using Hamilton's Principle and solved using perturbation technique. Next, the natural frequencies are examined numerically for different bending rigidities, internal support locations and translating velocities. Finally, nonlinear response and stability of the beam is searched.

PERTURBATION ANALYSIS and NUMERICAL EXAMPLES

An Euler-Bernoulli-type uniform beam, with density ρ , cross-sectional area A , modulus of elasticity E , the moment of inertia of the beam's cross section with respect to the neutral axis I , under an applied tension P , is moving axially at a slightly varying harmonic velocity v^* . In Fig. 1, u_1^* and u_2^* are the left and the right side axial displacements of the beam respectively, and w_1^* and w_2^* are the left and the right side transverse displacements of the beam respectively. Here, t^* is time, x_1^* and x_2^* are spatial variables. The Lagrangian for the beam is derived first. Then, the equations of motion are found through the Hamilton's Principle. Non-dimensional variables and parameters are employed [8, 9, 12]. A solution will be carried out by using the method of multiple scales [13].

^{a)} Corresponding author. Email: feridkostekci@hitit.edu.tr

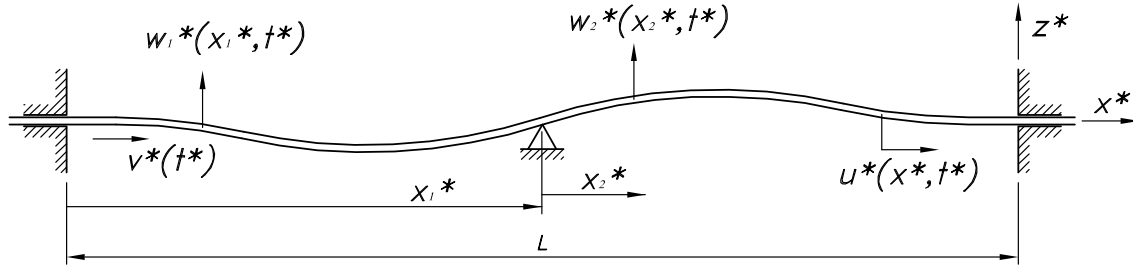


Fig. 1. Schematic model of a traveling beam passing through two fixed supports and one intermediate simple support.

Numerical examples are conducted to show effects of variations in the mean axial speed and the location of the intermediate support. Fig. 2 illustrates the variation of the first and second natural frequencies with mean translating velocity for different internal support locations, $\eta=0.1, 0.2, 0.3, 0.4,$ and 0.5 , for the flexural stiffness constant $v_f=0.3$.

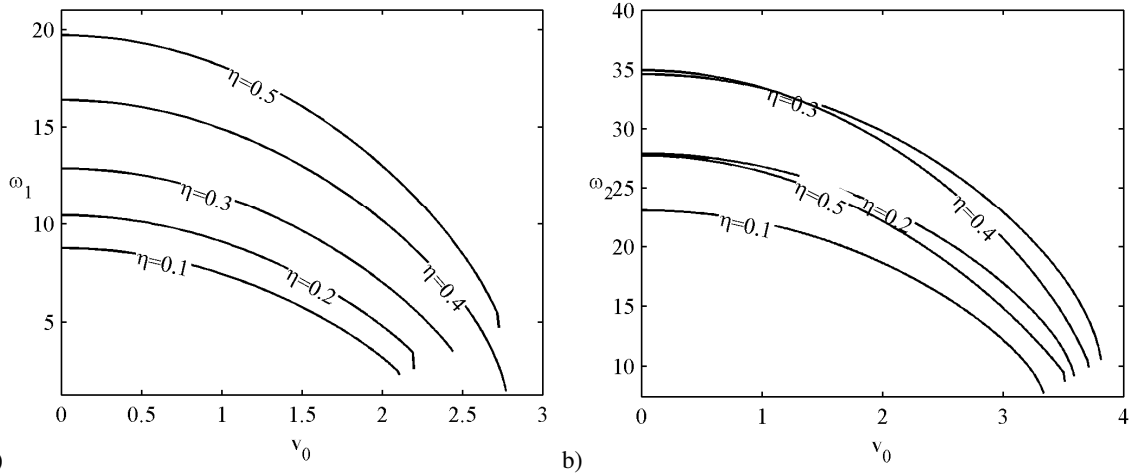


Fig. 2. Natural frequency variations vs. axially traveling speeds for different locations (η) of intermediate support: (a) the first mode and (b) the second mode.

CONCLUDING REMARKS

This paper addresses numerically the dynamic response and stability conditions of an axially moving beam. Increasing flexural rigidity increases linear frequency but higher mean velocities decreases linear frequency. Placing the intermediate support toward the middle of the beam also increases linear frequency.

References

- [1] G. Chakraborty, A.K. Mallik, H. Hatwal, Non-Linear Vibration of a Travelling Beam. *International Journal of Non-Linear Mechanics* 1999, 34: 655-670.
- [2] K.Y. Sze, S.H. Chen, J.L. Huang, The Incremental Harmonic Balance Method for Nonlinear Vibration of Axially Moving Beams. *Journal of Sound and Vibration* 2005, 281: 611-626.
- [3] L.H. Chen, W. Zhang, F.H. Yang, Nonlinear Dynamics of Higher-Dimensional System for an Axially Accelerating Viscoelastic Beam with In-Plane and Out-Of-Plane Vibrations. *Journal of Sound and Vibration* 2010, 329: 5321-5345.
- [4] M.H. Ghayesh, S. Balar, Non-linear Parametric Vibration and Stability Analysis for Two Dynamic Models of Axially Moving Timoshenko Beams. *Applied Mathematical Modelling* 2010, 34: 2850-2859.
- [5] J.A. Wickert, C.D. Mote, Jr., Classical Vibration Analysis of Axially Moving Continua. *ASME Journal of Applied Mechanics* 1990, 738-744.
- [6] M. Pakdemirli, H.R. Öz, Infinite Mode Analysis and Truncation to Resonant Modes of Axially Accelerated Beam Vibrations. *Journal of Sound and Vibration* 2008, 311: 1052-1074.
- [7] M. Pakdemirli, A.H. Nayfeh, Nonlinear Vibrations of a Beam-Spring-Mass System. *Journal of Vibration and Acoustics* 1994, 116: 433-439.
- [8] S.M. Bağdatlı, E. Özkaya, H.R. Öz, Dynamics of Axially Accelerating Beams with an Intermediate Support. *Journal of Vibration and Acoustics* 2011, 133: 031013.
- [9] S.M. Bağdatlı, E. Özkaya, H.R. Öz, Dynamics of Axially Accelerating Beams with Multiple Supports. *Nonlinear Dynamics* 2013, 74: 237-255.
- [10] Y.-Q. Tang, L.-Q. Chen, X.-D. Yang, Natural Frequencies, Modes and Critical Speeds of Axially Moving Timoshenko Beams with Different Boundary Conditions. *International Journal of Mechanical Sciences* 2008, 50: 1448-1458.
- [11] S.M. Bağdatlı, H.R. Öz, E. Özkaya, Non-Linear Transverse Vibrations and 3:1 Internal Resonances of a Tensioned Beam on Multiple Supports. *Mathematical and Computational Applications* 2011, 16: 203-215.
- [12] F. Kösteci, Effects of Flexural Stiffness, Axial Velocity and Internal Support Locations on Translating Beam's Natural Frequencies. *Applied Mechanics and Materials* 2014, 532: 316-319.
- [13] A.H. Nayfeh, Introduction to Perturbation Techniques, Wiley, 1993.

Nonlinear behavior of a Timoshenko nano-beam subjected to a displacement dependent pressure considering modified couple stress theory

H. Etemadi^{1*}, *R. Shabani*¹, *G. Rezazadeh*¹ and *V. Sadighi*
¹ *Department of Mechanical Engineering, Urmia University, Iran*
**.Hadi_Etemadi2007@yahoo.com*

Abstract:

In this paper, nonlinear static and dynamic behavior of electrostatically actuated Timoshenko nano-beams are analytically investigated on the basis of the modified couple stress theory in the elastic range. The modified couple stress theory is a non-classic continuum theory capable to capture the small-scale size effects in the mechanical behavior of structures. The governing equations of motion and boundary conditions are derived on the basis of Hamilton principle. In this paper, considering bending deformations and angle of rotation of the cross sections, an Timoshenko beam is proposed on the basis of the modified couple stress theory. Also in this study the effect of pull-in voltage, on static and dynamic behavior of the system are investigated. And the result indicates that the behavior of the beam significantly depends on the pull-in voltage. The static and dynamic pull-in voltages gained for nano Timoshenko beam using the modified couple stress theory are compared with those gained for nano Euler–Bernoulli beam using the modified couple stress theory [1]. And the results of this comparison showed slight difference between them.

Keywords: Timoshenko nano-beams, couple stress theory, bending deformations, angle of rotation of the cross sections, pull-in voltage

Introduction:

Thin (cantilever) beams have found important applications in micro- and nano-scale measurements such as those in biosensors and atomic force microscopes. In these applications the size effect is often observed (e.g., Lam *et al* (2003), McFarland and Colton (2005)). It is well-known that size-dependent behavior is an inherent property of materials which appears for a beam when the characteristic size such as thickness or diameter is close to the internal material length scale parameter [1]. Lacking an internal material length scale parameter, classical beam models cannot be used to interpret this microstructure-dependent size effect, therefore, need to be extended by using non-classical continuum theories such as modified couple stress theory. This theory is acceptably able to interpret the size-dependencies. Electrostatically actuated devices form a broad class of MEMS and NEMS devices due to their simplicity, as they require few mechanical components and small voltage levels for actuation [1]. In such devices, a conductive flexible beam/plate is suspended over a ground plate and a potential difference is applied between them. As the microstructure is balanced between electrostatic attractive force and mechanical (elastic) restoring force, both electrostatic and elastic restoring force are increased when the electrostatic voltage increases. When the voltage reaches the critical value, pull-in instability occurs. Pull-in is a situation at which the elastic restoring force can no longer balance the electrostatic force. Further increasing the voltage will cause the structure to have dramatic displacement jump causing structural collapse and failure [1]. The Timoshenko beam is a model for the study of behaviors of beams with less restrictive assumptions with respect to the Euler–Bernoulli beam. The Timoshenko beam is a complicated model with respect to the Euler–Bernoulli model, it possesses more capabilities and studying the behavior of beams based on the Timoshenko model gives closer results to the exact behavior [2]. Therefore the objective of this paper is to develop a model for Electrostatically actuated Timoshenko nano beams using the minimum total potential energy principle and the concepts of the modified couple stress theory of Yang *et al* (2002).

Results and Discussion

In this study the cantilever aluminum nano-beams properties are $b=200\text{nm}$, $h=150\text{nm}$, $g_0 = 100\text{nm}$ and $L = 8\ \mu\text{m}$ and $l = 0.5\ \mu\text{m}$ [1]. Fig. 2 depicts equilibrium points for the Aluminum nano-beam versus applied voltage as a control parameter based on couple stress theory. As shown in this figure for given $0 < V < V_{\text{pull-in}}$ there exist two physically fixed points. The first fixed point is a stable and the second one is an unstable. Therefore in Figs. 2 continuous and dashed curves present the stable and unstable branches, respectively. In the aforementioned nano beam, by increasing the control parameter V the physically possible fixed points are closing to each other and in the pull-in voltage, they coincide in the bifurcation point. In this study static pull-in voltage is 10.60 V. Fig. 3 shows pull-in voltage versus the initial

gap. As shown in these figure, with increasing the initial gap, pull-in voltage increases and the size effect of the nano-beam is also increased.

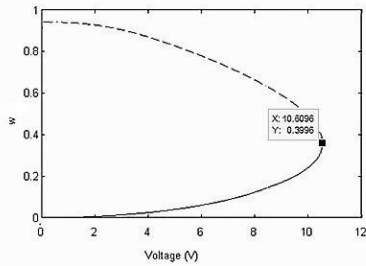


Fig. 2. Variation of the deflection of the nano-beams with applied DC voltage based on couple stress theory

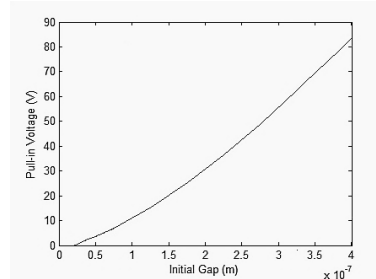


Fig. 3. pull-in voltage VS initial gap for nano-beam

Fig.4 showed Primary frequency-response for the Duffing equation .As shown in these figure with increasing the AC Voltage in frequency – response curves the bending of the frequency – response curves increases. Fig. 5 show the time history of dimensionless gap for this nano-beam with actuating step voltage of 9.4v. We note that the nano-beam oscillates with these voltages, and dose not collapse. But by a small increase of the actuating step voltage by only about 0.0 1V the nano-beam collapses. the calculated dynamic pull-in voltage based on couple stress theories is 9.41 The dynamic pull-in voltages are about 89% of the static pull-in voltages.

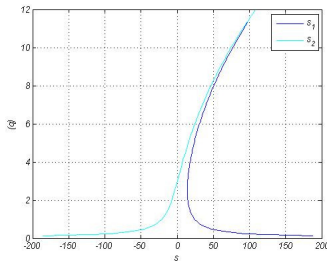


Fig. 4. Primary frequency-response for switch the Duffing equation ,effect of AC voltage [3]

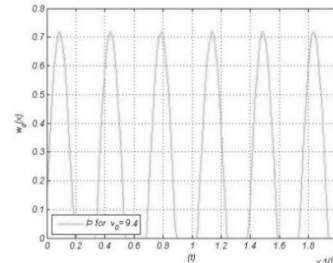


Fig. 5. Time history of aluminum nano subjected to step-wise $V_{DC}=9.4$ v

It is therefore concluded that the behavior of the beam significantly depends on the pull-in voltage. Beams show unstable behavior when are subjected to a fields created by potentials higher than pull-in voltage.

References

- [1]. *Hamed Mobki1, Morteza H. Sadeghi, Ghader Rezazadeh, Mohammad Fathalilou, Ali-asghar keyvani-janbaban. Nonlinear Behavior of a Nano-scale Beam Considering Length Scale-Parameter. Journal of Elsevier Editorial System(tm) Mathematical Modelling Manuscript Draft.*
- [2]. *M. Asghari, M. Rahaeifard, M.H. Kahrobaiyan, M.T. Ahmadian. The modified couple stress functionally graded Timoshenko beam formulation. Journal of ScienceDirect Materials and Design*
- [3]. *M. I. YOUNIS and A. H. NAYFEH. A Study of the Nonlinear Response of a Resonant Microbeam to an Electric Actuation. ScienceDirect Nonlinear Dynamics 31: 91–117, 2003.© 2003 Kluwer Academic Publishers.*
- [4]. *Kaveh Rashvanda, Ghader Rezazadeha, , Hamed Mobkib, Mergen H. Ghayeshc. On the Size-dependent Behavior of a Capacitive Circular Microplate Considering the Variable Length-scale Parameter. Journal of ScienceDirect Materials and Design .*

Effects of the Gap Distance on the Dynamics of a Nano-Resonant Beam Subjected to a Nonlinear Electrostatic Pressure

Mohammad Fathalilou¹, Morteza Sadeghi¹, Ghader Rezazadeh²

¹Mechanical engineering Department, University of Tabriz, Iran

²Mechanical engineering Department, Urmia University, Iran

Abstract

This paper presents a study on the gap dependent bifurcation behavior of an electrostatically-actuated nano-beam. The size-dependent behavior of the beam was taken into account by applying the couple stress theory. Two small and large gap distance regimes have been considered in which the intermolecular vdW and Casimir forces are dominant, respectively. It has been shown that changing the gap size can affect the fundamental frequency of the beam. The bifurcation diagrams for small gap distance revealed that by changing the gap size, the number and type of the fixed points can change. However, for large gap regime, where the Casimir force is the dominant intermolecular force, changing the gap size does not affect the quality of the bifurcation behavior.

Keywords: Nano-Beam, Electrostatic, Bifurcation, Fixed Point, Couple Stress

1. Introduction

Nowadays, with the rapid development in nano technology, the nano electro-mechanical systems (NEMS) have become one of the hottest research topics. High speed, accuracy and performance as well as low energy consumption have increased the possibility of substituting the nano technology with micro technology. Lin et al. [1] have studied the pull-in phenomena and calculated the pull-in voltage for a nano-electromechanical switch with the assumption of one degree of freedom for a nano switch without taking into account the effect of vdW force. Dequesnes et al. [2] have calculated the pull-in voltage for carbon-nano-tube-based nano-electromechanical switches. Moeenfard et al [3] have investigated the static behavior of nano and micro-mirrors under the effects of Casimir force. Palasantzas et al [4] have obtained for two parallel gold surfaces about 18 nm gap distance for the crossover from vdW to Casimir regime, whereas Lambrecht and Reynaud [5] have predicted theoretically about 13 nm for the transition.

On the other hand, many researches showed that in micro and nano scales the materials have strong size dependence in deformation behavior [6]. Size-dependent behavior is an inherent property of materials, which appears for a beam when the characteristic size such as thickness or diameter is close to the internal length-scale parameter of materials [6].

In spite of the mentioned works about the electrostatically actuated nano-beams, there is no comprehensive study about their stability from bifurcation view point. In this paper, distributed as well as the lumped models of the nano-beam

with nonlinear electrostatic actuation are introduced, considering the couple stress theory of elasticity. The vdW and Casimir forces are taken into account for small and large gap distances, respectively.

2. Mathematical Modeling and Numerical Solution

Figure 1 shows an electrostatically actuated fixed-fixed Euler-Bernoulli nano-beam.

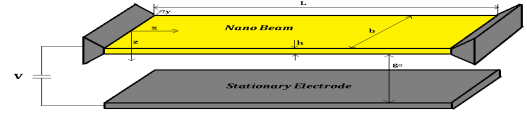


Fig. 1. An electrostatically actuated fixed-fixed nano-beam

The governing equation of motion considering the couple stress theory is obtained as following:

$$\left[\bar{E}I + 4\mu bhl^2 \right] \frac{\partial^4 w}{\partial x^4} + \rho b h \frac{\partial^2 w}{\partial t^2} = q_{ext} \quad (1)$$

Clearly, when the couple stress effect is suppressed by letting $l=0$, the present model will reduce to the classical Euler-Bernoulli beam model. In Eq. (1), q_{ext} is considered as the sum of the nonlinear electrostatic, vdW and Casimir forces as following [7]:

$$q_e = \frac{\epsilon_0 b V^2}{2(g_0 - \hat{w})^2}, \quad q_v = \frac{Ab}{6\pi(g_0 - \hat{w})^3}, \quad q_C = \frac{b\pi^2 \hbar c}{240(g_0 - w)^4} \quad (2)$$

Due to the nonlinearity of the derived static equation, the solution is complicated and time consuming. We adopted the step-by-step linearization method (SSLM) [6], followed by Galerkin method to solve the obtained linear set of algebraic equations. Dynamic loading response can be obtained using Galerkin-based reduced order model [6]. To achieve a reduced order model, $w(x,t)$ may be approximated as:

$$w(x,t) = \sum_{j=1}^n T_j(t) \phi_j(x) \quad (3)$$

By substituting Eq. (3) into Eq. (1) and multiplying by $\phi_i(x)$ as a weight function in Galerkin method and integrating the outcome from $x=0$ to L , the Galerkin based reduced order model is generated as:

$$\sum_{j=1}^n M_{ij} \ddot{T}_j(t) + \sum_{j=1}^n K_{ij} T_j(t) = F_i \quad (4)$$

3. Results and Discussion

For analyzing the bifurcation behavior, a capacitive gold nano-beam is considered with the specific geometries and material

properties. It is considered two gap distance regimes which in the small distances, $g_0 < 10 \text{ nm}$, the only intermolecular force is vdW force whereas in large distances, $g_0 > 15 \text{ nm}$, the Casimir force is the only dominant intermolecular force [4]. It can be seen in fig. 2. a. ($g_0 = 6 \text{ nm}$) that for the applied voltages, there are two voltage regimes with two fixed-points and an interval with no fixed-point in the bifurcation diagram. While, for $g_0 = 10 \text{ nm}$, instead of the regime with no fixed-point, we have a regime with four fixed-points in the diagram (Fig. 2.b). Figure 3 illustrates the stability of these fixed points. In Fig. 3, it can be found that for $V = 0V$ the first equilibrium position is a stable centre point and the second is an unstable saddle-node. There are two basins of attraction of stable centers and a basin of repulsion of unstable saddle node. Depends on the location of the initial condition the system can be stable or unstable. Also, it must be mentioned that for a given voltage there is a singular point (SP) at the substrate position.

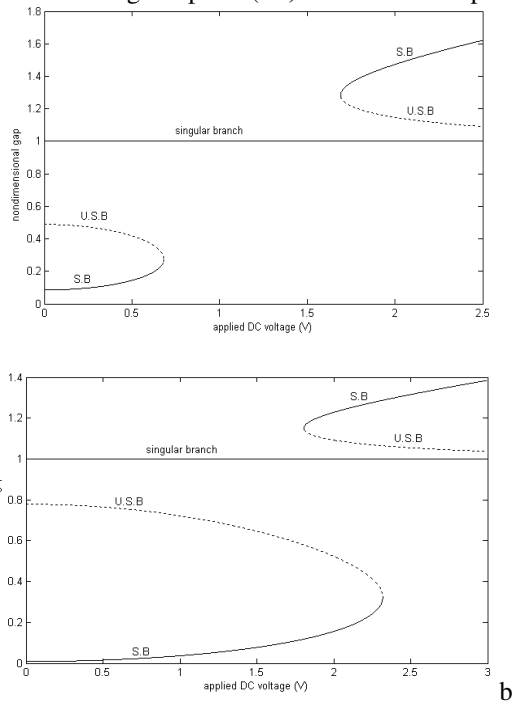


Fig. 2. Variation of the center gap of the nano-beam with applied DC voltage for a. $g_0 = 6 \text{ nm}$ b. $g_0 = 10 \text{ nm}$

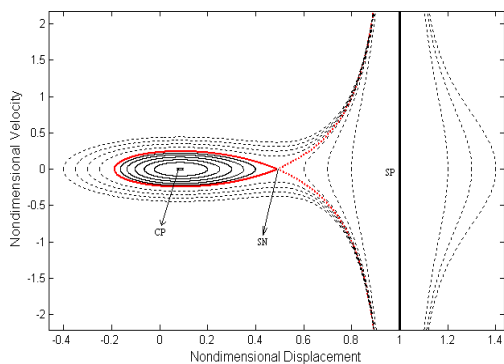


Fig. 3. Phase portrait of the nano-beam for $g_0 = 6 \text{ nm}$ and various initial conditions for $V=0V$

Figure 4 illustrates the bifurcation diagram of the nano-beam with $g_0 = 15 \text{ nm}$. It is understood that for all gaps above 15 nm there are three fixed points before pull-in voltage. One

of them is under the substrate which is physically impossible, but other two points are above the substrate. On the other hand, for voltages higher than pull-in voltage there is only one fixed point which is under the substrate.

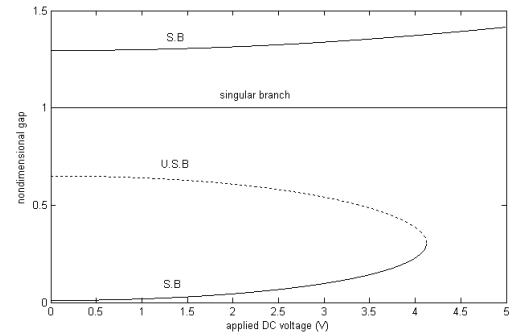


Fig. 4. Variation of the center gap of the nano-beam with applied DC voltage for $g_0 = 15 \text{ nm}$

4. Conclusion

In presented work, gap dependent bifurcation behavior of an electrostatically-actuated gold nano-beam was studied. Both distributed and lumped models were introduced to explain the nano-beam deformation considering couple stress theory. In bifurcation analysis, the following results were obtained:

1. In both small and large gap regimes, for voltages lower than pull-in voltage, two stable and unstable fixed points appear on upper side of the beam.
2. For small gap regime it can be found a voltage range in which no fixed point appears, whereas for large gaps there is not such a range.
3. For large gap distances, for all voltages, there is one mathematically stable fixed point under substrate plate which is physically impossible, whereas for small gaps we have two voltage ranges; in first range there is not any fixed point under the substrate and in second one two mathematically stable and unstable branches meet together in a saddle node. In this case the distance between two saddle nodes on upper and lower sides of the substrate plate varies with changing the gap size.

References

- [1] W.H. Lin, Y.P. Zhao, Nonlinear behavior for nanoscale electrostatic actuators with Casimir force, *Chaos Solutions and Fractals* 23 (2005) 1777–1785.
- [2] M. Dequesnes, S.V. Rotkin, N.R. Aluru, Calculation of pull-in voltages for carbon nano-tube-based nano electro mechanical switches, *Nanotechnology* 13 (2002) 120–131.
- [3] H. Moeenfar, A. Darvishian, M.T. Ahmadian, Static behavior of nano/micromirrors under the effect of Casimir force, an analytical approach, *Journal of Mechanical Science and Technology* 26 (2) (2012) 537–543.
- [4] G. Palasantzas, P.J. van Zwol, J. De Hosson, Transition from Casimir to van der Waals force between macroscopic bodies, *Applied Physics Letter*. 93 (2008) 121912.
- [5] A. Lambrecht, S. Reynaud, Casimir force between metallic mirrors, *European Physics Journal D* 8 (2000) 309–318.
- [6] M. Fathalilou, M. Sadeghi, G. Rezazadeh, M. Jalilpour, Study on the Pull-in Instability of Gold Micro-Switches Using Variable Length Scale Parameter, *International Journal of solid Mechanics* 3 (2011) 114–123.
- [7] F. Tahami, H. Mobki, A. Keyvani-Janbahan, G. Rezazadeh, Pull-in Phenomena and Dynamic Response of a Capacitive Nano-beam Switch, *Sensors & Transducers Journal* 110 (11) (2009) 26–37

Flexural–Torsional Vibration and Stability Analysis of Multilayer Beams Subjected to Axial Load and End Moment – A Dynamic Finite Element Formulation

¹Towliat, M.T., ²Hashemi, S. M.

Faculty of Aerospace Engineering, Ryerson University, Toronto, ON, Canada.

The coupled bending – torsion vibration and buckling of preloaded beams, subjected to axial load and end moment, is investigated. Based on the Euler-Bernoulli bending and St. Venant torsion beam theories, the differential equations governing coupled flexural–torsional vibrations and stability of a uniform, slender, isotropic, homogeneous and linearly elastic beam, undergoing linear harmonic vibration, are developed. Using the closed-form solutions of the uncoupled portions of the governing equations as the basis functions of approximation space, the Dynamic (frequency-dependent) Interpolation Functions are developed, which are then used in conjunction with the weighted residual method to develop the Dynamic Finite Element (DFE) of the system. Implementing the DFE in a MATLAB-based code, the resulting nonlinear Eigenvalue problem is then solved to determine the Eigensolutions of illustrative beam examples, subjected to various boundary conditions, and exhibiting geometric bending-torsion coupling. The validity and effectiveness of the proposed DFE are verified against the limited experimental data, and those obtained from analytical solution, conventional Finite Element Method (FEM), as well as commercial software (ANSYS®). A buckling analysis of the beam is also carried out to determine the critical buckling end moment and axial compressive force. The DFE produces exact results in absence of end moment, and exhibits a higher rate of convergence than the conventional FEM.

1. **Professor, Faculty of Aerospace Engineering, Ryerson University, Toronto, ON, Canada.
shashem@ryerson.ca**
2. **PhD Candidate, of Aerospace Engineering, Ryerson University, Toronto, ON, Canada.
mtowliat@ryerson.ca**

5th Conference on Nonlinear Vibrations, Localization and Energy Transfer
Istanbul, Turkey, July 2–4, 2014

SESSION 3

Discrete breathers in forced chains of oscillators with cubic nonlinearities

Francesco Romeo*, Michael Veremkroitt**, Oleg Gendelman**

**Dipartimento di Ingegneria Strutturale e Geotecnica, Sapienza University of Rome, Rome, Italy*

***Faculty of Mechanical Engineering, Technion - Israel Institute of Technology, Haifa, Israel*

Summary. The forced dynamics of chains of linearly coupled mechanical oscillators characterized by on site cubic nonlinearity is investigated. The study aims to highlight the role played by the harmonic excitation on the nonlinear localised dynamics of the system. Towards this goal, a map approach is employed in order to identify the chain nonlinear propagation regions under 1:1 resonance conditions. Given the latter assumption, the governing second-order difference equation refers to a perturbation of the stationary resonant response. Therefore, at first, the map dependence on the perturbation amplitude is neglected and the dependence of the propagation regions as well as the ensuing period-1 orbits on the excitation amplitude is described. Discrete breathers (DB) obtained as map homoclinic and heteroclinic orbits are compared with analytic approximations. Simple, soliton-like solutions are identified with sequences of homoclinic or heteroclinic primary intersection points and their analytic approximation is based on the idea that the nonlinearity is taken into account only in the central part of the breather whilst the tails are treated as linear excitations.

Equations of motion

A forced chain of linearly coupled nonlinear oscillators is studied by considering the dynamics governed by the following equation of motion for the generic n -th oscillator

$$\ddot{u}_n + u_n + u_n^3 + c(2u_n - u_{n-1} - u_{n+1}) = A \cos \omega t \quad (1)$$

in which c represents the linear coupling stiffness and the harmonic forcing amplitude and frequency are given by A and ω , respectively. Time periodic solutions of equation (1) are sought for by assuming the harmonic solution $u_n = a_n \cos(\omega t)$. Equating coefficients of $\cos(\omega t)$, thereby assuming 1:1 resonance conditions, gives

$$(1 - \omega^2)a_n + \frac{3}{4}a_n^3 + c(2a_n - a_{n-1} - a_{n+1}) = A \quad (2)$$

Equation (2) describes the motion of a perturbation of the underlying stationary resonant response; by substituting $a_n = \gamma_n + \mu$ and $1 - \omega^2 = \sigma$, equation (2) leads to

$$\sigma(\gamma_n + \mu) + \frac{3}{4}(\gamma_n + \mu)^3 + c(2\gamma_n - \gamma_{n-1} - \gamma_{n+1}) = A \quad (3)$$

The cubic nonlinearity allows to set

$$\sigma\mu + \frac{3}{4}\mu^3 = A \quad (4)$$

Among the real roots μ_i , $i = 1, \dots, 3$ of (4), the ones corresponding to stable solutions are selected and substituted into the map

$$\alpha\gamma_n + \beta(\gamma_n^3 + 3\gamma_n^2\mu + 3\gamma_n\mu^2) + \gamma_{n-1} + \gamma_{n+1} = 0 \quad (5)$$

where $\alpha = -\frac{\sigma}{c} - 2$, $\beta = -\frac{3}{4c}$. As known, the frequency dependent nonlinear map defined by (5) belongs to the class of area preserving maps such that $\det(\mathbf{DT}(\gamma_n, \mu)) = 1$, where \mathbf{DT} is the Jacobian or tangent map with reciprocal eigenvalues [1]. By setting $\gamma_{n+1} = x_{n+1}$ and $\gamma_n = y_{n+1}$ and exploiting the map symmetry lines, the period-1 orbits can also be obtained as $y = \frac{1}{2}x(\alpha + \beta(x^2 + 3x\mu + 3\mu^2))$. As expected, the period-1 orbits coincide with the saddle-node boundaries (blue curves in Figure 1).

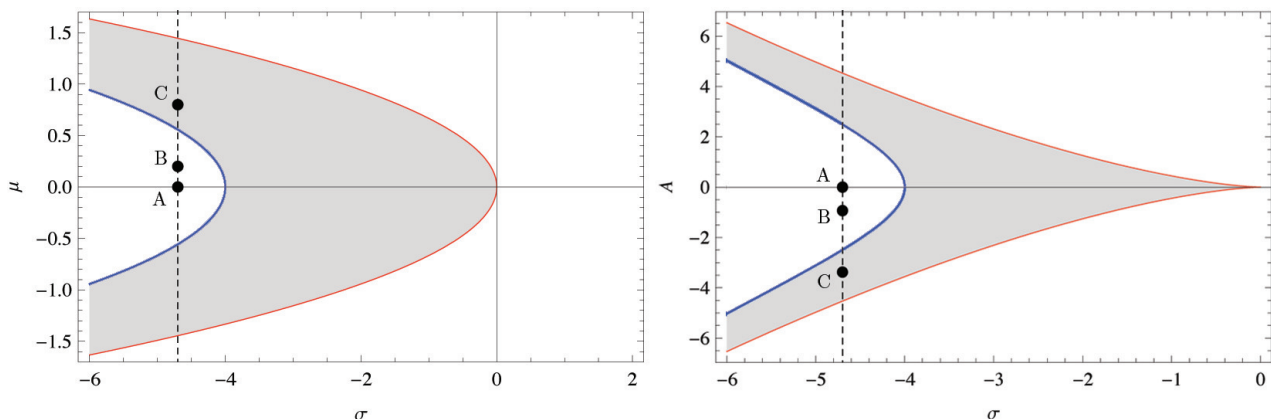


Figure 1: Propagation regions on the $\sigma - \mu$ (left) and $\sigma - A$ (right) planes for $c = 1$.

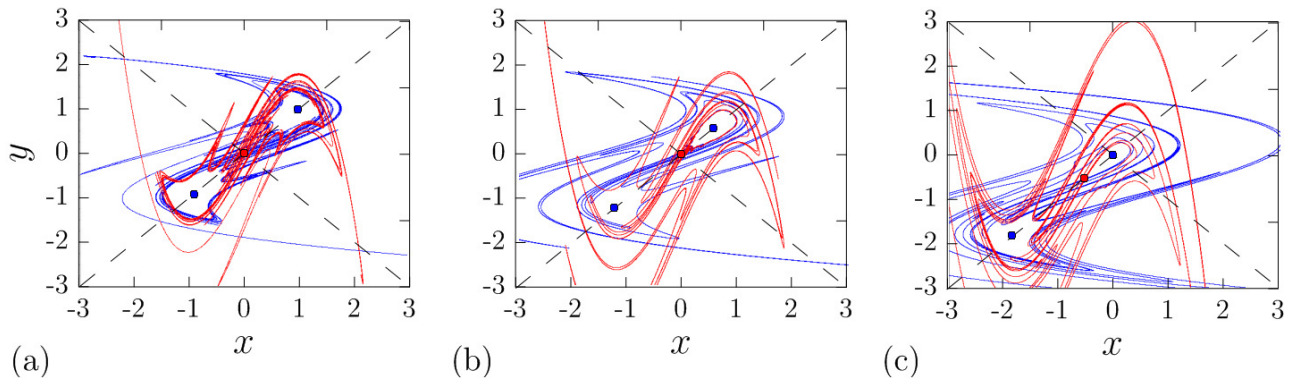


Figure 2: Invariant manifolds scenarios for increasing forcing amplitude level; stable (blue) and unstable (red) manifolds and fixed points for $\sigma = -4.7$: a) $\mu = 0.0$ ($A = 0.0$), point A in Figure 1; b) $\mu = 0.2$ ($A = -0.93$), point B in Figure 1; c) $\mu = 0.8$ ($A = -3.34$), point C in Figure 1.

Nonlinear propagation regions and discrete breathers

By neglecting γ_n , the excitation effect is retained by the map through dependence on μ , therefore the propagation regions boundaries can be easily identified by $|\text{tr}(\mathbf{DT})| = 2$, leading to the nonlinear propagation regions shown on the $\sigma - \mu$ and on the plane $\sigma - A$ planes (Figure 1). Interestingly enough, the dependence on μ (Figure 1, left) of the forced propagation regions coincides with that of the unforced ones with respect to the response amplitude. The presence of the forcing term alters the position of the fixed points along the symmetry line $x = y$. In essence, as the forcing amplitude level increases, the stable fixed points (blue dots in Figure 2) are no longer symmetric with respect to $x = -y$. Therefore for points lying outside the bounded regions (e.g. points A,B in Figure 1), the fixed points $(0, 0)$ are hyperbolic and the invariant manifolds can emanate from them (see Figure 2a,b). Differently, by entering the bounded region (e.g. point C in Figure 1), the fixed points $(0, 0)$ become elliptic and the unstable ones move along the main symmetry line $x = y$ (see Figure 2c). Exact analytical approaches for the analysis of DB are seldom available [2]. In this work, following [3, 1], discrete breathers are identified with sequences of homoclinic intersection points of the mapping (Figure 3a) corresponding to the DB centered in $n = 0$ shown in Figure 3b. Then, the DB map-based analysis is compared with an analytic approach based on a single particle DB approximation (Figure 3c) and harmonic balance method [4]. The prediction of DB existence zone in the space of parameters provided by the two approaches is eventually discussed.

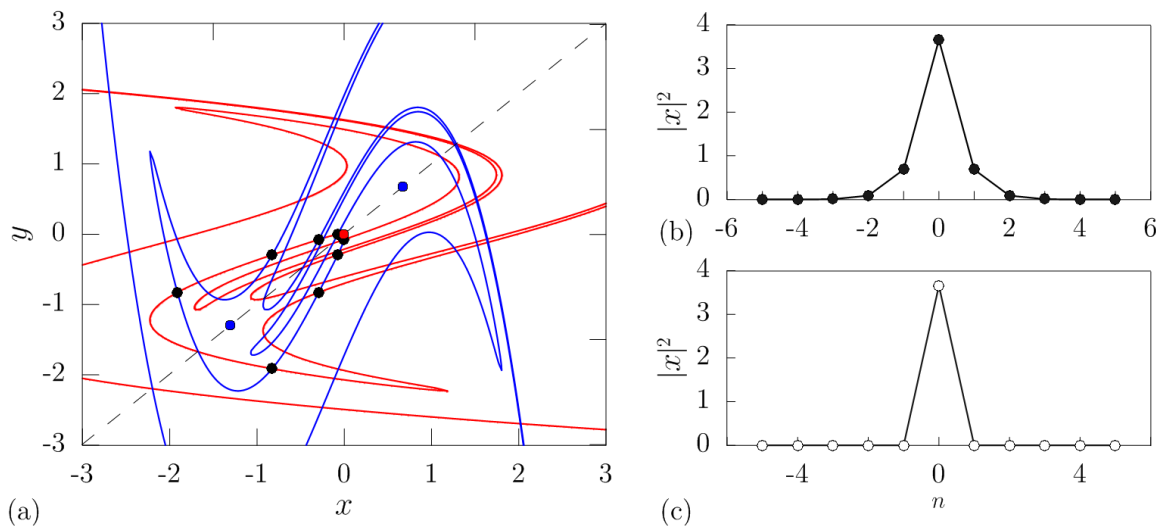


Figure 3: Stable (blue) and unstable (red) manifolds and fixed points for $\sigma = -4.7$, $\mu = 0.2$ and one homoclinic orbit (black); a) global view; b) discrete breather corresponding to the homoclinic orbit of $(0, 0)$; c) single particle discrete breather approximation.

References

- [1] Romeo F, Rega G (2014) Periodic and localized solutions in chains of oscillators with softening or hardening cubic nonlinearity, *Meccanica*, submitted.
- [2] Gendelman O, (2013) Exact solutions for discrete breathers in a forced-damped chain, *Phys. Rev. E*, 87:062911.
- [3] Bountis, T., Capel, H.W., Kollmann, M., Ross, J.C., Bergamin, J.M., van der Weele J.P., (2000) Multibreathers and homoclinic orbits in 1-dimensional nonlinear lattices, *Phys. Lett. A*, 268:50-60.
- [4] Veremkroit M, (2014) Analytic Exploration of Discrete Breathers in a Forced-Damped Klein-Gordon type Chain, Master Thesis, Technion - Israel Institute of Technology.

Microscopic approach to shear localization and plasticity in amorphous solids

O.V.Gendelman

Faculty of Mechanical Engineering, Technion – Israel Institute of Technology

e-mail: ovgend@tx.technion.ac.il

This presentation is devoted to a review of recent achievements in the field of microscopic foundations of plasticity in amorphous solids. It is well – known that traditional approaches based on dislocations and their motion fail in such systems due to the lack of long-range order. As a result, it is very difficult to define unambiguously the structural defects, and even less than that – to figure out any mechanisms for their motion. This difficulty caused many theoretical developments based on phenomenological definitions of local structural defects arising in the process of plastic deformation. Perhaps, most well-known example of such phenomenological concepts is that of shear transfer zones.

I am going to describe recent *ab initio* approach to the problem based on direct study of a potential relief related to the microstructure of the glass. Plastic events are thus identified with changes of the structure of this relief. This somewhat vague definition can be made rigorous by consideration of Hessian matrix of the potential energy as a function of the particle's coordinates. Plastic event may be identified with nullification of one of eigenvalues of this Hessian matrix through saddle-node bifurcation. It can be shown that the eigenfunction corresponding to this eigenvalue is generically localized on relatively small number of particles. Therefore, the idea of appearance of local structural defects is justified; however, the size of these localization zones is essentially larger than standard parameters used in the phenomenological theories.

The basic notion of the structural defect allows consideration of an interaction between the defects, preferable configurations and structural formation. These ideas allow explanation of some macroscopic phenomena, like formation of shear bands, nonlinear elasticity, and some others. In particular, the microscopic consideration allows one to offer the theoretical explanation for observed asymmetry of shear bands orientation for uniaxial tension and compression, and to explain why experimentally observed angle between the shear band and the direction of deformation almost never exceeds 60° . This phenomenon is illustrated in Figure 1.

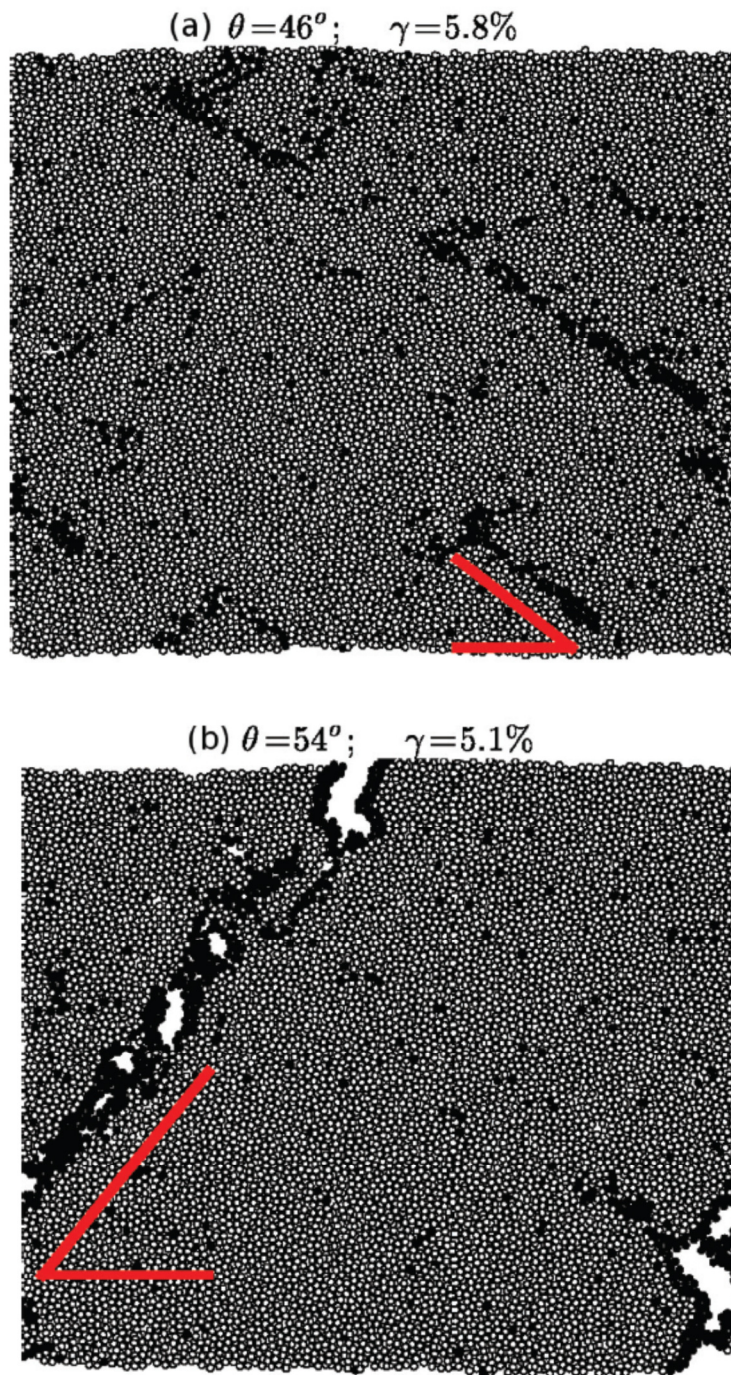


Figure 1. The shear band that occurs in a two-dimensional amorphous solid upon uniaxial (a) compression and (b) extension.

Discrete Breathers in 2D Chains with Vibro-Impact

Itay Grinberg* and Oleg V. Gendelman†

Faculty of Mechanical Engineering, Technion - Israel Institute of Technology, Haifa, Israel

A widely studied topic in recent years is localization in nonlinear discrete lattice or oscillator arrays. Such localization may appear even in perfectly homogeneous systems. It is commonly referred to as Discrete Breathers (DBs), Intrinsic Localized Modes (ILM) or Discrete Solitons in lattices or oscillatory arrays.

The discussed system includes the strongest type of nonlinearity – vibroimpact (VI). It consists of an array of linear chains connected by linear springs where each mass has two barriers bounding its movement such that when interacting there's impact – elastic or inelastic depending on the model. The forced model with inelastic impact is presented in fig. 1.

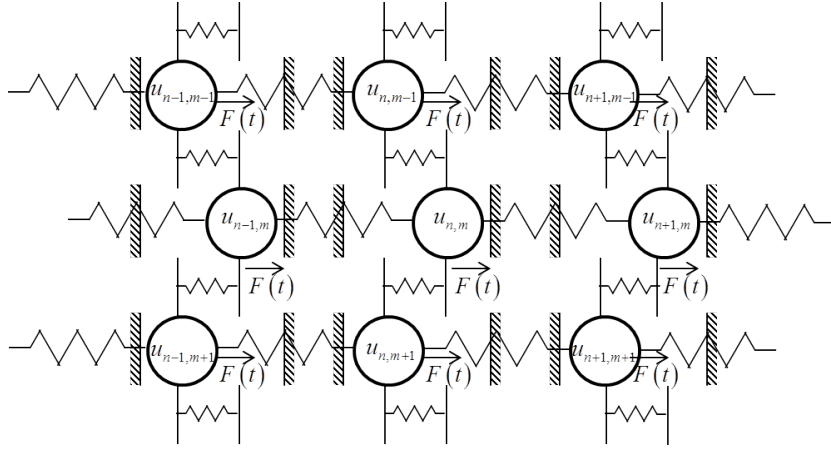


Fig. 1: System schematics.

Based on works by Gendelman and Manevich[2, 3] an exact solution of a symmetric DB is developed for the Hamiltonian model, and more importantly, a forced-damped model. Additionally, the zone of existence is determined and it's stability is examined via Floquet multipliers[4], i.e. eigenvalues of the Monodromy matrix that is described explicitly for an approximate finite system, hence the Floquet multipliers are not extracted numerically from the mapping as is usually the case but are derived directly from the Monodromy matrix. It is important to note that since both models are VI models, producing the Monodromy matrix is not a simple task and must be done separating the linear regime from the instance of the impact where one must use a saltation matrix [1].

The equations of motion for the system in between the impacts is as follows for the forced-damped model:

$$\ddot{v}_{n,m} + k_1 (2v_{n,m} - v_{n-1,m} - v_{n+1,m}) + k_2 (2v_{n,m} - v_{n,m-1} - v_{n,m+1}) = F(t) \quad (1)$$

where $F(t)$ is a periodic anti-symmetric excitation with period 2π , k_1 is stiffness of the linear chain and k_2 is the stiffness of the connection between the chains. Using a simple transformation and seeking a single-site symmetric (which is periodic) the equations of motion can be written as follows:

$$\begin{aligned} \ddot{u}_{n,m} + k_1 (2u_{n,m} - u_{n-1,m} - u_{n+1,m}) + k_2 (2u_{n,m} - u_{n,m-1} - u_{n,m+1}) = \\ = 2p\delta_{m0}\delta_{n0} \sum_{j=-\infty}^{\infty} (\delta((t-\phi) + \pi(2j+1)) - \delta((t-\phi) + 2j\pi)) \end{aligned} \quad (2)$$

Note that after the transformation the equations are conservative and p is the impulse of the impact.

Using an ansatz similar to that used in [2] based on the the fourier transform of the impacts the following solution is derived:

$$v_{n,m} = \sum_{l=0}^{\infty} u_{0,0,l} f^{|n|} g^{|m|} \cos((2l+1)(t-\phi)) + h(t) \quad (3)$$

where $\ddot{h}(t) = F(t)$.

*gitay@technion.ac.il

†ovgend@technion.ac.il

$$\begin{aligned}
f &= \frac{(2k_1 - (2l+1)^2) + (2l+1)\sqrt{(2l+1)^2 - 4k_1}}{2k_1} & g &= \frac{(2k_2 - (2l+1)^2) + (2l+1)\sqrt{(2l+1)^2 - 4k_2}}{2k_2} \\
g &= \frac{(2k_2 - (2l+1)^2) + (2l+1)\sqrt{(2l+1)^2 - 4k_2}}{2k_2} & & \\
u_{0,0,l} &= \frac{4p}{\pi(2l+1)(\sqrt{(2l+1)^2 - 4k_1} + \sqrt{(2l+1)^2 - 4k_2} - (2l+1))} & &
\end{aligned} \tag{4}$$

The parameter p and the function h are then determined via:

$$p\chi + h(\phi) = 1 \quad \dot{h}(\phi) = \frac{1-e}{1+e}p \tag{5}$$

where e is the coefficient of restitution of the impacts and $\chi = \sum_{l=0}^{\infty} \frac{4}{\pi(2l+1)(\sqrt{(2l+1)^2 - 4k_1} + \sqrt{(2l+1)^2 - 4k_2} - (2l+1))}$. Numerical verification on an approximate model is presented in fig. 2.

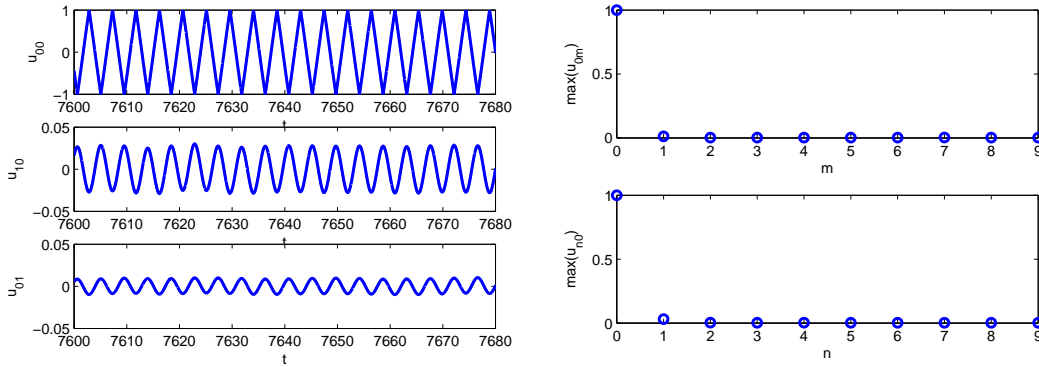


Fig. 2: Displacements and oscillation amplitudes for $k_1 = 0.06$, $k_2 = 0.02$, $a = 0.0001$ and $e = 1 - 10^{-16}$

The stability analysis revealed two mechanisms of loss of stability, one via Neimark-Sacker (Hopf) bifurcation and the later via pitchfork bifurcation which corresponds to appearance of two stable asymmetric DBs in the single chain model[2]. Example of the map of loss of stability is shown in fig. 3 where the upper loss of stability is the pitchfork bifurcation and the lower loss of stability is the Neimark-Sacker bifurcation.

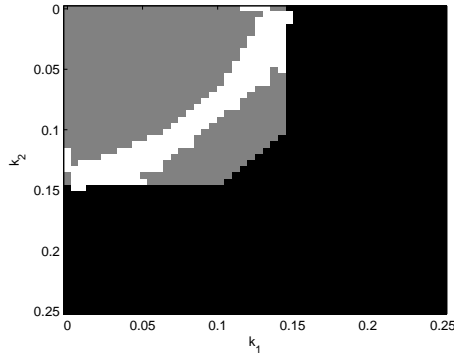


Fig. 3: Stability of the zone of existence for $a = 0.68$, $e = 0.8$. Gray denotes unstable region whereas white is stable.

References

- [1] Mats H Fredriksson and Arne B Nordmark. On normal form calculations in impact oscillators. *Proceedings of the Royal Society of London. Series A: Mathematical, Physical and Engineering Sciences*, 456(1994):315–329, 2000.
- [2] O. V. Gendelman. Exact solutions for discrete breathers in a forced-damped chain. *Phys. Rev. E*, 87:062911, Jun 2013.
- [3] O. V. Gendelman and L. I. Manevitch. Discrete breathers in vibroimpact chains: Analytic solutions. *Phys. Rev. E*, 78:026609, Aug 2008.
- [4] Ali H Nayfeh and Balakumar Balachandran. *Applied nonlinear dynamics*. Wiley. com, 2008.

Equation-Free Computations for Data Driven Studies of Granular Chains

M. O. Williams, D. Pozharskiy, R. W. Hölzel, C. Chong, F. Li,
J. Yang, P. G. Kevrekidis, C. Daraio, and I. G. Kevrekidis

April 4, 2014

Introduction

In many modeling problems, numerical bifurcation studies are an indispensable tool for obtaining a qualitative (and quantitative) understanding of the types of dynamics that arise, and when they can be observed experimentally. To perform such a study, we employ a combination of *numerical continuation* techniques, which locate where a desired type of behavior exists, *linearized stability analysis*, which determines if the resulting solutions persist in the face of perturbations, and *unstable manifold computations*, which provide some guidance on locating the new behaviors that arise when the branch becomes unstable. Furthermore, the knowledge obtained from these components is useful when subsequently conducting “systems level” tasks such as optimization or fixed point stabilization.

One set of solutions where these techniques can be applied are the “dark breather” solutions in an engineered granular chain (EGC). Dark breathers are a subset of “discrete breathers” [1] that have received far less attention than their “bright” counterparts. However, such structures naturally arise in engineered granular chains, which consist of closely packed arrays of particles [2] that interact elastically, and are relevant in numerous applications such as shock and energy absorbing layers [3], acoustic lenses [4], and sound scramblers [5]. Therefore, understanding the dynamics of such breathers is crucial in future applications of EGCs.

For a particular experimentally realized EGC, it is possible to identify an effective set of governing equations [6] that can be used to compute bifurcation diagrams. The purpose of our current work is to develop data driven algorithms and methods that perform the same task by wrapping equation-free algorithms around “black box” numerical simulators (and even, possibly, physical experiments). In this way, we could compute the needed solution branches as well as their stability and bifurcations without the need to develop explicit governing equations.

Experimental and Computational Tools

To perform a data driven bifurcation study, we require two sets of tools: experimental tools that generate data, and computational tools that analyze and exploit it. The experimental tool needed to accomplish this is the physical experiment shown in Fig. 1a, which consists of a 21-bead granular chain with piezoelectric actuators on both ends –to provide the forcing– and a laser Doppler vibrometer to non-intrusively measure the velocity of the beads that comprise the chain. Each bead in the chain is a chrome steel sphere (with radius $R = 9.53$ mm, Young’s modulus $E = 200$ GPa, Poisson ratio $\nu = 0.3$, and mass $M = 28.2$ g). The actuation frequency f_b and amplitude a can be controlled experimentally; typical values of $f_b \in [5, 7.5]$ kHz and $a = 0.2$ μm . In this parameter regime, dark breathers (or multi-breathers) with 1-, 3-, 5- and more spatial dips appear depending upon the precise values of f_b chosen. As a result, the experimental setup enables us to “select” a specific type of dark breather (by tuning the forcing frequency) and *measure* the state of the resulting system. To test our computational tools, we instead work with a “black box” numerical code that has been specifically calibrated to match the physical system described above [6]; the algorithms described below could be just as easily applied to a physical experiment, but this allows us to avoid the non-trivial step of experimentally specifying initial conditions.

The computational tools are a combination of the Equation-Free (EF) paradigm [7] developed by a subset of the present authors and the so called “matrix free” methods, which were originally designed to solve the linear system $\mathbf{A}\vec{x} = \vec{b}$ using only matrix–vector products (i.e., $\mathbf{A}\vec{x}$) rather than obtaining and decomposing the full matrix [8]. These matrix–vector products can also be *estimated* by “probing” the system with judiciously initialized perturbations without the need for explicit governing equations, which makes them ideal for use with black box systems. The three computational tasks that comprise our bifurcation study are

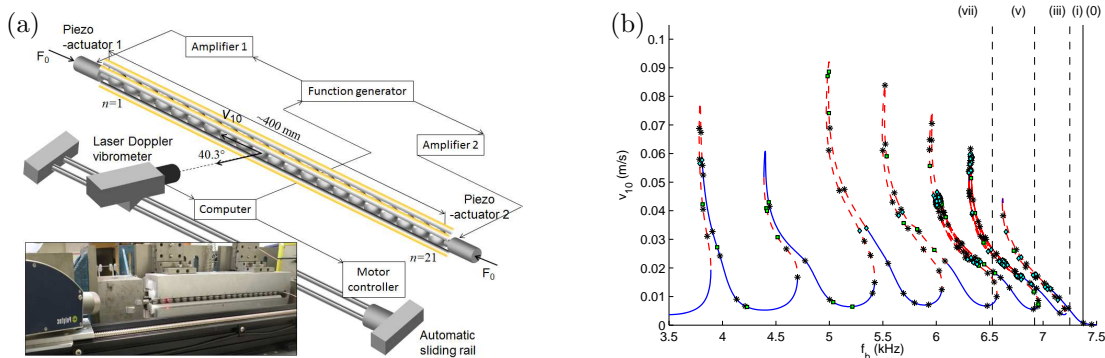


Figure 1: (a) Schematic and photograph of the experimental setup [6]. (b) The bifurcation diagram obtained using the EF framework with matrix-free linear algebra. The blue regions are stable, and the red regions are unstable as defined by Ref. [6]. The markers denote the location of different bifurcation points: cyan diamonds denote pitchfork bifurcations, green squares denote period-doubling bifurcations, and black asterisks denote Neimark–Sacker bifurcations.

accomplished with Newton–GMRES [8], the Implicitly Restarted Arnoldi Method (IRAM) [9], and manifold continuation techniques [10]. Each of these algorithms has been implemented in a matrix-free fashion and is suitable for use in the EF framework.

Results and Conclusions

We generated the bifurcation diagram shown in Fig. 1b using the computational tools described above on our black box systems. This study reveals that this conceptually simple EGC is a true playground for nonlinear dynamics, and contains numerous pitchfork, period-doubling, and Neimark–Sacker bifurcations all on one single, “snaking” branch of solutions. This single solution branch connects the dark-breathers with the n -dip multi-breathers that were observed at lower forcing frequencies, which is in agreement with the “equation aware” study performed in Ref. [6]. Note in that figure, we only plot half the total number of Neimark–Sacker bifurcations to avoid obscuring the main branch.

In addition to the main solution branch, there are numerous secondary branches including branches with higher period, which were generated either by a period-doubling bifurcation or within an Arnold tongue, (temporally) quasi-periodic solutions, which appear as invariant circles on the stroboscopic map and were generated by supercritical Neimark–Sacker bifurcations, and branches that break symmetry and were generated by pitchfork bifurcations. Each of these secondary branches has its own and often complex bifurcation substructure and often generates tertiary branches with yet more complexity. There are even hints of chaotic behavior that can be observed at higher forcing frequencies. A non-exhaustive study of the subsequent tertiary branches shows that they too have a complex structure and additional bifurcations; however, these branches are often only stable for short intervals (if they are stable at all). As such, we conjecture that they will not frequently appear experimentally unless the system is specifically modified to stabilize them.

Ultimately, EF computations with the assistance of matrix-free linear algebra are an effective suite of computational tools for conducting bifurcation studies on “black box” systems, and there is excellent agreement between the bifurcation diagram computed here and the one obtained with AUTO [11]. Although the black box in this example was a numerical code, these methods could in principle be applied to experiments if the *experimental* initial conditions could be specified at will. In addition to their engineering applications, EGCs are valuable as a testbed for new data driven algorithms and procedures because they contain highly nontrivial dynamics and are approachable experimentally. As such, they will be useful in developing new “seamless” algorithms for the EF framework that are more compatible with experiments where the state of the system cannot easily be prescribed in detail.

References

- [1] S. Flach and A. V. Gorbach, “Discrete breathers — advances in theory and applications,” *Physics Reports*, vol. 467, no. 1, pp. 1–116, 2008.
- [2] V. F. Nesterenko, *Dynamics of heterogeneous materials*. Springer, 2001.
- [3] C. Daraio, V. Nesterenko, E. Herbold, and S. Jin, “Energy trapping and shock disintegration in a composite granular medium,” *Phys. Rev. Lett.*, vol. 96, no. 5, p. 058002, 2006.
- [4] A. Spadoni and C. Daraio, “Generation and control of sound bullets with a nonlinear acoustic lens,” *Proceedings of the National Academy of Sciences*, vol. 107, no. 16, pp. 7230–7234, 2010.
- [5] C. Daraio, V. Nesterenko, E. Herbold, and S. Jin, “Strongly nonlinear waves in a chain of Teflon beads,” *Physical Review E*, vol. 72, no. 1, p. 016603, 2005.
- [6] C. Chong, F. Li, J. Yang, M. Williams, I. Kevrekidis, P. Kevrekidis, and C. Daraio, “Damped-driven granular crystals: An ideal playground for dark breathers and multibreathers,” *Phys. Rev. E*, (In press).
- [7] I. G. Kevrekidis, C. W. Gear, J. M. Hyman, P. G. Kevrekidis, O. Runborg, C. Theodoropoulos, *et al.*, “Equation-free, coarse-grained multiscale computation: Enabling microscopic simulators to perform system-level analysis,” *Communications in Mathematical Sciences*, vol. 1, no. 4, pp. 715–762, 2003.
- [8] C. T. Kelley, *Solving nonlinear equations with Newton’s method*, vol. 1. Siam, 2003.
- [9] R. B. Lehoucq, D. C. Sorensen, and C. Yang, *ARPACK users’ guide: solution of large-scale eigenvalue problems with implicitly restarted Arnoldi methods*, vol. 6. Siam, 1998.
- [10] B. Krauskopf and H. Osinga, “Growing 1d and quasi-2d unstable manifolds of maps,” *J. Comput. Phys.*, vol. 146, no. 1, pp. 404–419, 1998.
- [11] E. J. Doedel, “AUTO: A program for the automatic bifurcation analysis of autonomous systems,” *Congr. Numer.*, vol. 30, pp. 265–284, 1981.

Basins of attraction of coupled nonlinear resonators in periodic lattices

Diala Bitar, Najib Kacem and Nouredine Bouhaddi

FEMTO-ST Institute, UMR 6174, Applied Mechanics Department, 24 Chemin de l'Épitaphe, F 25000, Besançon, France

Summary

Collective dynamics in periodic lattices of coupled nonlinear Duffing-Van Der Pol oscillators is modeled and investigated under simultaneous external and parametric resonances. The resonators are coupled with linear and nonlinear springs. Numerical simulations have been performed in the case of two coupled oscillators for which the basins of attraction have been analyzed in the multistability domain in order to check the efficiency of the multimode branches.

Introduction

Interest in the nonlinear dynamics of periodic nonlinear lattices has grown rapidly over the last few years. Actually, it exists a practical need to understand nonlinearities and functionalize them in order to efficiently exploit the collective nonlinear dynamics of smart structures. For instance, Lifshitz et al. [1] investigated the dynamic behavior of an array of N coupled micro-beams using a discrete model. Manktelow et al. [2] focused on the interaction of wave propagation in a cubically nonlinear mono-atomic chain, while Bitar et al. [3] investigated the bifurcation and energy transfers in periodic lattices of coupled nonlinear Duffing-Van Der Pol oscillators under an external excitation. Particularly, the basins of attraction can be used for qualitative as well as quantitative analysis of the collective dynamics robustness. In a nonlinear nanomechanical resonator, Kozinsky et al. [4] experimentally probe the basins of attraction of two fixed points. Moreover, Sliwa et al. [5] investigated the basins of attraction of two coupled Kerr oscillators. Furthermore, Ruzziconi et al. [6] studied frequency response curves, behavior charts and attractor-basins phase portraits of a considered NEMS constituted by an electrically actuated carbon nanotube. In this context, an array of coupled Duffing-Van Der Pol oscillators under simultaneous primary and parametric resonances is developed and the distribution of the basins of attractions is analyzed for multistable solutions including single and multi-modes branches.

Model and basin of attraction analysis

The proposed model presents an array of a finite coupled Duffing-Van Der Pol oscillators, under simultaneous external and parametric excitations. The scaled equation of motion (EOM) governing the behavior of the n^{th} resonator can be written as:

$$\ddot{u}_n + \varepsilon \frac{\omega_0}{Q} \dot{u}_n + \omega_0^2 u_n + \varepsilon h \cos[2(\omega_0 + \varepsilon\Omega)t] u_n + \frac{1}{2} \varepsilon d (-u_{n+1} + 2u_n - u_{n-1}) + \alpha [(u_n - u_{n+1})^3 + (u_n - u_{n-1})^3] + \eta u_n^2 \dot{u}_n = \varepsilon^{\frac{3}{2}} g \cos[(\omega_0 + \varepsilon\Omega)t], \quad (1)$$

where u_n is the displacement of the n^{th} oscillator, with fixed boundary conditions $u_0 = u_{N+1} = 0$, ω_0 and Ω are respectively the natural frequency and the detuning parameter. Q is the quality factor, d represents the linear coupling, α is the cubic spring constant and η represents the Van Der Pol damping coefficient, h and g are parametric and external excitation amplitudes respectively, and ε is a small dimensionless parameter.

The method of multiple time scales was used to solve the coupled EOM analytically. With the expectation that the motion of the resonator far from its equilibrium will be on the order of $\varepsilon^{\frac{1}{2}}$, we try a solution of the form:

$$u_n(t) = \varepsilon^{\frac{1}{2}} \sum_{m=1}^N (A_m(t) \sin(\frac{nm\pi}{N+1}) e^{i\omega_0 t} + c.c.) + \varepsilon^{\frac{3}{2}} u_n^{(1)}(t) + \dots \quad n = 1, \dots, N, \quad (2)$$

where $T = \varepsilon t$ is a slow time variable. The slowly varying amplitudes $A_m(T) = (a_m(T) + ib_m(T)) e^{i\omega_0 t}$ obeys to $2N$ differential equations. In Figure 1, we display the response amplitude of the first oscillator, in function of the detuning parameter of two coupled oscillators, for specific design parameters. Remarkably, there are frequency bands where four stable solutions can exist. The multivaluedness of the response curves due to the nonlinearity has a significance from the physical point of view because it leads to jump phenomena which are localized at the bifurcation points.

The basins of attraction are numerically plotted to investigate the trajectories of the system response and the probability for which the system follows either the resonant or non-resonant, for single or double mode branches. Although, they are usually plotted in the phase plane (u_n, \dot{u}_n) , we chose to represent them in the Nyquist plane. Several numerical integrations of differential equations have been performed for a specific domain of initial conditions, in order to localize the maximum amplitude $|A_1|^2$ in the steady-state domain. As shown in Figure 1, $|A_1|^2$ takes one of four values, depending in the chosen initial conditions which allows for the representation of the corresponding basins of attraction.

Conclusion

The collective nonlinear dynamics of periodic nonlinear lattices was modeled for specific discrete systems of coupled Duffing-VDP oscillators under simultaneous primary and parametric excitations. The case of two coupled oscillators was investigated for a specific design parameters for which, the basins of attraction have been analyzed in the multistability domain for two coupled nonlinear oscillators to quantitatively assess the efficiency and reliability of additional branches

when used in energy harvesting applications.

Acknowledgments

This project has been performed in cooperation with the Labex ACTION program (contract ANR-11-LABX-01-01).

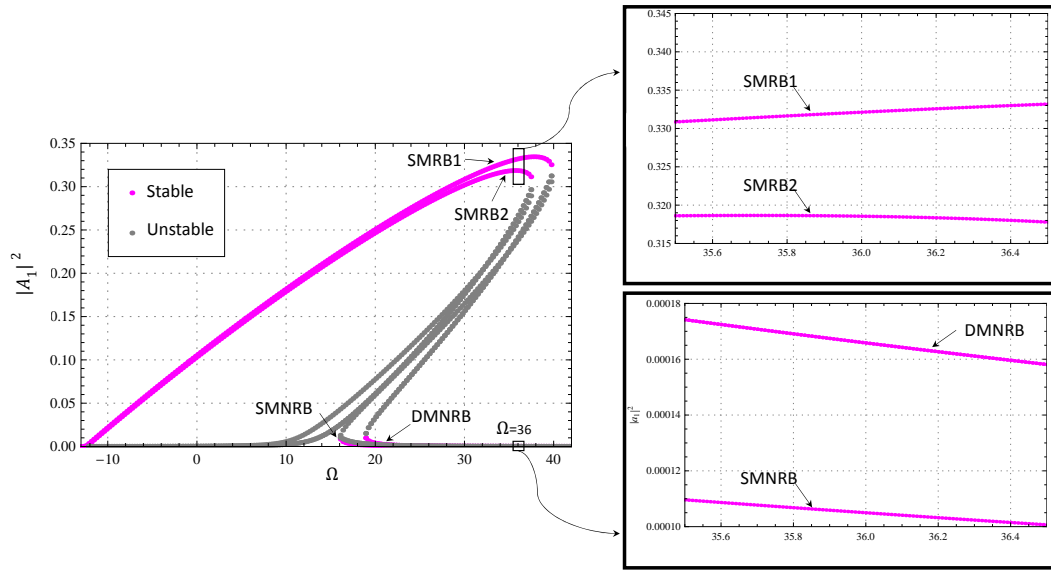


Figure 1: Response intensity as a function of the detuning parameter Ω for the first oscillator, where SMRB1 and SMRB2 are Single Mode Resonant Branches due respectively to primary and parametric resonances, SMNRB and DMNRB are respectively Single and Double Mode Non Resonant Branches.

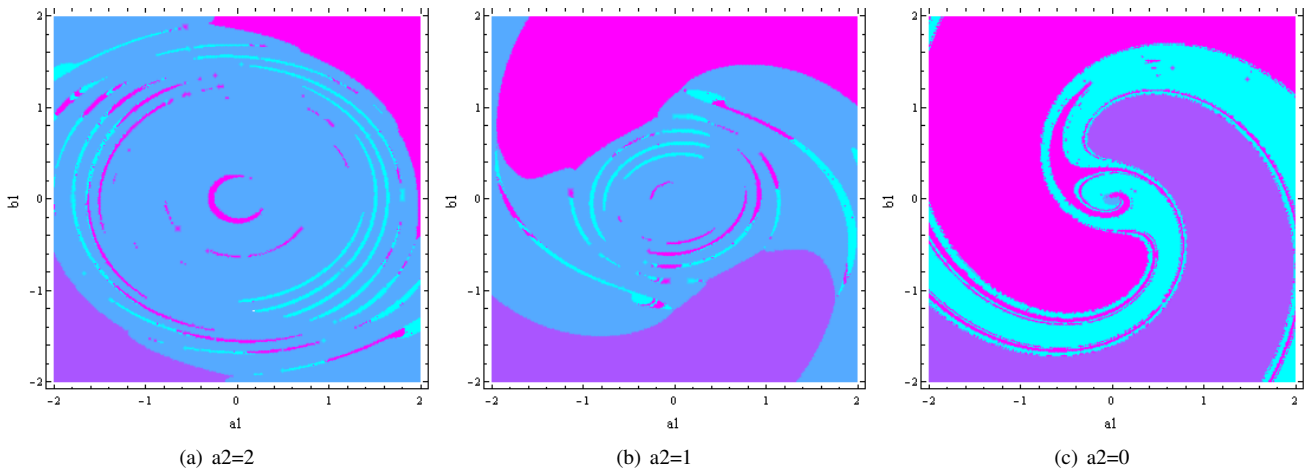


Figure 2: Variation of the basins of attraction in the Nyquist plane (a_1, b_1), with respect to the initial condition a_2 for fixed detuning parameter $\Omega = 36$ and $b_2 = 0$. Magenta, purple, blue and cyan colors indicate respectively SMRB1, SMRB2, SMNRB and DMNRB.

References

[1] R. Lifshitz and M. C. Cross, (2008) Nonlinear dynamics of nanomechanical and micromechanical resonators. *Review of Nonlinear Dynamics and Complexity*, 1:1-52.

[2] K. Manktelow, M. J. Leamy and M. Ruzzene, (2011) Multiple scales analysis of wave interactions in a cubically nonlinear monoatomic chain. *Nonlinear Dyn.* **63**:193-203.

[3] D. Bitar, N. Kacem, N. Bouhaddi and M. Collet, (2014) Energy transfer in externally driven periodic nonlinear structures. ENOC 2014, July 6-11, 2014, Vienna, Austria.

[4] I. Kozinsky, H. W. Ch. Postma, O. Kogan, A. Husain and M. L. Roukes, (2007) Basins of attraction of a nonlinear nanomechanical resonator. *Phys. Rev. Lett.*, **99** 207201.

[5] I. Śliwa, K. Grygiel, (2012) Periodic orbits, basins of attraction and chaotic beats in two coupled Kerr oscillators. *Nonlinear Dyn.* **67**:755-765.

[6] L. Ruzziconi, M. I. Younis, S. Lenci, (2013) Multistability in an electrically actuated carbon nanotube a dynamical integrity perspective. *Nonlinear Dyn.* **74**:533-549.

Modal analysis of nonlinear dissipative systems: Application to vibration damping with shape memory materials

Malte Krack^{1,*}, Lars Panning-von Scheidt¹ and Jörg Wallaschek¹

¹ University of Hannover, Appelstr. 11, 30167 Hannover, Germany, www.ids.uni-hannover.de

* presenting author, krack@ids.uni-hannover.de

Keywords: *Nonlinear Normal Modes, nonlinear dynamics, shape memory effect, reduced order modeling, design.*

The concept of nonlinear modes is well-known for its ability to extract the energy-dependent vibration signature of nonlinear dynamical systems in terms of natural frequencies and vibration deflection shapes. Modal analysis also facilitates the qualitative understanding of nonlinear phenomena such as the localization of vibration energy, the change of stability of modes and internal resonances at high energies. It can generally be stated that in contrast to the linear case, modal analysis is far less established in the nonlinear case. An important reason for this is possibly that most approaches are strictly limited in their scope of applicability. In particular, fundamental research in the field of nonlinear modes focused primarily on conservative systems with low-order polynomial nonlinearities. This clearly limits their usefulness to investigate (dissipative) vibration control mechanisms and strongly nonlinear or even non-smooth forces induced e.g. by contact interactions and phase transformations.

The presented method is based on the periodic motion conception of nonlinear modes [2]. An artificial mass-proportional damping term is introduced in order to compensate the non-conservative forces and thus to make the motion periodic. Conventional methods such as the shooting and the harmonic balance method can be utilized for the direct computation of the energy-dependent natural frequency, modal damping ratio and the vibration deflection shape. The treatment of quite generic nonlinear, including non-smooth forces is therefore straight-forward. The method is currently limited to the investigation of isolated resonances, i. e. to the dynamic regime where internal resonances are absent.

The capabilities of the approach are demonstrated for a mechanical system with SMM attachments [1], cf. figure 1. The dissipative character of the shape memory effect is described by a piecewise linear hysteresis. The proposed method is employed for the assessment of the vibration damping performance of the assembly. The amplitude-dependent natural frequency and modal damping ratio of the considered system are illustrated in figure 2. In contrast to alternative methods for damping assessment, the proposed approach explicitly accounts for the variation of the vibration deflection shape with amplitude and the possible multi-harmonic vibration content, which generally leads to an improved

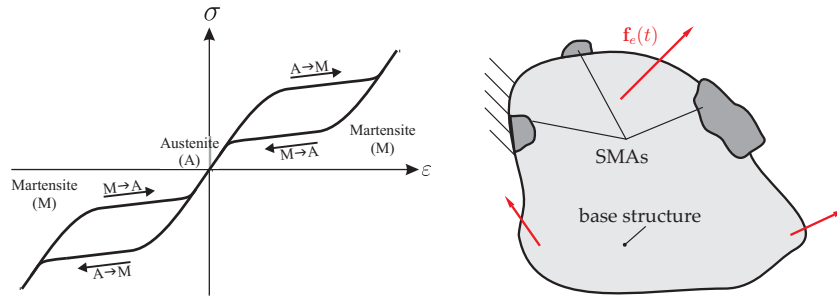


Figure 1: Passive vibration damping using shape memory materials (SMMs) (a) pseudoelastic stress-strain behavior, (b) schematic setup of base structure with SMM attachments

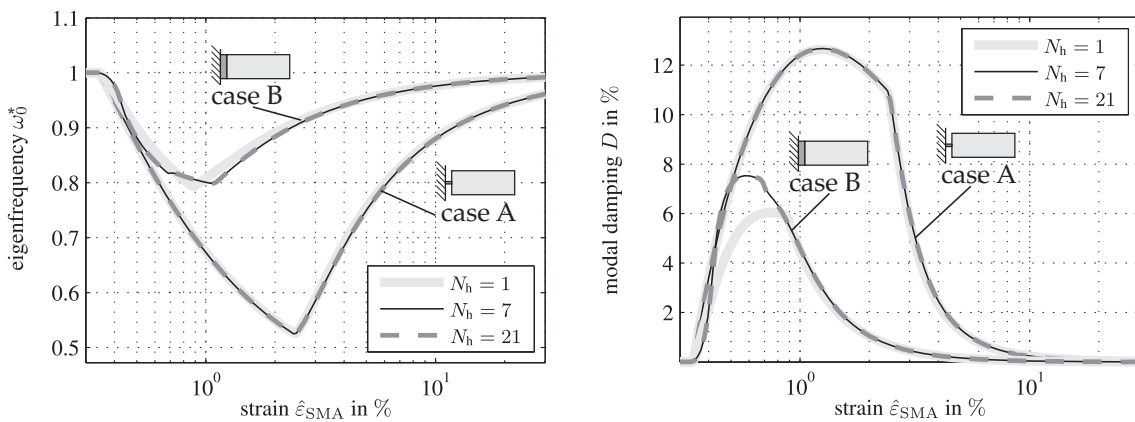


Figure 2: Modal properties of the first axial vibration mode of a rod with SMM attachment for two different radii of the SMM section ((a) natural frequency, (b) modal damping ratio)

accuracy of the results. If one is interested in reducing near-resonant vibrations, the proposed computational method gives directly rise to relevant measures that characterize the autonomous vibration behavior of structures damped with SMMs. These modal characteristics can also be utilized to predict the vibration behavior under various operation conditions (model reduction) [2, 3]. The approach is therefore regarded as particularly useful for the design of nonlinear vibration control mechanisms.

REFERENCES

- [1] M. Krack and J. Boettcher. A Method for the Computational Assessment of the Damping Performance of Shape Memory Alloys. *Smart Materials and Structures*, 2014, (under review).
- [2] M. Krack, L. Panning-von Scheidt, and J. Wallaschek. A method for nonlinear modal analysis and synthesis: Application to harmonically forced and self-excited mechanical systems. *Journal of Sound and Vibration*, 332(25):6798–6814, 2013.
- [3] M. Krack, L. Panning-von Scheidt, and J. Wallaschek. On the computation of the slow dynamics of nonlinear modes of mechanical systems. *Mechanical Systems and Signal Processing*, 42(1-2):71–87, 2014.

Delayed Feedback Control of Nonlinear Surge Response of Multi-point Mooring System under Harmonic Waves

A K Banik & R K Mitra, National Institute of Technology Durgapur, WB, India 713209

Extended Abstract

The complex behaviour of nonlinear system such as periodic, aperiodic and chaotic solutions is generally dealt with active vibration control based on time delayed feedback control. The delay in the feedback control is expected for several reasons or sometimes introduced intentionally for obtaining desired performance of nonlinear dynamical systems. Generally, the presence of delay either natural or intentional results in the more complex behaviour of the dynamic system. The classical control theory limited to linear system cannot be applied for the time delay control of nonlinear system which is essentially in the form of nonlinear delay differential equations.

In the recent past, time-delayed feedback control has been successfully used to control vibrations and stability of various linear and nonlinear systems using various analytical, semi-analytical and numerical methods. Application of these techniques cover a wide range of problems including standard problem of van-der-Pol Oscillator, Duffing Oscillator, Mathieu's Equation etc. The present study is motivated by the need for a better semi-analytical prediction of complex periodic (ultra-subharmonic) via incremental harmonic balance method (IHB), as previous theoretical analysis focused on weakly nonlinear regimes (via both multiple-scales asymptotic (1, 2, 3, 4, 5, 6, 7) and a straight forward harmonic balance analysis (8). This apart, these methods are mostly suitable for systems with small amplitude of excitation. On the other hand, numerical integration techniques are able to solve strongly nonlinear problems and gives both transient and steady-state responses for given initial conditions. There are some distinct drawbacks of these methods. It is highly expensive for stiff equations and longer period responses. Also, point-to-point integration makes it inefficient for parametric studies. Further, NI cannot generally capture unstable solutions, which are necessary for better understanding of the system behaviour, particularly the bifurcation behaviour of the nonlinear system. If the system or the feedback control law (which will be developed and introduced in the feedback path) is strongly non-linear, the method of incremental harmonic balance along with continuation technique, a systematic computer method seems to be useful (9, 10 & 11). Therefore, in the present study, a comprehensive numerical schemes based on IHBC is developed to analyze all possible stationary resonances of nonlinear dynamical systems under non-linear time-delayed feedback.

With this back ground, time delay feedback control of nonlinear surge response behaviour of multipoint mooring system under harmonic wave is investigated by incremental harmonic balance method along with continuation technique (IHBC). The two-point mooring system has fairly strong

stiffness nonlinearity and is, therefore, expected to show fundamental and subharmonic resonances. The nonlinearity of the restoring force is represented by a cubic polynomial and the forcing function on the mooring system is idealized as monoharmonic excitation. The period-one as well as the subharmonic solutions obtained by the incremental harmonic balance IHB method are compared with the solutions obtained by the numerical integration of the equation of motion.

The objective of this paper is to study the amenability of IHBC Technique for analysis of time delay feedback control of two point mooring system and study its efficiency in obtaining suppression of various fundamental and subharmonic resonances present in the strongly nonlinear multi point mooring system with delayed feedback. Appreciable reductions in the peak of resonance curves obtained with appropriate choices of the feedback gains and the time-delay from the viewpoint of vibration control are also discussed. The control of complex nonlinear responses such as periodic, aperiodic and chaotic responses present in the strongly nonlinear dynamical system is successfully investigated.

References

1. Hu, H., Dowell, E. H. and Virgin, L. N., 1998, "Resonances of a Harmonically Forced Duffing Oscillator with Time Delay State Feedback", *Non-linear Dynamics*, 15 pp. 311-327.
2. Ueda, Y., 1991, "Survey of regular and chaotic phenomena in the forced Duffing oscillator", *Chaos, Solitons Fractals* 1, pp. 199-231.
3. El-Bassiouny, A F, and El-kholy, S., 2009, "Resonances of a non-linear SDOF system with time-delay in linear feedback control", *PhysicaScripta*, 81 no. 1.
4. Ji, J. C. and Leung, A. Y. T., 2002, "Resonances of a non-linear s.d.o.f. system with two time-delays in linear feedback control", *Journal of Sound and Vibration*, 253, pp. 985-1000.
5. Zhao, Y. and Xu, J., 2007, "Effects of delayed feedback control on non-linear vibration absorber system", *Journal of Sound and Vibration*, 308 pp. 212-230.
6. Alhazza, K A., Daqaq, M. F., Nayfeh, A H., and Inman, D J., 2008, "Non-linear Vibrations of Parametrically-Excited Cantilever Beams subjected to Non-linear Delayed-Feedback Control", *International Journal of Non-Linear Mechanics*, 43 pp.801-812.
7. Li, X., Ji, J. C., Hansen, C H. and Tan, C., 2006, "The response of a Duffing-van der Pol oscillator under delayed feedback control", *Journal of Sound and Vibration*, 291 pp. 644-655.
8. Liu, L. and Nagy, T., 2010, "High-dimensional Harmonic Balance Analysis for Second-order Delay-differential Equations" ,*Journal of Vibration and Control* 00(0): 1-20.

9. Banik, A. K., and Datta, T. K., 2008, "Stability Analysis of an Articulated Loading Platform in Regular Sea," *ASME J. Comput. Nonlinear Dyn.*, 3 (1), p. 011013.
10. Banik, A. K., and Datta, T. K., 2009, "Stability Analysis of TLP Tethers Under Vortex-Induced Oscillations," *ASME J. Offshore Mech. Arct. Eng.*, 131(1), pp. 011601.

Experimental Study of Acoustic Bands and Propagating Breathers in Ordered Granular Media Embedded in Matrix

M. Arif Hasan¹, Shinhu Cho¹, Kevin Remick¹, D. Michael McFarland²,
Waltraud Kriven³, Alexander F. Vakakis¹

¹*Department of Mechanical Science and Engineering*

²*Department of Aerospace Engineering*

³*Department of Materials Science and Engineering*

*University of Illinois at Urbana – Champaign
Urbana, IL 61801*

We study experimentally pass and stop-bands, and propagating breathers in ordered granular chains composed of steel beads embedded in elastic matrix, subject to single point harmonic excitation [1]. We consider three different matrix materials with varying stiffness and damping properties: PDMS, polyurethane and geopolymer. Moreover, we experimentally test single and coupled granular chains over varying frequency and amplitude ranges. In all cases we experimentally prove the existence of low-frequency acoustic pass-bands where the embedded granular chains exhibit strongly nonlinear dynamics. In this case the applied harmonic excitation generates discrete pulses in the granular metamaterial due to negligible effective compression. In these low-frequency regimes the granular interactions in the time series of the transmitted pulses can be clearly identified. These pulses are highly tunable with frequency and force intensity. At high-frequencies stop-bands are realized, characterized by strongly localized standing waves in the acoustic metamaterial. In this case the granular medium is strongly compressed and its response is almost linear. This leads to complete elimination (filtering) of transmitted waves, and the embedded granular medium oscillates as a low-dimensional system of spring-mass coupled oscillators. Such strongly attenuating dynamic response is important in applications where shock isolation is desired. The more interesting dynamic regime is realized at intermediate frequency ranges. In these ranges we conclusively prove the propagation of breathers in the embedded granular chains. These are oscillatory wavetrains with localized envelopes, and can be robustly and predictably excited in all three granular metamaterials tested in our study. We investigate the effects of matrix properties and of the distance between coupled granular chains on the propagation of these breathers, and study energy exchanges between coupled embedded chains in this strongly nonlinear regime. To our knowledge this is the first experimental demonstration of propagating breathers in a practical, highly nonlinear acoustic granular metamaterial. Applications of these results will be discussed.

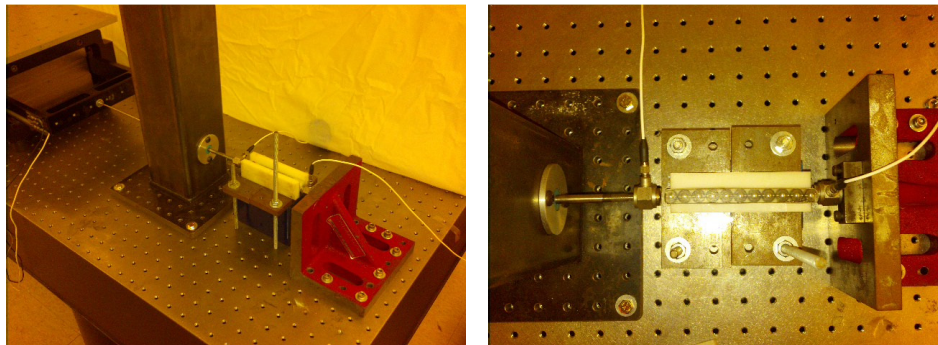


Figure 1. Experimental fixture

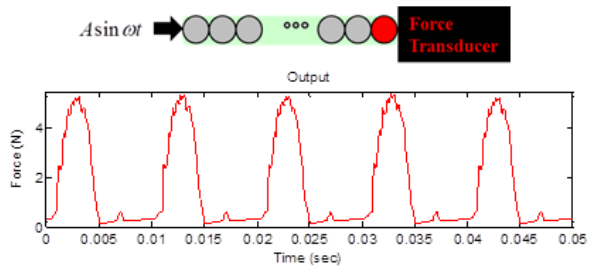


Figure 2. Pass band dynamics in a single granular chain of 11 steel beads embedded in PDMS matrix under relatively high amplitude excitation at 100 Hz: Force transmitted at the end of the chain.

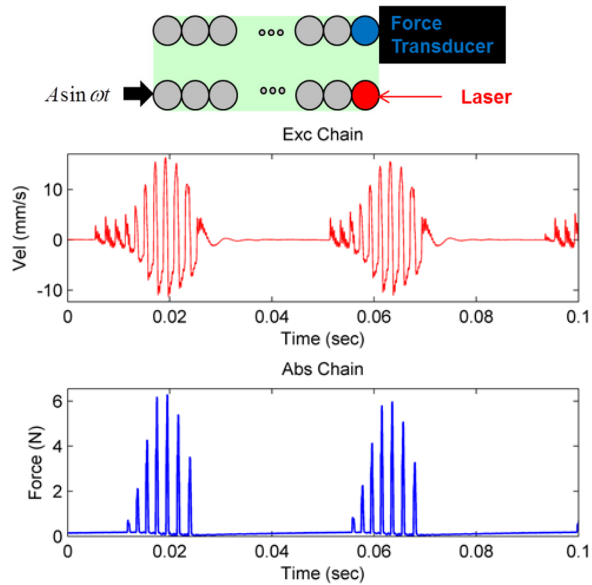


Figure 3. Propagating breathers two coupled granular chains of 11 steel beads embedded in polyurethane matrix at 500 Hz: Velocity of the last bead of the excited chain and force transmitted at the end of the unexcited chain.

References

[1] M.A. Hasan, K. Remick, S. Cho, A.F. Vakakis, D.M. McFarland, W.M. Kriven, ‘Acoustic Bands and Propagating Breathers in Ordered Granular Media Embedded-in-Matrix’ (under review).

5th Conference on Nonlinear Vibrations, Localization and Energy Transfer
Istanbul, Turkey, July 2–4, 2014

SESSION 4

Estimation of nonlinear frequency response for a system with backlash nonlinearity using multi-term harmonic balance method

Osman Taha Sen, Research Associate, senos@itu.edu.tr, Department of Mechanical Engineering, Istanbul Technical University, Istanbul, 34437, Turkey

Rajendra Singh, Professor, singh.3@osu.edu, Department of Mechanical and Aerospace Engineering, The Ohio State University, Columbus, OH, 43210, USA

Most real-life structures include inherent nonlinearities, and their responses (such as unstable motions, limit cycles, bifurcations and chaotic motions) are of significant interest to researchers. The harmonic balance method is a powerful tool to approximate the dynamic response in a more tractable form since it converts the nonlinear ordinary differential equations into a set of manageable nonlinear algebraic equations.

The goal of this study is to apply the multi-term harmonic balance method to a mechanical oscillator with clearance nonlinearity as depicted in Fig. 1. As shown in Fig. 1, a mass m moves with $x(t)$ due to the external excitation force $F(t)$, and two sets of elastic (k) and dissipative (c) elements are located on both sides of m with a backlash (clearance) of b . Elements of gear rattle in vehicles can be simulated using this model. The chief objective of the current study is to estimate the nonlinear frequency responses using the multi-term harmonic balance method.

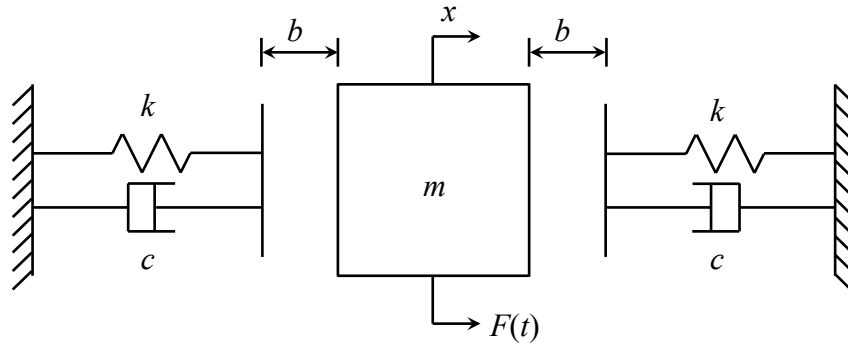


Figure 1. Single degree of freedom model with clearance nonlinearity.

The governing equation of the system of Fig. 1 is given with $g(x, \dot{x})$ and $h(x)$ as dissipative and elastic functions, respectively,

$$m\ddot{x} + cg(x, \dot{x}) + kh(x) = F(t). \quad (1)$$

The piecewise linear functions are described as:

$$g(x, \dot{x}) = \begin{cases} \dot{x} \\ 0 \\ \dot{x} \end{cases} ; \quad h(x) = \begin{cases} x - b & x > b \\ 0 & -b \leq x \leq b \\ x + b & x < -b \end{cases} . \quad (2a, b)$$

The excitation force $F(t)$ is assumed to be periodic of order M with a constant mean value, i.e. $F(t) = F_0 + \sum_{m=1}^M F_m \sin(m\omega t)$. For the multi-term harmonic balance solution, Eq. (1) is first transformed from t domain to spatial θ domain by assuming $\theta = \omega t$ with $\theta \in [0, 2\pi)$. Second, the Fourier series expansion is assumed for the solution of Eq. (1), as: $x(\theta) = a_0 + \sum_{n=1}^{\infty} a_{2n-1} \sin(n\theta) + a_{2n} \cos(n\theta)$. Third,

the discrete Fourier transform operator (Γ) and differential operator (D) are defined, and the nonlinear elastic and dissipative functions along with $x(\theta)$ are discretized as $g(x, x') = \Gamma\gamma$, $h(x) = \Gamma\eta$ and $x(\theta) = \Gamma a$, where $(\cdot)' = d(\cdot)/d(\theta)$. Finally Eq. (1) is rewritten as follows.

$$m\omega^2\Gamma D^2 a + c\omega\Gamma\gamma + k\Gamma\eta = \Gamma Q. \quad (3)$$

Equation (3) can now be transformed to the frequency domain by pre-multiplying it with the pseudo-inverse of Γ ($\Gamma^+ = (\Gamma^T \Gamma)^{-1} \Gamma^T$), and the residue equation is defined as:

$$R = m\omega^2 D^2 a + c\omega\gamma + k\eta - Q. \quad (4)$$

Equation (4) represents a set of nonlinear algebraic equations; therefore it is iteratively solved using the Newton-Raphson method. In the solution, the pseudo arc-length continuation method is also applied in order to successfully track the nonlinear frequency response curve, especially in the vicinity of turning points [1, 2]. The calculated nonlinear frequency response curve is shown in Fig. 2 in terms of the maximum normalized \bar{x} amplitudes, where $\bar{x} = x/b$. First, observe multiple peaks due to the multiple orders in $F(t)$. Peaks are well separated at the higher frequency range; however, they are closer in the lower frequency range. Second, higher orders of $F(t)$ do not excite the nonlinearity due to their lower amplitudes, hence the response is linear in the lower frequency region. The bending of the resonant peaks is clearly seen at first and second orders. This demonstrates the amplitude dependent response of a nonlinear system.

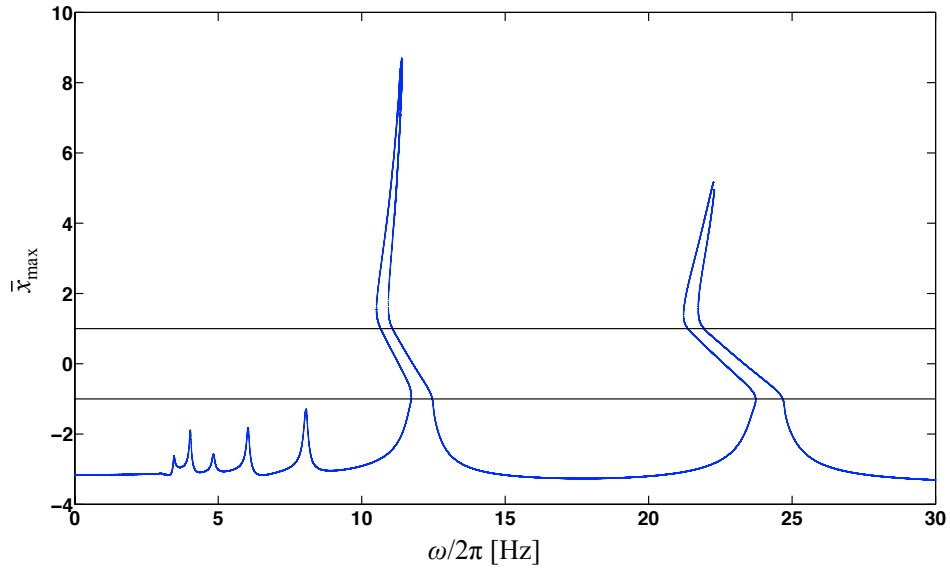


Figure 2. Nonlinear frequency response of the model of Fig. 1.

In order to better observe the interactions between adjacent peaks, the DC value of the $F(t)$ (F_0) is halved and the calculated nonlinear frequency response, in the lower frequency regime only, is displayed in Figure 3. An isolated branch emerges over the lower frequency range, which is away from the peaks of Fig. 2. It is believed that this branching is due to interactions between adjacent orders. Furthermore, the frequency response curve follows an interesting path as shown in the zoomed view of Fig. 3.

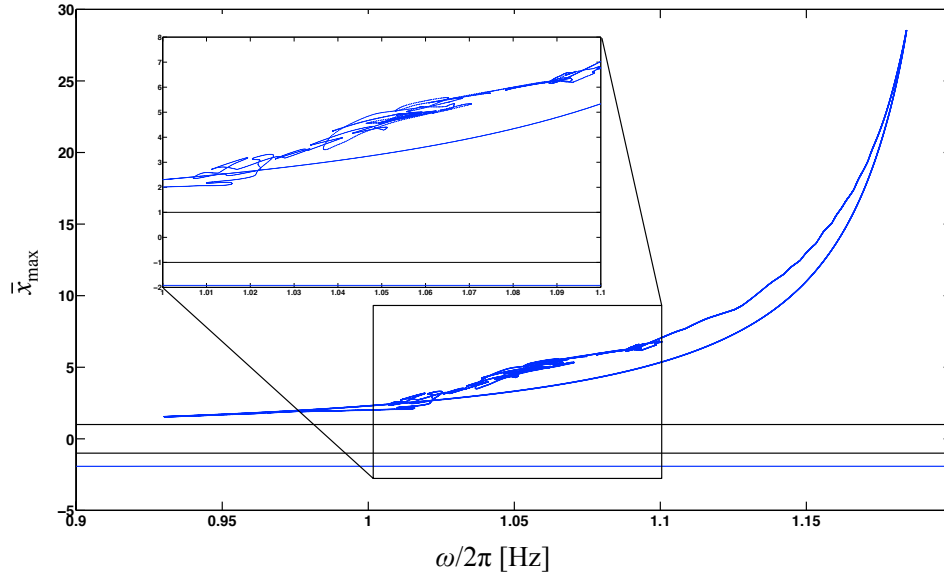


Figure 3. Isolated branch over lower frequency region.

In summary, this study examines the application of multi-term harmonic balance method for a system with backlash nonlinearity. It is shown that even a single degree of freedom system with a discontinuous nonlinearity can exhibit a wide class of dynamic responses. Furthermore, the stability of the solutions is also checked using the Hill's method [1-3]. In addition, the method is utilized to track and identify the bifurcations, though such results are not included in the text due to page limitations.

References

- [1] O.T. Sen, J.T. Dreyer, R. Singh, Envelope and order domain analyses of a nonlinear torsional system decelerating under multiple order frictional torque, *Mechanical Systems and Signal Processing* 35(2013) 324-344.
- [2] A. H. Nayfeh, B. Balachandran, *Applied Nonlinear Dynamics: Analytical, Computational, and Experimental Methods*, John Wiley & Sons, 1995.
- [3] T. Detroux, L. Renson, G. Kerschen, The harmonic balance method for advanced analysis and design of nonlinear mechanical systems, *IMAC XXXII Conference and Exposition on Structural Dynamics*, 3-6 Feb. 2014, Orlando, USA.

Parameter identification of a nonlinear beam with hardening behavior using Volterra series

Sidney B. Shiki, *sbshiki@gmail.com*, Cristian Hansen, *engcristianhansen@gmail.com*, Samuel da Silva, *samuel@dem.feis.unesp.br*

UNESP - Univ Estadual Paulista, Faculdade de Engenharia de Ilha Solteira, Departamento de Engenharia Mecânica, Av. Brasil 56, 15385-000, Ilha Solteira, SP, Brasil

1 Contributions of the paper

Linear parameter identification in structural dynamics is an already well-developed topic and is fundamentally based on modal parameters [1]. However, the nonlinear counterpart is still not consolidated since these features are not valid for nonlinear systems in a way that classical linear techniques can drastically fail to identify representative models [2].

An interesting technique to treat nonlinearities is the Volterra series since it is a generalization of the linear convolution [3]. In this model the linear part of the response of the system is represented with the first Volterra kernel (i.e impulse response function), while the nonlinear part is represented by the higher-order kernels. Many papers have already applied the continuous-time version of this technique however it is very limited to cases where the motion equation is known [4]. Recent investigations have been focused on discrete-time representation and the estimation of Volterra kernels using only the input/output time-series [5, 6] In this work, the discrete-time version of this tool is applied to identify nonlinear parameters in a clamped beam subjected to an axial preload which exhibits hardening stiffness nonlinearity.

2 Application in a buckled beam

The experimental setup was composed by a clamped aluminum beam with $460 \times 18 \times 2$ mm excited by a shaker placed 65 mm from the clamped end and with the velocity measured by a laser vibrometer in the center of the beam (Figure 1).

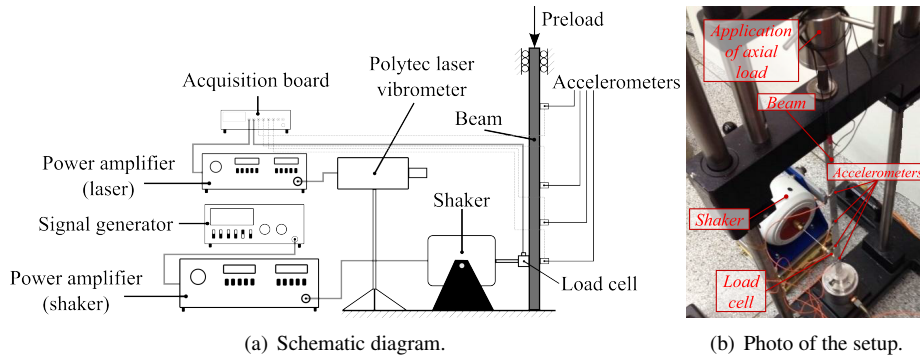


Figure 1: Experimental setup.

A chirp input sweeping frequencies around the first mode (20 to 50 Hz) in three different magnitudes (0.01, 0.05 and 0.10 V) was used to identify the Volterra kernels \mathcal{H}_η . Since third-order harmonics and hardening behavior was observed in the response of the system, a model considering until the $\eta = 3$ kernel was identified which can be represented by [3]:

$$y(k) = \sum_{m=1}^{\eta} \left[\sum_{n_1=0}^{N_1} \dots \sum_{n_\eta=0}^{N_\eta} \mathcal{H}_\eta(n_1, \dots, n_\eta) \prod_{i=1}^{\eta} u(k - n_i) \right] \quad (1)$$

where N_1, \dots, N_η is the memory length of the η -th kernel, $y(k)$ is the output signal and $u(k)$ is the input signal. Since the model is linear in the parameters a least-squares approximation can be used to estimate the first three kernels for this problem. With the reference kernels representing the structure, the deviation between the experimental kernels with the ones identified with the integration of the motion equation can be used as a metric to update the parameters of the model.

Using the lowest input amplitude, the linear part of the motion equation was estimated (mass m , damping ratio ζ and stiffness k) using the proposed metric considering only the first kernel. The higher amplitudes were then used to compute the nonlinear cubic stiffness that describes the hardening behavior of the system. The values obtained mapping the objective function were: $m = 0.082$ kg, $k = 4130$ N/m, while $k_3 = 1.73 \times 10^8$ N/m³ for the highest level of input amplitude. The damping ratio however showed to significantly vary with the magnitude of excitation obtaining $\zeta = [0.016, 0.033, 0.047]$ for a growing level of chirp input which may indicate some nonlinear behavior in the damping as well. The performance of the identified oscillator with the estimated parameters is depicted in the Figures 2 and 3 which shows the FRF and the stepped sine frequency response respectively comparing the experimental and the model response. The model showed to reproduce the hardening behavior and also the jump phenomenon, however some discrepancy can be found in this last response since force drop-out is inevitable in the experimental test.

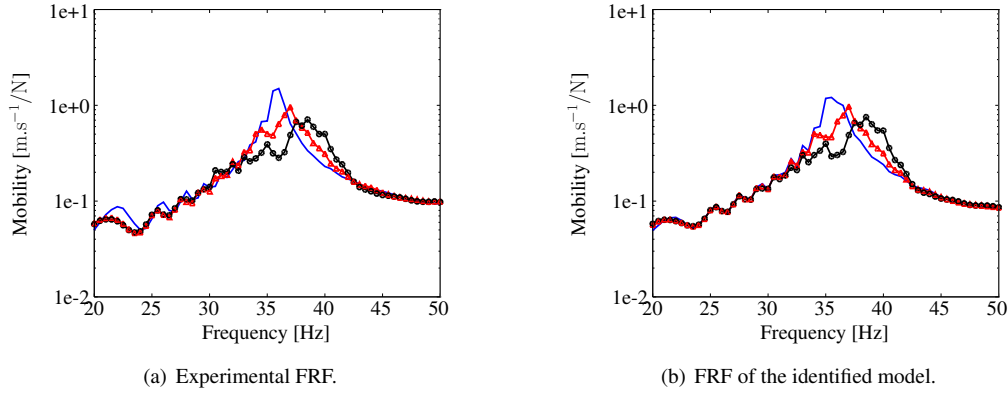


Figure 2: Comparison between the experimental and the model FRFs. The continuous line is the low input (0.01 V), \triangle is the medium input (0.05 V) and \circ is the high input (0.10 V)

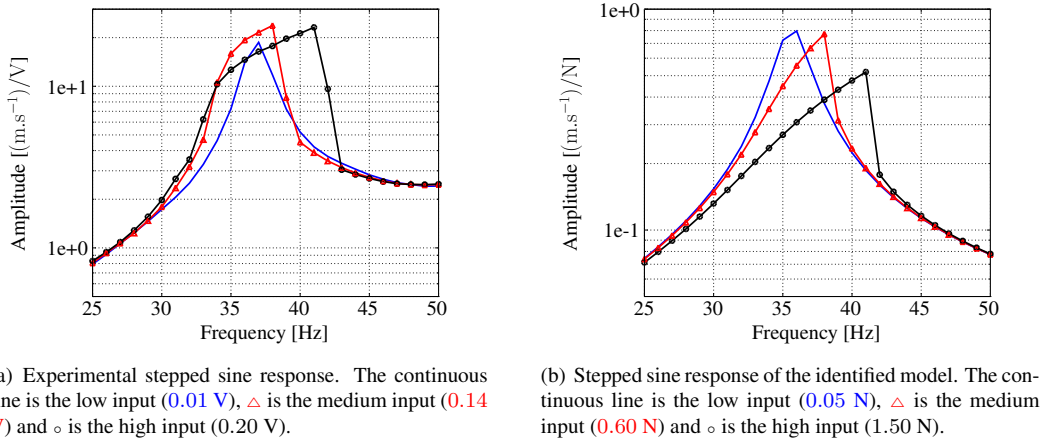


Figure 3: Comparison between the experimental and the model stepped sine responses.

3 Final remarks

This paper applies the Volterra model to identify parameters of the motion equation. This is a powerful tool since it separates the linear and nonlinear responses with a generalization of the linear convolution. In this way, the linear and nonlinear inverse problems can be treated in a separated way. This allows to apply other classical metrics for the identification of linear parameters and then employ Volterra series to treat the nonlinear part of the system. The FRF and stepped sine response of the identified oscillator showed to reproduce similar behavior to the experimental system.

4 Acknowledgments

The authors acknowledge the financial support provided by FAPESP (grant numbers 13/25148-0, 13/09008-4, 12/09135-3), CNPq (grant number 470582/2012-0) and INCT-EIE.

References

- [1] G. Kerschen, K. Worden, A. F. Vakakis, and J. C. Golinval. Past, present and future of nonlinear system identification in structural dynamics. *Mech Syst Signal Pr*, 20:502–592, 2006.
- [2] K. Worden and G. R. Tomlinson. *Nonlinearity in Structural Dynamics*. London : Institute of Physics Publishing, 2001.
- [3] M. Schetzen. *The Volterra and Wiener theories of nonlinear systems*. New York: Wiley, 1980.
- [4] S Cafferty and G. R. Tomlinson. Characterization of automotive dampers using higher order frequency response functions. *Proc Instn Mech Engrs Part D*, 211(3):181–203, 1997.
- [5] S. da Silva. Non-linear model updating of a three-dimensional portal frame based on Wiener series. *Int J Nonlin Mech*, 46(1):312 – 320, 2011.
- [6] S. B. Shiki, V. Lopes Jr, and S. da Silva. Identification of nonlinear structures using discrete-time Volterra series. *J Braz Soc Mech Sci*, pages 1–10, 2013.

Comparison between a finite-element-based and a trajectory-based method for computing damped nonlinear normal modes

Ludovic Renson and Gaëtan Kerschen

Aerospace and Mechanical Engineering Department, University of Liège, Belgium.

Pioneered in the 60s by Rosenberg, nonlinear normal modes (NNMs) were initially defined as families of synchronous periodic oscillations of the autonomous conservative system. The NNM concept was then further generalized to non-conservative systems by Shaw and Pierre. Based on geometric arguments, they defined a NNM as a two-dimensional invariant manifold in phase space [1]. Inspired by the center manifold approach, they used a single pair of state variables for manifold parameterization (a displacement and a velocity) and derived a set of partial differential equations (PDEs). These PDEs globally describe the manifold's geometry in terms of the remaining state-space variables which are functionally related to the chosen master pair. The first attempt to numerically solve these PDEs and to compute NNMs as invariant manifolds is that of Pesheck et al. [2]. PDEs were written in modal space and solved using a Galerkin projection. In recent contributions, Touzé and co-workers [3] solved the same set of PDEs using finite differences whereas Renson and Kerschen [4] used a specific finite element method in configuration space.

In this paper, the recently-developed finite element approach is compared to a new trajectory-based method. For this study, a two-degree-of-freedom system including regularized Coulomb friction is considered. The governing equations of motion are

$$\begin{aligned}\ddot{x}_1 + (2x_1 - x_2) + F_{\max} \tanh(R\dot{x}_1) &= 0, \\ \ddot{x}_2 + (2x_2 - x_1) &= 0.\end{aligned}\tag{1}$$

with $F_{\max} = 1.5$ N and $R = 1$ rad.s/m.

The finite-element-based (FE-based) method grows the two-dimensional invariant manifold as a collection of annular strips for which the manifold-governing PDEs are solved in configuration space. Recognizing that the PDEs are of hyperbolic nature, it was shown that solving these equations requires specific numerical treatments including a particular finite element formulation and appropriate boundary conditions [4]. The invariant manifold obtained for the in-phase NNM of the 2DOF (1) is presented in Figure 1(a). It was computed using 9 annular regions. For the last annular domain, the invariant surface becomes almost vertical. This indicates a failure of the parameterization and that it is not possible to further describe the invariant manifold using the preselected pair of master variables. This occurs because the invariant manifold generally presents a complex folding structure that is embedded in the full phase space. To circumvent this issue, Shaw and co-workers introduced the concept of multi-modal NNMs where the invariant manifold is described by multiple pairs of variables [5]. While effective, this method still assumes an explicit and global description of the NNM which does not completely solve the intrinsic parameterization issue.

The second (new) method considered here is a trajectory-based method which computes the invariant surface as a collection of trajectories defined using boundary value problems (BVPs). It is an alternative method for computing invariant manifolds that does not rely on a predefined parameterization. Originally proposed by Doedel [6, 7] in the general context of two-dimensional (un)stable invariant manifold calculations, the method covers the manifold using trajectories defined as a one parameter-family of curves. More precisely, the method considers successive BVPs to (i) compute a trajectory on the invariant manifold, (ii) continue the trajectory to cover the manifold. For stable systems, the computation of the first trajectory is similar to backward time integration with initial conditions that, close to the equilibrium point of the system, lie in the tangent space of the NNM. The in-phase NNM computed with this trajectory-based approach is the blue surface presented in Figure 1(b). It was obtained by constructing a mesh between the adjacent trajectories. In the center of the figure, the solution obtained with the FE-based approach in Figure 1(a) is presented in orange. It perfectly overlaps the trajectory-based results. The blue mesh also appears to fold in several regions recognizable by the darker blue color. The projection in Figure 1(c) of three trajectories onto the master's coordinate plane used by the FE-based method confirms this observation. The trajectories intersect each other in two different regions around $(x_2, y_2) = (-5, 2)$ and $(x_2, y_2) = (2, 5)$. Clearly, the FE-based method is limited in amplitude by those regions whereas the trajectory-based approach captures the manifold without limitation.

In summary, the finite-element-based method accurately captures the NNM and, based on the manifold's parameterization, allows to reduce the system's dynamics onto the invariant surface (i.e., a SDOF oscillator). However, the explicit parameterization limits the amplitude up to which the manifold can be computed. The trajectory-based method is an alternative approach where no explicit parameterization is assumed. It provides a means to calculate invariant manifolds with complex topologies. However, contrary to the FE-based method, the absence of parameterization prevents from obtaining a reduced-order model of the system.

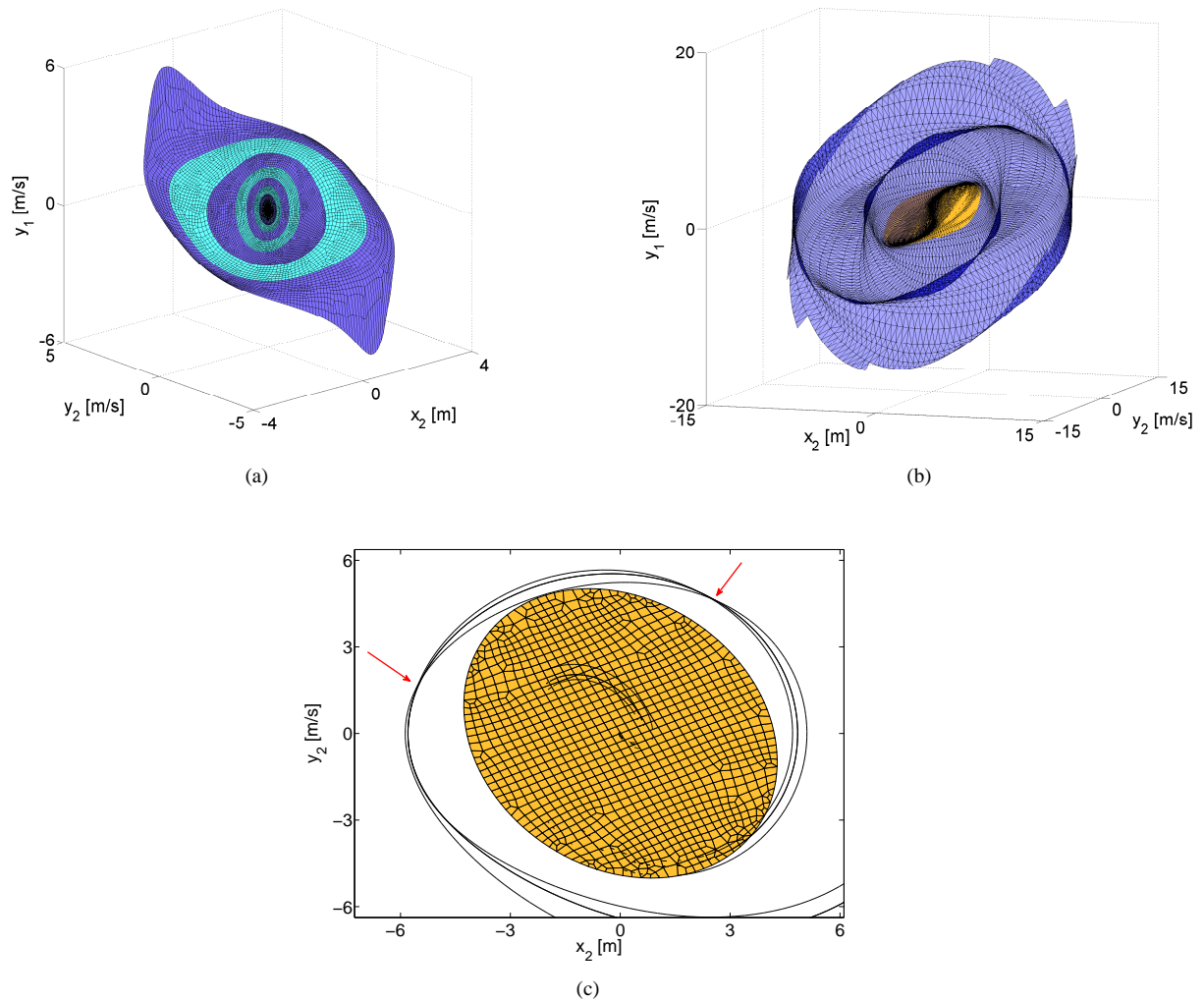


Figure 1: In-phase NNM of the 2DOF system (1). (a) Invariant manifold computed with the finite-element-based method; (b) Comparison between the trajectory-based method (in blue) and the FE-based results in orange; (c) top view of three trajectories computed with the BVP formulation.

References

- [1] S. W. Shaw and C. Pierre. Normal modes for non-linear vibratory systems. *Journal of Sound and Vibration* **164**:40, 1993.
- [2] E. Pesheck, C. Pierre, S. W. Shaw. A new Galerkin-based approach for accurate non-linear normal modes through invariant manifolds. *Journal of Sound and Vibration* **249**(5):971-993, 2002.
- [3] F. Blanc, C. Touzé, J. F. Mercier, K. Ege, A. S. Bonnet Ben-Dhia. On the numerical computation of nonlinear normal modes for reduced-order modeling of conservative vibratory systems. *Mechanical Systems and Signal Processing* **36**(2):520-539, 2013.
- [4] L. Renson, G. Deliège and G. Kerschen. An effective finite-element-based method for the computation of nonlinear normal modes of nonconservative systems. *Meccanica*, 2014.
- [5] D. Jiang, C. Pierre, S. W. Shaw. The construction of non-linear normal modes for systems with internal resonance. *International Journal of Non-Linear Mechanics* **40**(5):729-746, 2005.
- [6] E. J. Doedel, R. C. Paffenroth, A. R. Champneys, T. F. Fairgrieve, Yu. A. Kuznetsov, B. E. Oldeman, B. Sandstede, and X. J. Wang. AUTO2000: Continuation and bifurcation software for ordinary differential equations, available via <http://cmvl.cs.concordia.ca/>, 2000.
- [7] B. Krauskopf and H. M. Osinga. Computing Invariant Manifolds via the Continuation of Orbit Segments. *Numerical Continuation Methods for Dynamical Systems*, Springer Netherlands, 4:117-154, 2007.

A Comparison between Two Reduced-Order approaches in Nonlinear Capacitive Micro-Resonators

Mohammad Fathalilou¹, Ghader Rezazadeh², Morteza Sadeghi¹, A.M. Abazari³

¹Mechanical engineering Department, University of Tabriz, Iran

²Mechanical engineering Department, Urmia University, Iran

³Mechanical engineering Department, Isfahan University of Technology, Iran

Abstract

This paper presents a comparison between two reduced-order approaches of electrostatically actuated microbeams. The governing equations of motion have been derived considering nonlocal theory of elasticity. Galerkin-based reduced order model has been applied to solve the governing nonlinear equation with two approaches. In the first approach as used by many researchers in the literature, both sides of the equations are multiplied with the denominator of the electric term and then the Galerkin method is applied. In the second approach direct Galerkin method has been applied to solve the equation. The results show that for a given beam, although the both approaches predict same pull-in voltage in most cases, but the first approach cannot predict the pull-in instability in some cases and also misses some fixed points. So the bifurcation diagrams and phase portraits have different quality in the two approaches. Also, the results show that the singular point which is the position of the substrate plate acts as a strong attractor in the capacitive structures.

Keywords: Electrostatic, Fixed Point, Nonlinearity, Nonlocal theory

1. Introduction

Over the last decades, microelectromechanical systems (MEMS) have taken root firmly in research and technology world.

Numerous researches have shown that study on the mechanical behavior in electrostatically actuated microsystems is faced with various challenges due to existence of nonlinearities, which arise from a number of sources such as inherently nonlinear electric excitation.

From elasticity view of point, many researchers show that at micron and sub-micron scales the materials have strong size dependence in deformation behavior [1].

Eringen in 1962 [2] introduced the nonlocal elasticity theory in which he has assumed that in a material body, stress at point is not only a function of the strain at that point but also strain at all points in the continuum.

Some researchers have proposed various approaches in the literature focusing on the nonlinear electric force term, which is difficult to analyze directly. A complete review have been given by Nayfeh et al. [3] where different reduction methods based on the reduction of nodes of the discretized system and on the reduction of domains have been presented.

The purpose of this paper is to report that multiplying both sides of the governing equation with the denominator of the electric term proposed by some researchers may not be applicable in some cases.

2. Electrostatic Actuation Structure

Figure 1 shows an electrostatically actuated fixed-fixed Euler-Bernoulli micro-beam.

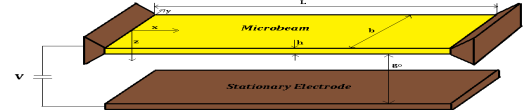


Fig. 1 An electrostatically actuated fixed-fixed micro-beam

Using the Hamiltonian principle, the governing non-dimensional equation for transverse vibrations of the beam in nonlocal theory is written by:

$$\frac{\partial^4 \hat{w}}{\partial \hat{x}^4} + \frac{\partial^2 \hat{w}}{\partial \hat{t}^2} + D_1 \frac{V^2}{(1-\hat{w})^4} \left(\frac{\partial \hat{w}}{\partial \hat{x}} \right)^2 + D_2 \frac{V^2}{(1-\hat{w})^3} \frac{\partial^2 \hat{w}}{\partial \hat{x}^2} + D_3 \frac{\partial^4 \hat{w}}{\partial \hat{x}^2 \partial \hat{t}^2} = D_4 \frac{V^2}{(1-\hat{w})^2} \quad (1)$$

In order to analyze the bifurcation of the microbeam, we use two approaches: in first one introduced by some researchers, firstly both sides of the static form of Eq. 1 are multiplied by $(1-\hat{w})^4$, then, assuming $\hat{w} = \sum_{i=1}^{\infty} a_i \varphi_i(\hat{x})$, considering the first term

of this series, substituting in static equation, multiplying with $\varphi(\hat{x})$ and integrating the outcome from zero to one, the following algebraic equation will be written as:

$$c_1 a^5 + c_2 a^4 + c_3 a^3 + c_4 a^2 + c_5 a + c_6 = 0 \quad (2)$$

In the second method (proposed approach), direct Galerkin method is applied to obtain the following relation:

$$V = \left(\frac{-a \int_0^1 \varphi \varphi^{iv} d\hat{x}}{\int_0^1 \varphi \left[\frac{D_1}{(1-a\varphi)^4} a^2 \varphi'^2 + \frac{D_2}{(1-a\varphi)^3} a \varphi'' - \frac{D_4}{(1-a\varphi)^2} \right] d\hat{x}} \right)^{\frac{1}{2}} \quad (3)$$

Now, one can obtain the variation of the applied voltage with changing the coefficient a , and consequently \hat{w} .

In order to investigate the stability of the fixed points obtained by the above analysis, we use two mentioned approaches as well. The first approach includes multiplying both sides of Eq. 1 with $(1-\hat{w})^4$ and then applying the Galerkin method to achieve a reduced order model by assuming $\hat{w}(\hat{x}, \hat{t}) = \sum_{j=1}^n T_j(\hat{t}) \varphi_j(\hat{x})$. Now, the following reduced order model is obtained:

$$\sum_{j=1}^n M_{ij} \ddot{T}_j(\hat{t}) + \sum_{j=1}^n K_{ij} T_{ij}(\hat{t}) = F_i \quad (4)$$

In second approach, direct Galerkin method similar to the static case is applied.

3. Results and Discussion

Position of the fixed points in the state-control space versus given voltage are shown in Figs. 2a and 2b using the first and second approach, respectively. These figures are plotted for different values of the nonlocal parameter, μ . As shown, for $\mu = (0.02L)^2$, five voltage ranges appear. In the first and fifth ranges there is only one fixed point, in the second and fourth ranges three fixed points and in the third one, five fixed points are observed in bifurcation diagram. For $\mu = (0.1L)^2$, for all given voltages there is only one fixed point. As shown in Fig. 2a, for $\mu = (0.02L)^2$ and $(0.04L)^2$ two stable and unstable branches meet together at pull-in point (saddle node bifurcation), but for $\mu = (0.1L)^2$ it is not seen such a position. So, for this case one cannot predict the position of the pull-in point in bifurcation diagram. Figure 2b illustrates the bifurcation diagrams for mentioned values of the nonlocal parameter using the second approach. As shown, for all given voltages under pull-in voltage we have two fixed points on upper side of the substrate. As shown, for the all values of the nonlocal parameter one can see the position of the pull-in point in bifurcation diagram.

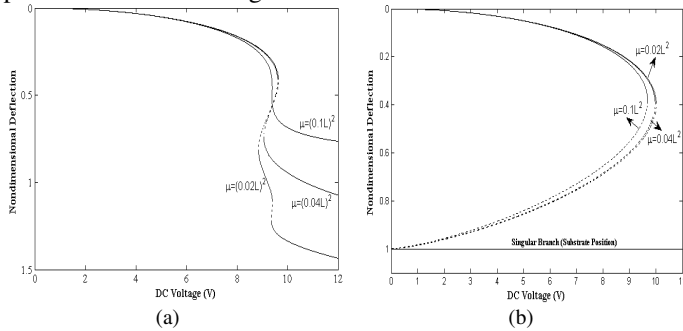


Fig. 2 Bifurcation diagram of the beam for $\mu = (0.02L)^2$, $(0.04L)^2$ and $(0.1L)^2$ using a) the first approach, b) the second approach

Now, the phase portraits using the first and second approaches are plotted to investigate the stability of the fixed points. Figure 3 shows the phase portrait for $\mu = (0.02L)^2$ and $V = 9.4V$ using the first approach. With attention to this figure one can recognize the stable and unstable branches in bifurcation diagrams. As obtained from Fig. 3, the first approach cannot predict the singular point (position of the substrate).

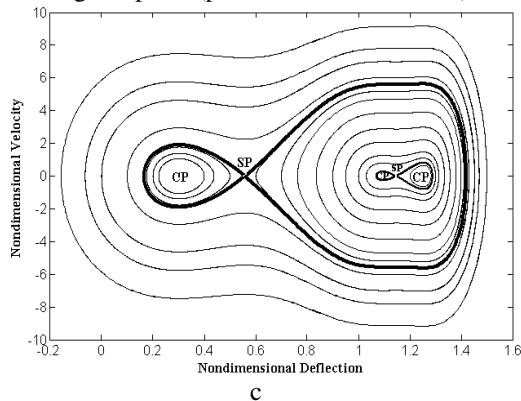


Fig. 3 Phase portrait for $\mu = (0.02L)^2$ and $V = 9.4V$

In Fig. 4 for $V = 8V$ (smaller than the pull-in voltage) one stable center point and one unstable saddle point are shown. It must be mentioned that unlike the first approach, the second one predicts the singular point which occurs at $\hat{w} = -1$. This type of singular points, which is the fixed position of the substrate, is introduced as an attractor because any motion which starts in the neighborhood of this point will attract to it with infinite speed. It should be mentioned that the singular point can be considered as a stronger attractor than the center point, because as shown in figure 4 the basin of attraction of the singular point is greater than the center point. On the other hand, only the motions which start at a finite neighborhood of the center point orbit around it whereas the motions which start at any other point in phase plane will attract to the singular point. Thus, we can conclude that the basin of attraction of the singular point is an infinite basin.

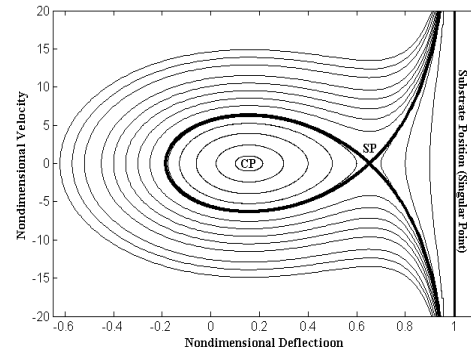


Fig. 4 Phase portrait for $\mu = (0.1L)^2$ and $V = 8V$

4. Conclusion

In presented work we used two Galerkin-based reduced order approaches to treat the governing equation of motion of an electrostatically actuated microbeam which were derived considering the nonlocal theory of elasticity. The results showed that in most cases the both approaches calculate the same pull-in voltage. But, from bifurcation view of point there were a qualitative difference between two approaches. Using the first approach missed some fixed points in the bifurcation diagram. The results showed that this approach cannot predict the singular points in motion trajectories which clearly were shown by the second approach. Also, the results showed that the singular point acts as a strong attractor where the basin of attraction of it is an infinite basin in phase plane, because any motion which start from the outside of the basin of attraction of the center point will attract to the singular point. Another remarkable result is that the first approach cannot predict the pull-in instability for one range of the nonlocal parameter values.

References

1. Fathalilou, M., Sadeghi, M., Rezazadeh, G., Jalilpour, M.: Study on the Pull-in Instability of Gold Micro-Switches Using Variable Length Scale Parameter. *Int. J. solid Mechanics*. 3, 114-123 (2011)
2. Eringen, A.C.: *Nonlinear Theory of Continuous Media*. McGraw-Hill, New York (1962)
3. Nayfeh, A.H., Younis, M.I. and Abdel-Rahman, E. M.: Reduced-order models for MEMS applications. *Nonlinear Dyn.* 41, 211-236 (2005)

Nonlinear Model Updating Based on Global/Local Nonlinear System Identification Approach

Mehmet Kurt¹, Melih Eriten², D. Michael McFarland³,

Lawrence A. Bergman³, Alexander F. Vakakis¹

¹*Department of Mechanical Science and Engineering*

University of Illinois at Urbana – Champaign

Urbana, IL 61801

²*Department of Mechanical Engineering*

University of Wisconsin at Madison

Madison, WI 53706

³*Department of Aerospace Engineering*

University of Illinois at Urbana – Champaign

Urbana, IL 61801

Tools for analyzing the strongly nonlinear dynamics of these systems have been developed, such as wavelet spectra superpositions on frequency-energy plots – FEPs of Hamiltonian dynamics and complexification/averaging analysis [1]. As shown previously in literature, two-dimensional FEPs provide a synoptic global description of the frequency and energy dependencies of periodic orbits of Hamiltonian n-degree of freedom (DOF) dynamical systems, and can be used to interpret complex dynamical transitions of weakly damped systems possessing even strong, non-smooth nonlinearities [2].

In this paper, we propose a new nonlinear model updating strategy based on global/local nonlinear system identification of a broad class of nonlinear systems. The approach relies on analyzing the system in the frequency-energy domain by constructing Hamiltonian or forced and damped frequency – energy plots (FEPs). These plots depict the steady-state solutions of the systems based on their frequency-energy dependencies. The backbone branches, branches that correspond to 1:1 resonances, are calculated analytically (for fewer DOFs) [3] or numerically (e.g., shooting method) [4]. The system parameters are then characterized and updated by matching these backbone branches with the frequency-energy dependence of the given system by using experimental/computational data. The main advantage of this method is that, no type of nonlinearity model is assumed a priori and the system model is updated solely based on time simulations and/or experimental results. We hope that our methodology will stand as a first step towards a nonlinear model updating methodology of broad applicability.

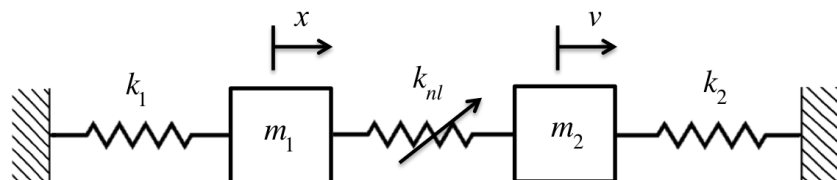


Figure 1. 2-DOF system with a nonlinear connection depicted in Figure 2.

In order to apply our proposed nonlinear model updating strategy, we consider the 2-DOF system depicted in Figure 1, with parameters $k_1 = 8400$ N/m, $k_2 = 6470$ N/m, $m_1 = 0.066$ kg, $m_2 = 0.060$ kg. The system can be regarded as a reduced order model of a larger system, consisting of two cantilever beams with a nonlinear coupling in between them. The nonlinear coupling between the two masses is given in Figure 2. Until some breaking point, which is negative 4 mm in this example, the connection is an essential, cubic-type nonlinearity. After the breaking point, the connection suddenly softens and behaves as a “zero-stiffness” member. This behavior suggests that the connection has membrane-like properties. Due to these hardening and softening effects, we expect to see interesting and very complicated transitions in the frequency-time domain for this system, which makes it a good candidate to apply our nonlinear model updating strategy.

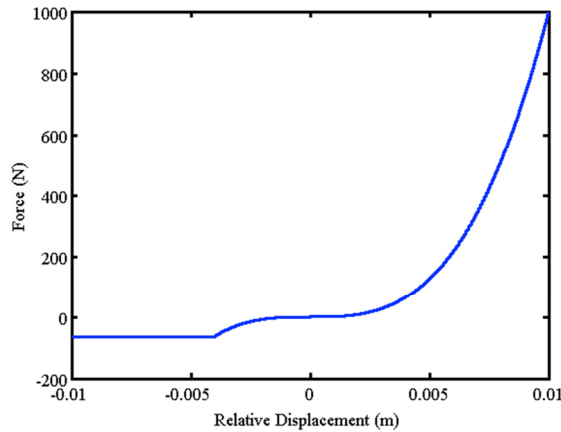
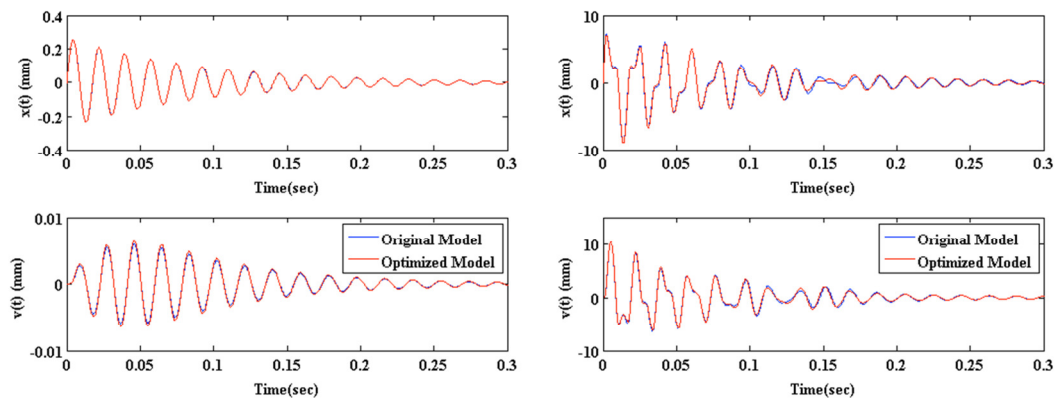


Figure 2. a) The force-displacement relationship of the nonlinear connection in Figure 1.

The nonlinear model updating strategy for this system is applied as follows. In order to find the global frequency-energy behavior of this system, we analyze it numerically with multiple impulse tests and find the transient frequency-energy behavior. Then, by looking at this frequency-energy dependence, we decide a nonlinearity model, whose parameters are optimized by comparing the numerical frequency-energy dependence from the time simulations to the Hamiltonian FEPs computed by NNMcont developed by Peeters *et al* [4]. In Figure 3, a comparison of the time series for the original and optimized models is depicted for an impulse with maximum amplitude of 100 N, depicting the linear region and 5000 N, depicting the strongly nonlinear region. As observed in Figure 3, the optimized model captures the nonlinear behavior very accurately for both cases. For the time simulations, low damping values are used in order to be able to use the Hamiltonian FEPs as our reference models.



(a)

(b)

Figure 3. Comparison of the time series for (a) 100 N impulse test (b) 5000 N impulse test

References

- [1] A.F. Vakakis, O. Gendelman, L.A. Bergman, D.M. McFarland, G. Kerschen, Y.S. Lee, *Passive Nonlinear Targeted Energy Transfer in Mechanical and Structural Systems: I and II*, Springer Verlag, Berlin and New York, 2008.
- [2] Y.S. Lee, F. Nucea, A.F. Vakakis, D.M. McFarland, L.A. Bergman, 'Periodic Orbits, Damped Transitions and Targeted Energy Transfers in Oscillators with Vibro-Impact Attachments,' *Physica D*, 238(18): 1868-1896, 2009.
- [3] M. Kurt, M. Eriten, D.M. McFarland, L.A. Bergman, A.F. Vakakis, 'Frequency-Energy Plots of Steady State Solutions for Forced and Damped Systems and Vibration Isolation by Nonlinear Mode Localization,' *Communications in Nonlinear Science and Numerical Simulation* 19(8): 2905-2917, 2014.
- [4] M. Peeters, R. Vigié, G. Sérandour, G. Kerschen, J.C. Golinval, Nonlinear normal modes, Part II: Toward a practical computation using numerical continuation, *Mechanical Systems and Signal Processing* 23: 195-216, 2009.

On the Properties of the POD Modes of Geometrically Exact Acceleration Space-Time Databases of Beam Structures Sensed by a Triad of Relocated and Fixed Accelerometers

Ioannis T. Georgiou

National Technical University of Athens, Zografos-Athens, Greece 15710

Test and evaluation methodologies targeted for model identification and structural health monitoring of physical one-dimensional solid continua are interesting topics of basic research-both at the theoretical and experiment levels-with measurable economic and societal impacts in real live applications. For example, some core elementary structures in technology and biology are essentially one-dimensional continua; and their function may depend on reliable monitoring of their dynamics response. Regarding structural health monitoring, one challenge is spatial measurements of flexible rod dynamics with embedded sensors in such a way as to record the interactions of the slow bending motions and fast torsion and extension motions. As the rod structure is the paradigm of the structure used to establish the modern geometric mechanics framework, here it is used as a prototypical structural system to cultivate novel ideas for distributed sensing of continuum slow-fast dynamics in a geometrically exact manner. We exploit the geometric concepts of the Slow Invariant Manifold (SIM) and the transversal fiber of Fast Invariant Manifolds (FIM) to conduct geometry consistent measurements in space using limited resources of sensors: here a triad of light weight acceleration sensors. They follow the local geometry of the deforming beam and thus they sense naturally the acceleration with reference to a local time varying coordinate system.

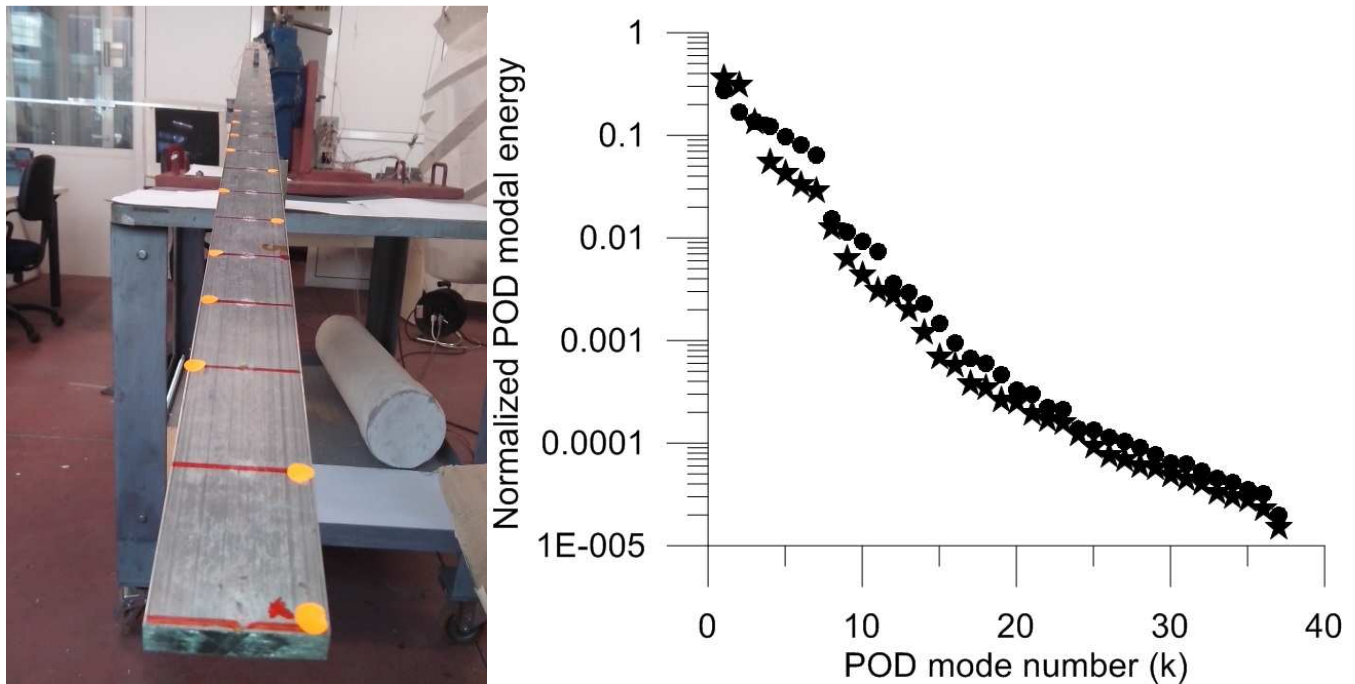


Figure 1 Left part: Photographic view of a physical long aluminum alloy beam whose transverse acceleration is measured by a pair of relocated accelerometers controlled by a fixed one. Right part: Distribution of the energy (right) of the mined space-time database over its intrinsic POD modes: local motion (circle) vs global motion (star).

We have tested long aluminum alloy beams both with rectangular and square cross-sections, Fig 1a. The sensing direction of the accelerometer intersects the gravitational field direction. The question that arises naturally is whether the sensed dynamics reflect the fact that the sensor is forced by the gravitational field. First, we answer the question whether the space-time database mined by the pair of the relocated sensors has physical meaning. The pair of relocated sensors is controlled by a fixed sensor. By this way we create indirectly nearly simultaneous spatial measurements. The dynamics are not restricted to small amplitudes and in the plane: The beams are excited in such a way as to create free motions that are a mixture of bending-extension-torsion in three-dimensional space. The typical space-time database collected by the two relocated sensors is evaluated in terms of its intrinsic proper orthogonal decomposition modes and the associated POD energy distribution, Fig. 1b. Despite the introduced errors, the experiments are repeatable, a fact that verifies the merit of the sensing technique. We follow the

following method of analysis: We create a sequence of geometric objects which initially are local and gradually become global to cover the whole time horizon of the motion. We find that the shape of the dominant POD mode changes as a function of the considered time horizon. For short time horizons, the time modulation of the POD mode has a single resonant frequency but as the time horizon expands the shapes change, Fig. 2b, quantitatively and this is reflected in the time modulation as the presence of two resonant frequencies. We see this very clearly in Fig. 3. This is either the effect of a space-time modulation stemming from the fact that the accelerometer interacts with the gravitational field or/and also indicates that the spatial coupled vibration of the beam is nonlinear. These two issues are topics of an ongoing investigation. The work contributes in the area of identification of vibration mode in experimental continuous structural dynamics.

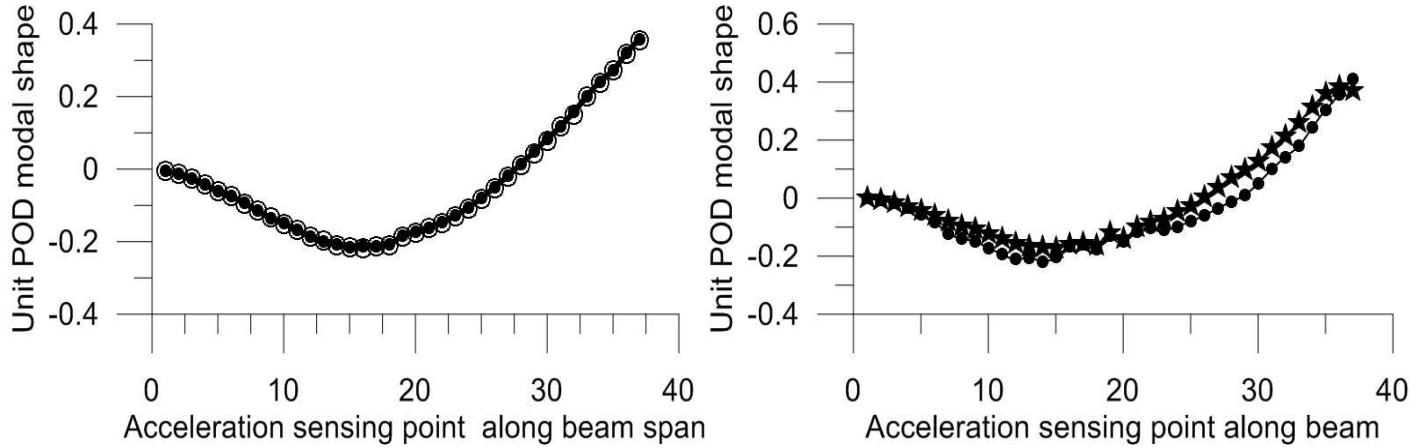


Figure 2 Experiment repeatability: dominant POD mode: Test 1 vs Test 2 (left). Dominant POD modal shape: local (circle) versus global (star) space-time database.

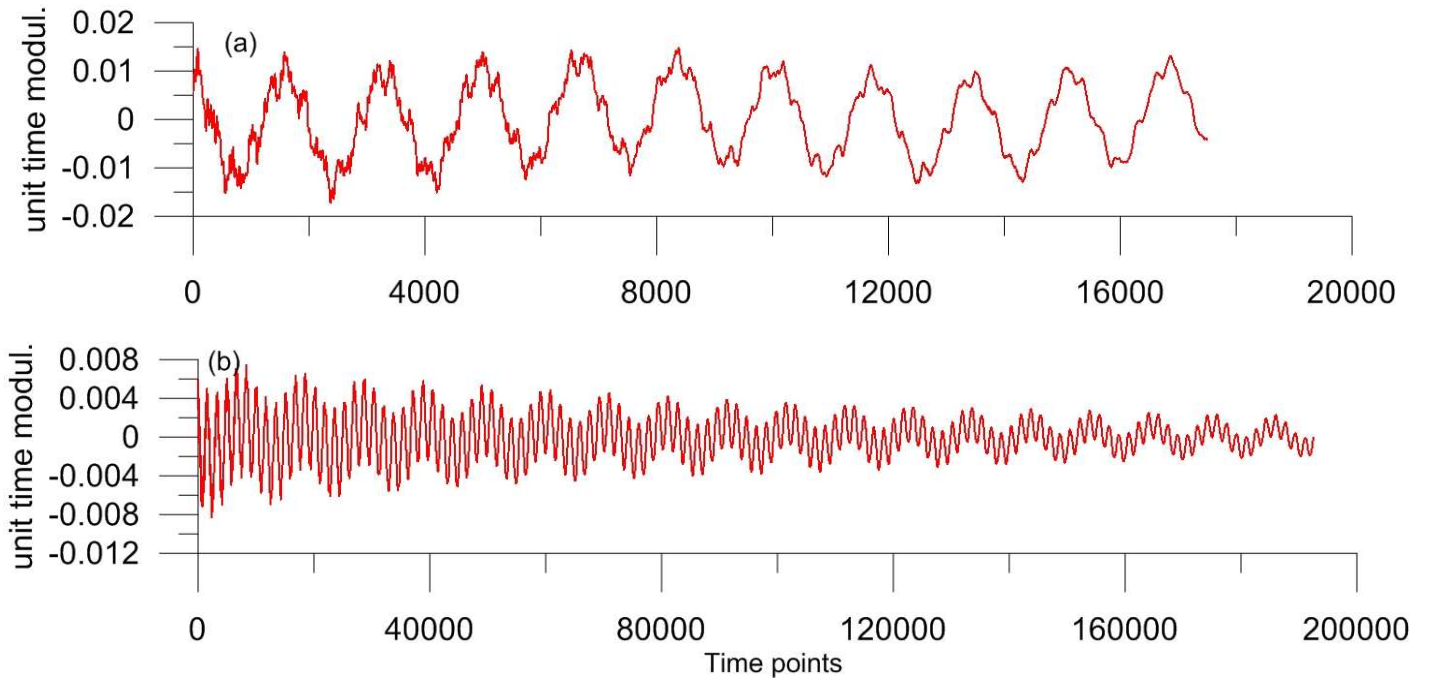


Figure 3: POD time modulation of dominant POD mode: (a) local database (17500 time points) , (b) global database (192500 time points).

Acknowledgments:

5th Conference on Nonlinear Vibrations, Localization and Energy Transfer
Istanbul, Turkey, July 2–4, 2014

SESSION 5

Nonlinear Dynamics of a Capacitive Micro-Resonator Considering Nonlocal Theory

Mohammad Fathalilou¹, Ghader Rezaadeh², Morteza Sadeghi¹, A.M. Abazari³

¹Mechanical engineering Department, University of Tabriz, Iran

²Mechanical engineering Department, Urmia University, Iran

³Mechanical engineering Department, Isfahan University of Technology, Iran

Abstract

This paper investigates the nonlinear dynamics of a capacitive micro-resonant beam considering the nonlocal theory of elasticity. Presenting a mathematical modeling, the microbeam has been deflected by a DC voltage and then the dynamic equation has been obtained by small motions about the deflected position. The governing nonlinear equation of motions has been solved using the perturbation method. The results have shown that, the nonlocality has softening effect in the beam motions against the hardening effect of the stretching term.

Keywords: Nonlocal theory, stretching, frequency response, perturbation method.

1. Introduction

Beams are key component of many structures from nano to macro scales in science and technology world. At small scales many researches show that the beams have size dependent mechanical behavior. Ignoring the microstructure of the beam material, classic elasticity cannot predict this behavior properly. In classical elasticity the deformation behavior is described by the local parameters of stress.

In the classical elasticity theory, stress at a point is considered to be a function of a strain at that point. On the other hand, Eringen in 1972 [1] introduced the nonlocal elasticity theory, in which they have assumed that in a material body, stress at a point is not only a function of the strain at that point but also strain at all points in the continuum. This hypothesis leads to introduce atomic forces and internal length scale parameter in constitutive equations.

The fixed-fixed microbeams represent an example of the structures suffering from the geometric nonlinearity stretching generated by mid-plane. For large deflections this nonlinearity becomes more significant. The stretching term hardens the beam with increasing the transverse deformation.

Microelectromechanical systems (MEMS) technology has already taken root firmly in today's world. Electrostatically actuated devices form a broad class of MEM devices due to their simplicity, as they require few mechanical components and small voltage levels for actuation.

In this paper, contrast effect of the stretching term and nonlocality of the beam theory in nonlinear dynamics of the electrostatically-actuated microbeam is investigated. In spite of the existence of the nonlinearity in the system, this conflict effect can result in a linear frequency response curve for some values of the nonlocal parameter.

2. Model Description

Fig.1 shows a schematic view of an electrostatically-actuated micro-resonant beam. This resonator consists of an elastic beam with fixed-fixed boundary conditions which is suspended over a stationary conductor plate. When a voltage is applied between two electrodes, an attractive electrostatic force pulls down the upper deformable electrode.

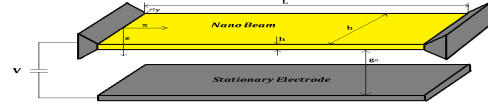


Fig.1. An electrostatically actuated fixed-fixed microbeam

Using the Hamiltonian principle, the governing equation for transverse vibrations of the beam in nonlocal theory by considering the stretching term is written by: [2]

$$EI \frac{\partial^4 w(x,t)}{\partial x^4} + \rho A \frac{\partial^2 w(x,t)}{\partial t^2} + \mu \left(\frac{-3\epsilon b V^2}{(g_0 + w)^4} \left(\frac{\partial w}{\partial x} \right)^2 + \frac{\epsilon b V^2}{(g_0 + w)^3} \frac{\partial^2 w}{\partial x^2} - \rho A \frac{\partial w}{\partial t} \right) - \left(\frac{EA}{2l} \int_0^l \left(\frac{\partial w(x,t)}{\partial x} \right)^2 dx \right) \frac{\partial^2 w}{\partial x^2} + c \frac{\partial w}{\partial t} = \frac{\epsilon_0 b}{2(g_0 + w)}$$

In order to solve the governing equation, we apply the Galerkin method to obtain a reduced order model. So, the $w_d(x,t)$ is considered as following:

$$w_d(x,t) = \sum_{j=1}^n \varphi_j(x) T_j(t) \quad (2)$$

Substituting this relation in Eq. (1), one can obtain the following n coupled ordinary differential equations:

This equation can be written in matrices form as following:

$$\sum_{j=1}^n M_{ij} \ddot{T}_j(t) + \sum_{j=1}^n C_{ij} \dot{T}_j(t) + \sum_{j=1}^n K_{1ij} T_j(t) + \sum_{j=1}^n \sum_{k=1}^n K_{2ijk} T_j(t) T_k(t) + \sum_{j=1}^n \sum_{k=1}^n \sum_{m=1}^n K_{3ijkm} T_j(t) T_k(t) T_m(t) = F_{1i} V_{ac} \cos \Omega t + f_{1i} V_{ac}^2 \cos^2 \Omega t + V_{ac} \cos \Omega t \sum_{j=1}^n F_{2ij} T_j(t) + V_{ac}^2 \cos^2 \Omega t \sum_{j=1}^n f_{2ij} T_j(t) \quad (3)$$

To determine a uniformly valid approximate solution of Eq. (3), the method of multiple time scales [3] (MMTS) is used.

3. Results and Discussion

For dynamic analysis, we study the effects of the applied DC voltage, stretching and nonlocality on the frequency response of the beam. To this end we consider an epoxy fixed-fixed microbeam with the specific geometrical and material properties.

Figure 6 exhibits the nonlocality effects on the frequency response for the DC voltage of 3.5V. As shown, increasing the nonlocal parameter tend the curve from hardening behavior to softening behavior.

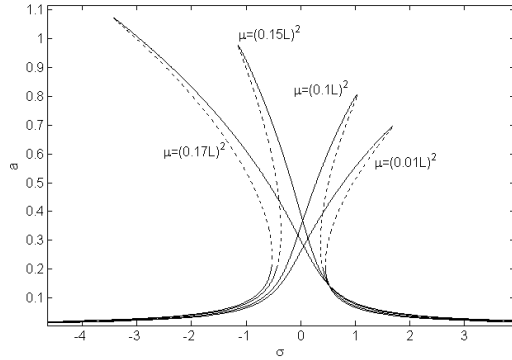


Fig 2. Frequency response of the beam for various values of the nonlocal parameter

The hardening effect of the nonlocality illustrated in figure 6, is in conflict with the hardening effect of the stretching. This matter is illustrated in figure 7, where considering the nonlocal theory for $\mu = (0.1L)^2$ modifies the nonlinear frequency response curve by destroying the hardening effect of the stretching.

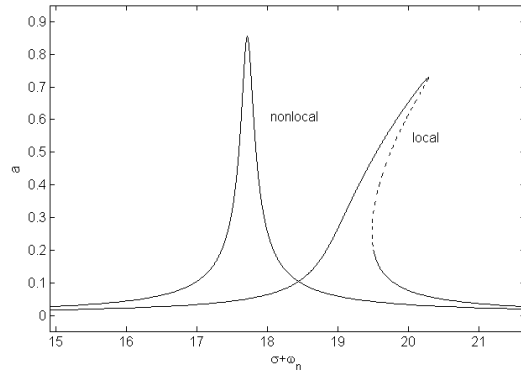


Fig. 3. Frequency response of the beam for considered local and nonlocal theories

4. Conclusion

In the presented work, the nonlocal theory of elasticity was used to obtain governing equation of motion of a capacitive microbeam. In dynamic analysis, first a DC voltage was applied to deflect the beam and then by applying an AC voltage, small motions of the beam was considered about the deflected position. The Galerkin method was applied to reduce the governing equation to a single ordinary differential equation. Then, the perturbation method was used to treat the nonlinear

dynamical behavior. We investigated the effects of the nonlocality on the frequency response of the beam. The results showed that, the nonlocality has softening effects while the stretching term hardens the system with increasing the amplitude of the motion. Also, it was shown that for specific values of the design parameters the nonlinear frequency response in local theory can be changed to a conventional curve (without the hardening or softening effects) when we consider the nonlocal theory of elasticity. These results can be useful for precise designing of the micro-resonators in which the frequency response curves have a significant role in analyzing their performance.

5. References

1. Eringen, A.C. [1972] "Nonlocal polar elastic continua," *Int. J. Eng. Sci.* **10**, p. 1–16.
2. Reddy, J.N. [2007] "Nonlocal theories for bending, buckling and vibration of beams," *Int. J. Eng. Sci.* **45**, p. 288–307.
3. Nayfeh, A.H.: *Introduction to Perturbation Techniques*. John Wiley & Sons, New York, 1-24 (1981).

TRANSVERSAL VIBRATION OF A MICRO-BEAM IN INTERACTING WITH A MICRO-SCALE FLUID MEDIA BASED ON MICRO-POLAR THEORY

Mina Ghanbri^{*1}, Siamak Hossainpour², Ghader Rezazadeh³

^{1,2}Mech. Eng. Dept., Sahand University of Technology, Tabriz, Iran

^{1*} minaghanbari@yahoo.com ; ² hossainpour@sut.ac.ir,

³Mech. Eng. Dept., Faculty of Eng., Urmia University, Urmia, Iran

³ g.rezazadeh@urmia.ac.ir

Abstract: In this paper Transversal vibration of a micro-beam in interacting with a micro-scale fluid media based on micro-polar theory has been investigated. The proposed model for this study that appears in the most of MEMS devices especially in micro-resonators consists of a clamped-clamped micro-beam bounded between two fixed layers. The gap between the micro-beam and the layers is filled with air. Fluid field affects the behavior of the micro-beam. Transversal vibration of the micro-beam squeezes the air, causes the squeeze film damping phenomenon to be occurred. This phenomenon occurs as a result of massive movement of the air underneath the beam which is resisted by the viscosity of air. Equation of motion governing the transverse deflection of the micro-beam based on non-local elasticity theory and also non-linear Reynolds equation of the fluid field based on micro-polar theory have been non-dimensionalized, linearized and solved simultaneously to calculate the quality factor of the squeeze film damping. The effect of non-dimensional length scale parameter of the air and micro-beam for different values of micro-polar coupling parameter has been investigated. The quality factor of the squeeze film damping for different values of length-to-width ratio of the micro-beam, squeeze number and non-dimensional pressure have been calculated and compared to the obtained values of quality factor based on classic theory.

Key words: MEMS, Micro-polar theory, Squeeze film damping.

Introduction

Recently, progress in technology of micro-electromechanical systems (MEMS) can be seen in fabricating new devices and creating innovative applications. The fact that they can be produced at low cost in large volumes, with light weight, small size and low-energy consumption, make them attractive and cause a great interest among scientists and engineers due to their several advantageous. The effect of squeeze film damping on the response of microstructures that appears in most of MEMS devices as micro-resonators have been studied extensively in recent years. Damping characteristics for the first three flexural modes of vibration of the resonator were obtained by Pandey and Pratap in which static deflection due to DC load was neglected [1]. Younis and Nayfeh obtained bias deflection of the micro-plate under different ambient pressures by using perturbation method [2]. Squeeze film characteristics of cantilever micro-resonators for higher modes of vibration under large DC load were obtained operating in different ambient pressure conditions by Chatterjee and Pohit [3-4]. Khatami and Rezazadeh [5] studied the dynamic response of actuators to electrostatic force and mechanical shock. They showed that the combined effect of a shock load and an electrostatic actuation makes the instability threshold much lower than the predicted threshold, considering the effect of shock force or electrostatic actuation alone.

Although several studies have been done on the dynamic behavior of the micro-structures under squeeze film damping but most of them have used the linearized Reynolds equation obtained by classic theories, for simulating the fluid field. Numerous experimental results indicate that, as fluid flow moves differently in the micro-scale than that in the macro scale, in the study of micro and nano-scale fluid mechanics, the Navier-Stokes equations derived from classical continuum, become incapable of explaining the micro scale fluid transport phenomena [6]. A novel approach was developed by Eringen [7] which includes the effect of local rotary inertia and couple stresses and offers mathematical foundation to capture the motions of the micro-scale fluids. Today, researches show that in the field of micro-scale fluids, applying micro-polar fluid theory can be a useful tool in modeling of the micro-flows and micro-structures.

In this paper, free vibration of the clamped-clamped micro-beam under the effect of squeeze film damping based on micro-polar fluid theory is studied. The coupled governing equations of motion of the beam based on non-local elasticity theory and the fluid pressure field based on micro-polar theory is solved simultaneously using Galerkin based reduced order model. The effect of length scale and coupling parameter of the micro-polar theory on the values of calculated quality factor is investigated. The values of calculated quality factor are compared to the values obtained based on classic theory, and these differences are discussed and investigated.

Methodology and results

The proposed model for this study is shown in Fig.1. It consisted of a clamped-clamped micro-beam with two fixed layers on the upper and lower surfaces of it. The distance between the micro-beam and the parallel layers is filled with air.

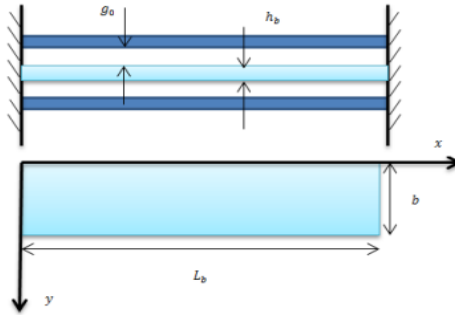


Fig.1. proposed model for studying the effects of the fluid field on the behavior of the micro-beam

The coupled equations of motion of the transverse deflection of the beam based on non-local elasticity theory and non-linear Reynolds equation of the fluid field based on micro-polar theory are non-dimensionalized, linearized and then discretized by applying Galerkin-based reduced order model. These coupled equations are solved simultaneously to calculate natural frequencies of the beam for obtaining damping coefficient and quality factor of the micro-beam. Effects of micro-polar parameters of the fluid and non-dimension length scale parameter of the micro-beam on the obtained values of quality factor are investigated and are compared to the values that are obtained based on classic theories. The results are shown in Fig.2 in which N refers to coupling parameter of the fluid field.

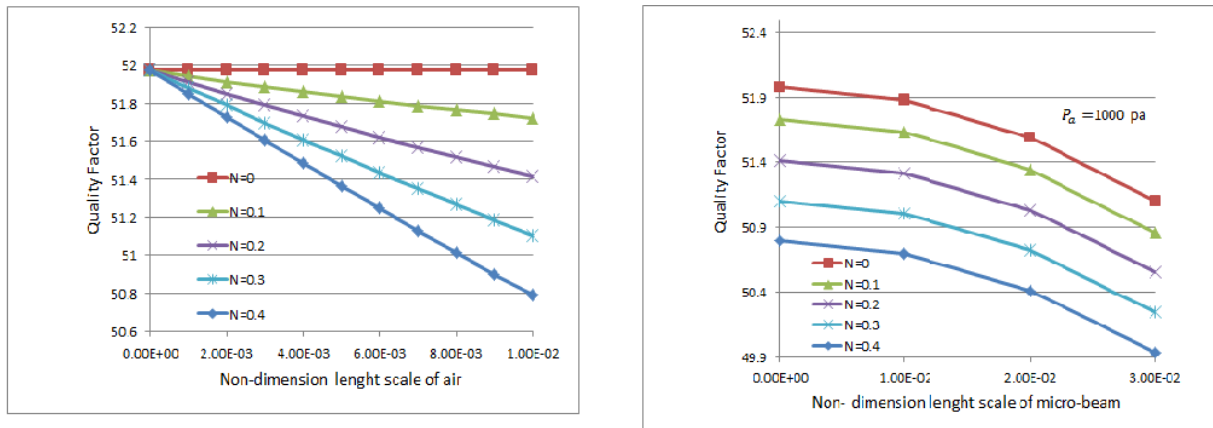


Fig.2. Effect of micro-polar parameters and non-dimension length scale of the micro-beam on the values of quality factor

Conclusion

Results showed that increasing micro-polar parameters causes the quality factor to decrease. The results also showed that applying micro-polar theory and also non-linear elasticity theory underestimates the values of quality factor that are obtained based on classic theory.

References

1. A. K. Pandey and R. Pratap, "Effect of flexural modes on squeeze film damping in MEMS cantilever resonators," *J. Micromech. Microeng.*, vol. 17, pp. 2475-2484, Oct. 2007.
2. M. I. Younis, A. H. Nayfeh, "Simulation of squeeze-film damping of micro-plates actuated by large electrostatic load", *ASME. J. Comput. Nonlinear Dynam.*, vol.2, pp. 101-112, Jan. 2007.
3. S. Chatterjee, G. Pohit, "A large deflection model for the pull-in analysis of electrostatically actuated micro cantilever beams," *J. Sound and Vib.*, vol. 322, pp. 969-986, May.2009.
4. S. Chatterjee, G. Pohit, "Squeeze- film characteristics of cantilever micro-resonators for higher modes of flexural vibration," *Int. J. Eng. Sci and Technol.*, vol.2, pp. 187-199, May. 2010.
5. F. Khatami, G. Rezazadeh, "Dynamic response of a torsional micro-mirror to electrostatic force and mechanical shock," *Microsyst. Technol.*, vol.15, pp. 535-545, Apr.2009.
6. A. Kucaba-Pietal, "Microchannels flow modelling with the micro-polar fluid theory," *Bull. Pol. Acad. Sci.*, vol. 52, pp. 209-213, 2004.
7. A.C. Eringen, "Theory of micro-polar fluids," *J.Math.Mech.*, vol.16, pp. 1-18, 1966.

Nonlinear Solutions in BEC for Different Potentials

Eren Tosyali¹ and Fatma Aydogmus²

¹ *Istanbul Bilgi University, School of Advanced Vocational Studies, Istanbul, TURKEY*

² *Istanbul University, Department of Physics, Istanbul, TURKEY*

e-mails: eren.tosyali@bilgi.edu.tr, fatmaa@istanbul.edu.tr

After the first experimental observation of Bose-Einstein Condensation (BEC) in 1995 [1], many physicists and applied mathematicians focus on this topic significantly. Different theories were developed to describe the BEC depending various ranges of temperature and interaction. In the low temperature regime, a BEC is well described by the non-linear Schrödinger equation known as the Gross-Pitaevskii Equation (GPE) with the macroscopic wave function $\psi = \psi(x,t)$ which evaluates with time and space. The GPE was first developed independently by Gross [2] and Pitaevskii [3] in 1961 to describe the vortex structure in superfluid. The 1-D Gross-Pitaevskii equation is given as

$$i\hbar \frac{\partial}{\partial t} \psi(x,t) = -\frac{\hbar^2}{2m} \frac{\partial^2}{\partial x^2} \psi(x,t) + \left[V_{ext}(x) + g_0 |\psi(x,t)|^2 \right] \psi(x,t), \quad (1)$$

where m is the mass of the atoms of the condensate, g_0 describes the interaction between atoms in the condensate. GPE possesses a very rich dynamics and exhibits soliton type solutions.

Many theoretical studies have been performed on nonlinear properties in Bose-Einstein Condensate (BEC) for different optical lattice potential [4,5,6]. Recently, super lattice potential has been fulfilled chaotic behavior in BEC [7,8]. In this work, we study the dynamics of 1D Gross-Pitaevskii equation (GPE) for different external trapping potentials. we consider that the external potential $V_{ext}(x)$ in Eq. (1) is a tilted bichromatical potential

$$V_{ext}(x) = V_1 \cos^2(w_1 x) + V_2 \cos^2(w_2 x) + Fx, \quad (2)$$

where F is inertial force, which accelerates the atoms in the x direction, V_1 and V_2 are the respective amplitudes. Firstly we briefly present an analytical study of GPE for the tilted bichromatic optical lattice potential. After that we perform numerical simulations of the GPE for tilted bichromatic and Gaussian optical lattice potentials. We show that density of flow (J) affects behavior of BEC for different potential depths. In addition, for regular case with a number of density of flow under the bichromatic potential exhibits similar behavior with Wannier Stark lattice potential [5]. Regular and chaotic behaviors are investigated for different initial conditions with small and big tilted value. Regular behaviour is seen when the tilted force is really small and density of flow is big. Other cases BEC shows chaotic behaviour for two types of potential.

References:

- [1] M. H. Anderson, J. R. Ensher, M. R. Matthews, C. E. Wieman, and E. A. Cornell. Observation of bose-einstein condensation in a dilute atomic vapor. *Science*, 269(5221):198–201, 1995.
- [2] E. P. Gross. Structure of a quantized vortex in boson systems. *Nuovo. Cimento.*, 20, 454, 1961.
- [3] L. P. Pitaevskii. Vortex lines in an imperfect Bose gas. *Soviet Phys. JETP*, 13, 451, 1961.
- [4] Q. Thommen, J. Garreau and V. Zehnle, *Phys. Rev. Lett.* 91, 210405 (2003).
- [5] W. Hai, G. Lu, and H. Zhong, *Phys. Rev. A*, 79, 053610 (2009)
- [6] K. Zhang W. Chen, M. Bhattacharya, and P. Meystre, *Phys. Rev. A*, 81, 013802 (2010)
- [7] Vivien P. C., Mason A. P., *Jour. of Bif. and Chaos* 16, 945-959 (2004).
- [8] Priyanka V., Aranya B., Man M., *Jour. of Phys.: Conference Series* 350 (2012).

Detection of Hydrogen Sulphide agents using frequency shifting of a doubly clamped micro-beam based sensor considering Couple Stress effect

Mohsen Safavai¹, Amir Musa Abazari¹, Ghader Rezazadeh²

¹Mechanical engineering Department, Isfahan University of Technology, Iran

²Mechanical engineering Department, Urmia University, Iran

This paper relates to the continually advancing field of micro-electro-mechanical-systems (MEMS). With MEMS technology, there are many different areas of concentration available for research. This paper addresses analysis and preliminary characterization of a doubly-clamped type MEMS chemical gas sensor for detection of Hydrogen sulphide.

Hydrogen sulphide (H_2S) is a toxic gas with a peculiar foul smell. It is corrosive and is naturally occurring due to decomposition of some organic matter in wastewater. It is also used in large quantities to extract heavy water. Monitoring and control of H_2S in ambient is therefore important in laboratories and industrial areas where it is used as a process gas, generated as a byproduct or produced naturally in wastewater swamps. There currently exist several different types of MEMS chemical gas sensors. Each is based on a different detection method, e.g., capacitive, thermal, resistive, etc., and is used for specific tasks. Out of all currently available detection methods, the most common is the gravimetric method. The gravimetric sensor works by adsorbing the molecules in a special material, usually a polymer, which alters the overall mass of the sensing element that can then be measured, or detected, to identify the chemical adsorbed.

One of the more exciting developments in the field of gravimetric chemical MEMS has been with the advancement of beam-type sensors. These beams are small and usually on the order of only about $300\ \mu m$ in length. In order to utilize the gravimetric method, a beam is coated with a layer that allows an analyte to bond to it and change its mass, which in turn changes the resonant frequency of the beam. The change in frequency can then be measured and analyzed and from it, the amount of added mass can be calculated. For example, current research in the beam-type resonating sensors for the detection of hydrogen is developing measurement capabilities of under 1 ppm (part-per-million). Parametric analyses involving chemical adsorption processes will be discussed in this paper. Such analyses consider different parameters, e.g., damping and stiffness as well as changes in their values, to determine contributions they make to the quality of the frequency data and the effect they have on sensitivity of the MEMS beam-type gas sensor. Once these parametric analyses were completed, it was possible to estimate the sensitivity of the beam, or the ability for the beam to detect frequency shifts due to adsorption of the target gas.

In this paper, we will derive the required formulas for the effect of added mass on the resonant frequency of a doubly-clamped micro-beam (Fig. 1) due to the mass addition built up along the beam. In the main manuscript we will discuss that a net surface adsorption of mass is induced in a doubly-clamped beam, along its surface. For the resonators used here, this coincides with the adsorption in the active layer only; other parts of the beam do not contribute to the mass addition because the non-adsorptive surface to the analyte. The net mass addition determines the resulting effect on resonance frequency and/or stiffness of the device.

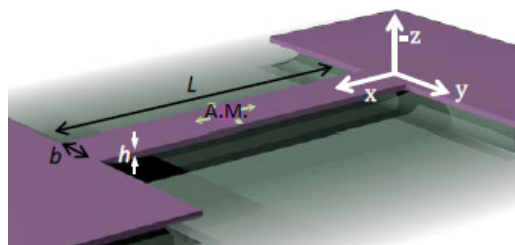


Figure 1. Graphical representation of a doubly-clamped beam with the dimensions used in the paper, as well as the axis definition, (A.M.: Adsorbent Mass)

The effect of added mass on the resonance frequency of a doubly-clamped beam is calculated to leading order for small mass loads, and thus gives a linear relationship between the resonant frequency shift and the applied added mass change. The main objective of this paper is to comprehensively analyze vibration characteristics of doubly-clamped microbeam-based sensors with application to ultra-small mass detection and low dimensional materials characterization. The work focuses on theoretical developments commercially named Active Probes, which are extensively used in most today's advanced Atomic Force Microscopy (AFM) systems. Due to micro structure of the beam, a general and comprehensive framework is introduced for forced vibration and modal analysis of the beam.

It is demonstrated that a significant enhancement on sensing accuracy of Active Probes can be achieved using the proposed model. The material properties are expressed in terms of added mass force acting on the surface as a result of response of material to applied electric field. Since the application of bias voltage to the beam results in the surface displacement in normal direction, the microbeam is considered to vibrate in one direction with transversal motion. In this respect, it is demonstrated that the system can be governed by a set of partial differential equations along with boundary conditions. Overall in this paper, a precise dynamic model is developed for doubly-clamped micro-beam for ultra-small mass detection purpose. A distributed model which is considering higher order elasticity theories for the problem is investigated assuming the beam as an electrode of a micro-capacitor. This model can also be utilized in AFM systems to replace laser-based detection mechanism with other alternative transductions. The dynamic response of a doubly-clamped microbeam due to application of an AC voltage in presence of a bias DC voltage will be studied. The frequency resonance of the beam is determined and it is illuminated that increasing in the bias voltage will make the frequency sensible.

For verification of our proposed micro-beam, a microbeam with the geometric and material properties listed in Table 1 was considered. In Table 2 the calculated pull-in voltage was compared to the results of existing work for the fixed-fixed micro-beams having properties shown in Table 1. As shown the calculated pull-in voltages are in good agreement with the results presented in previous work. As you seen in Table 2, 22.07 (V) is pull-in voltage for our proposed model, however this will be increased to 22.58 (V) when we consider the couple stress effect in our model. It could be explained that with considering couple stress effect, the stiffness parameter of vibration equation of the micro beam increases and then cause to higher pull-in voltage. In main manuscript we will discuss more on this effect.

Table 1. The values of design variables

Design Variable	Values for comparison pull-in voltage	Proposed Values for sensor
Length	350 μ m	600
Width	50 μ m	150
Thickness	3 μ m	5
Gap	1 μ m	1
Young's Modulus	169GPa	169GPa
Density	2331 kg/m ³	2329 kg/m ³
electrical permittivity of air	8.85 PF/m	8.85 PF/m
Poisson's Ratio	0.06	0.06

Table 2 Comparison of the pull-in voltage for a fixed-fixed microbeam

	Our result	Energy model	MEMCAD
Pull-in Voltage (V)	20.1	20.2	20.3

After considering adsorption of H₂S natural frequency shifting due to presence of gas molecules illuminated in frequency responses in both situations: considering couple stress effect and without its effect, that are plotted in Figure 2. As it can be seen in the figure frequency shifting is changed approximately 341.6 kHz in first case and 230.8 kHz in second state due to adsorption of gaseous molecules on the micro-beam that easily is detectable. Also, it is clear that with considering couple stress effect amplitude of the resonator will be reduced that it could be easily seen from the illustrated picture. It can be concluded that considering couple stress effect is effective in amount of frequency shifting and cause to increase it.

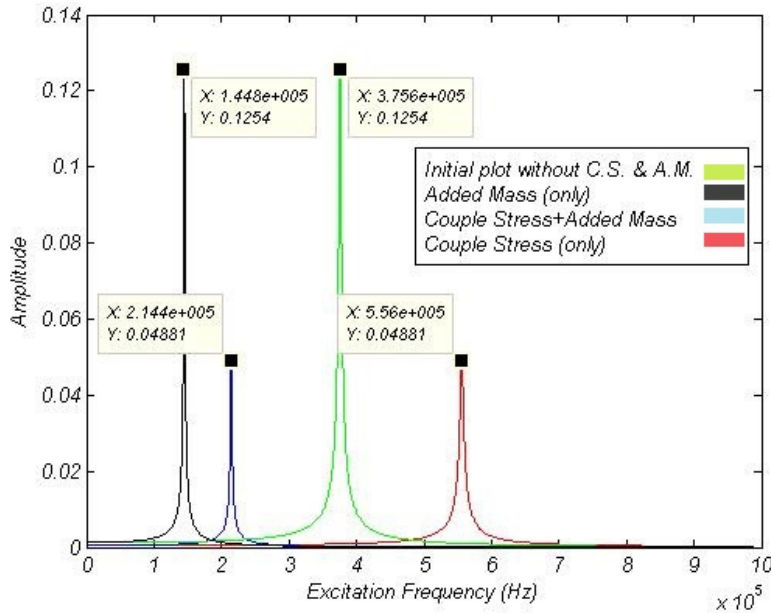


Figure 2- Frequency response: Shifting frequency with considering Couple Stress is about 110.8 KHz more than state without considering its effect due to added gaseous molecules

Nonlinear Dynamics of Adhesive Micro-spherical Particles on Vibrating Substrates

Armin Saeedi Vahdat¹, Saber Azizi², and Cetin Cetinkaya^{1*}

¹ Department of Mechanical and Aeronautical Engineering, Photo-Acoustics Research Laboratory Center for Advanced Materials Processing, Clarkson University, Potsdam, NY 13699-5725, USA

² Department of Mechanical Engineering, Engineering Faculty, Tarbiat Modares University, Tehran, Iran

EXTENDED ABSTRACT

Adhesion bond of a micro-spherical particle on a flat vibrating rigid substrate creates restitution force and rolling moment resisting to its out-of-plane and in-plane motions, respectively, (Fig. 1). The resistance of a micro-particle on a surface to rocking and rolling has relatively rarely been experimentally explored with few exceptions even though it is critical in particle removal and attachment [1]. Recently, based on ultrasonic base excitation and interferometric sensing technique, a non-contact method was introduced for observing dynamic behavior of adhesive micro-particles on rigid flat substrates (Fig. 2) [1]. However, complex and coupled dynamics of a vibrating particle can result in various natural frequencies in the experimentally obtained spectral domains of the particle which can lead to an ambiguity in adhesion characterization[2, 3]. For some spherical micro-particles on a vibrating flat substrate, in addition to their predicted rocking resonance frequencies, other resonance peaks at their doubles are observed (Fig. 3). Employing the vibrational spectroscopy approach reported in [2], the total out-of-plan displacement of a microparticle in temporal domain is acquired and then transformed into spectral domain for understanding their frequency contents. As depicted in Figs. 3. a pair of peaks in the spectral response of a PSL (polystyrene latex) at 45.16 and 82.70 kHz is observed. Employing the Newton's second law of motion and Euler law of angular motion, the equations of in-plane and out-of-plane motions are derived:

$$m \ddot{\delta} - m \delta \dot{\theta}^2 + F_R(\delta) = -m r \dot{\theta}^2 \quad (1.a)$$

$$(I_O + m(r - \delta)^2) \ddot{\theta} - (2m(r - \delta)\dot{\delta}) \dot{\theta} + M_R(\delta, \theta) = 0 \quad (1.b)$$

Substituting an approximated in-plane harmonic solution $\theta(t) = \Theta \sin(\omega_r t)$ into Eq. 1.a, the right-hand side of the resulting equation, acts as an excitation term and forces the system to oscillate at an additional frequency which is double of the rocking frequency ω_r . Therefore, due to the nonlinear coupling, the purely rocking motion can excite the out-of-plane motion with a frequency of $2\omega_r$. Note that, since the interferometer measures the out-of-plane movement of the top of a particle as it oscillates, as it was

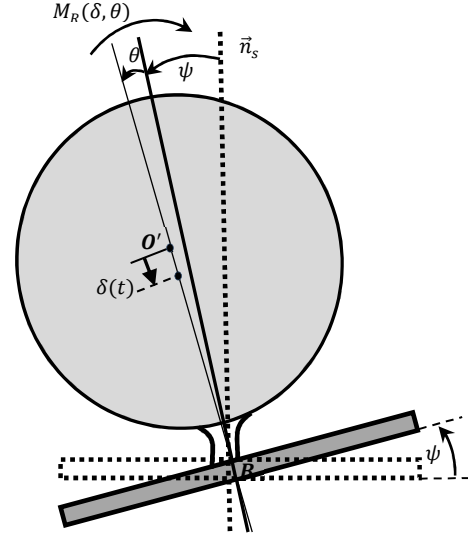


Figure 1. The independent coordinates of the proposed two-dimensional adhesion model for the simultaneous out-of-plane (δ) and in-plane (θ) motions of a spherical particle on a vibrating surface (not to scale).up).

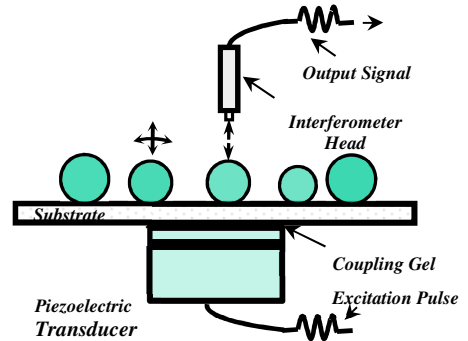


Figure 2. Schematics of the measurement zone of

explained in [2], only modifying the approximated solution $\theta(t)$ by adding a non-zero term ($\theta_0(\dots)$), as $\theta_m(t) = \Theta \sin(\omega_r t) + \theta_0(\dots)$, leads to the out-of-plane displacement oscillating not only at ω_r , but also at $2\omega_r$. The term $\theta_0(\dots)$, which causes the rocking resonance frequency doubling effect, attests that the rocking motion occurs around an inclined axis with respect to the substrate normal. This inclined rocking motion implies the existence of whirling-like motion of a particle and/or the nonlinear component coming from the presence of the nonlinear damping term in Eq. 1.b. In conclusion, based on the presented two-dimensional dynamic model of an adhesive micro-spherical particle on a flat substrate, it is found that nonlinear coupling between its in-plane (rocking) and out-of-plane modes of motion is the source of reported rocking frequency doubling phenomenon. It is explained that, in order to observe both the rocking resonant frequency and its double in the experimental measurements, the particle has to experience rocking motion around an inclined axis with respect to the surface normal. This implies the presence of whirling-like motion of particles in the reported experiments. The excitation modes/mechanisms and/or the nonlinear coupling effect could cause a whirling-like motion. By matching the rocking resonance frequency value of simulations and experimental results work-of-adhesion values can accurately be extracted while in previous studies, the doubling effect was leading to confusion in adhesion characterization since ambiguity existed in choosing the resonance frequency and corresponding mode of motion. Also by matching the amplitude ratios of the rocking resonance frequency and its doubled of simulation to the experimental ones the leaning angles of whirling particles can be approximated.

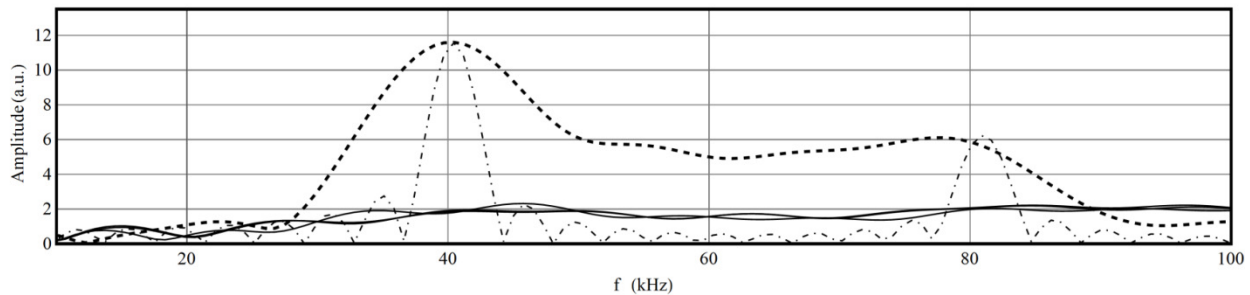


Figure 3. Comparisons of experimental spectral responses of the substrate (solid thin lines) and particle (dashed thick line) with those computationally obtained from the integration of the proposed model (dot-dashed thin line)

List of References

- [1] M.D.M. Peri and C. Cetinkaya, *Rolling Resistance Moment of Microspheres on Surfaces*, Philosophical magazine. 85 (2005), pp. 1347-1357.
- [2] A. Saeedi Vahdat, S. Azizi and C. Cetinkaya, *Nonlinear Dynamics of Adhesive Micro-Spherical Particles on Vibrating Substrates*, J.Adhes.Sci.Technol. (2012), pp. 1-15.
- [3] I. Akseli, M. Miraskari, H. Zhang, W. Ding and C. Cetinkaya, *Non-Contact Rolling Bond Stiffness Characterization of Polyvinylpyrrolidone (PVP) Particles*, Journal of Adhesion Science and Technology, 25. 4 (2011), pp. 407-434.

5th Conference on Nonlinear Vibrations, Localization and Energy Transfer
Istanbul, Turkey, July 2–4, 2014

SESSION 6

Nonlinear Energy Transmission in a Finite Dissipative Periodic Structure

Behrooz Yousefzadeh, A. Srikantha Phani

Department of Mechanical Engineering, University of British Columbia, Canada

behroozy@alumni.ubc.ca , phani@mech.ubc.ca

Abstract: We study nonlinear transmission of energy in a finite dissipative periodic structure, forced outside the linear wave transmission spectrum (the pass band). There exists a threshold for the driving amplitude above which a sudden increase occurs in the energy transmitted to the other end of the finite structure. The mechanism responsible for this steady nonlinear transmission is explained, and its connection to the resonance of the driving forcing with the shifted pass band is discussed.

Introduction: The vibrations of periodic structures is very well understood for small-amplitude motions; i.e. in the linear operating range [1]. Due to their dispersive nature, periodic structures attenuate any wave with a frequency component that is outside a particular frequency range known as the pass band. Waves with frequency components within the pass band can propagate freely through an undamped periodic structure.

It is known that if the amplitude of the driving force is large enough, energy transmission is possible even when the driving frequency is outside the pass band [2, 3]. This nonlinear energy transmission is accompanied by a large increase in the energy flux throughout the structure. This is clearly in contrast with the linear response of the structure.

Nonlinear transmission of energy from excitations outside the pass band has been predominantly studied in the physics literature, for non-dissipative and infinitely-long systems with governing equations that are not common in engineering applications; e.g. Morse potentials and FPU chains. In contrast, engineering structures inevitably possess some form of damping and have finite length. Dissipation results in spatial attenuation of waves even within the pass band and finite size results in reflection of waves from the boundaries.

In this work, we study energy transmission in a dissipative nonlinear periodic structure of finite length, driven harmonically at one end with a frequency outside the pass band. We demonstrate, using numerical computations, that nonlinear transmission of energy is possible even in short (six units) and dissipative periodic structures. Thus we show the relevance of this nonlinear phenomenon to engineering applications.

The mechanical system: The periodic structure consists of six weakly-coupled identical units. Each unit is made of a hanging cantilever vibrating in its fundamental mode shape, with the first beam excited at its base – see Figure 1. Nonlinear forces are introduced in each unit by the magnetic force between two electromagnets and a permanent magnet placed at the tip of each cantilever. These forces are tuneable, making it possible to realize different types of nonlinearities. The governing equations have nonlinearities that are relevant in engineering applications. In this abstract, we only present the results for softening cubic nonlinearity. Experimental validation of the results will be presented in the future.

Results: The nonlinear transmission phenomenon is shown here for a fixed forcing frequency, Ω , chosen below the pass band of the finite structure. For a chosen driving amplitude, F , the governing equations are solved for long time periods, and the average energy in the last unit, E_6 , is calculated. Figure 2(a) shows E_6 as a function of F . We can see a threshold around $F = 0.02$ above which there is a sudden increase in the energy at the end of the structure.

The frequency components of the response at the first and last units are shown for two cases: (1) $F = 0.19$, below the transmission threshold, in Figure 2(b); (2) $F = 0.21$, above the threshold, in Figure 2(c). We can see in Figure 2(b) that the driving frequency ($\Omega = 0.85$) is the predominant frequency component throughout the structure below the threshold. Above the threshold, Figure 2(c), the driven unit moves with a high amplitude and its response is highly nonlinear. Due to increased amplitude of motion, the pass band of the periodic structure shifts to lower frequencies [4] and the driving force resonates with the shifted pass band. This results in excitation of the spatially-extended propagating waves of the system. As these waves move through the structure their amplitude decrease due to dispersion and dissipation, and their frequencies change accordingly. Figure 2(c) shows that the frequencies of the transmitted waves are predominantly within the pass band of the linear structure, with a small component corresponding to the driving frequency.

We will further show that as the forcing frequency moves farther from the linear pass band of the structure, the transmission threshold increases. Qualitatively, this can be explained by the resonance of the driving force with the shifted pass band of the structure. The shift in the pass band can be calculated by considering the natural frequencies of its repeating unit. We will discuss the relation between the pass band resonance and transmission threshold, and compare with infinite undamped systems. In addition, we will discuss the influence of damping on the transmission threshold. Finally, results for the case of hardening nonlinearity will be presented as well.

Summary: It is possible to transfer energy steadily through a short dissipative periodic structure by driving it with a frequency outside its pass band. This happens due to the dependence of the dispersion characteristics of nonlinear periodic structures on the amplitude of motion. The spectrum of the transmitted waves is mainly within the linear pass band of the finite periodic structure, with a small component corresponding to the driving frequency.

References

- [1] D.J. Mead, *J. Sound Vib.*, 40, 1 (1975).
- [2] F. Geniet and J. Leon, *Phys. Rev. Lett.*, 89, 134102 (2002).
- [3] P. Maniatis et al., *Physica D*, 216, 121 (2006).
- [4] R.K. Narisetti et al., *J. Vib. Acoustics*, 132, 031001 (2010).

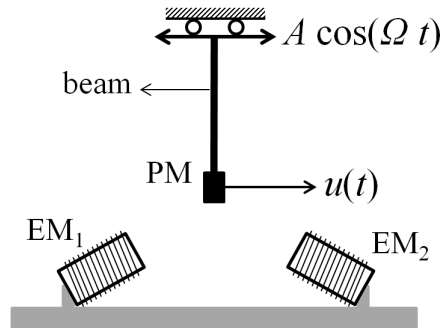


Figure 1: The schematic of the first unit of the mechanical setup. The first beam is harmonically excited at its base with frequency Ω and amplitude A ; for other units $A = 0$. PM is the permanent magnet placed at the tip of the beam. EM_1 and EM_2 are the two DC electromagnets. $u(t)$ denotes the horizontal displacement of the tip of the beam. The effective driving force acting on the tip of the beam has an amplitude F proportional to A .

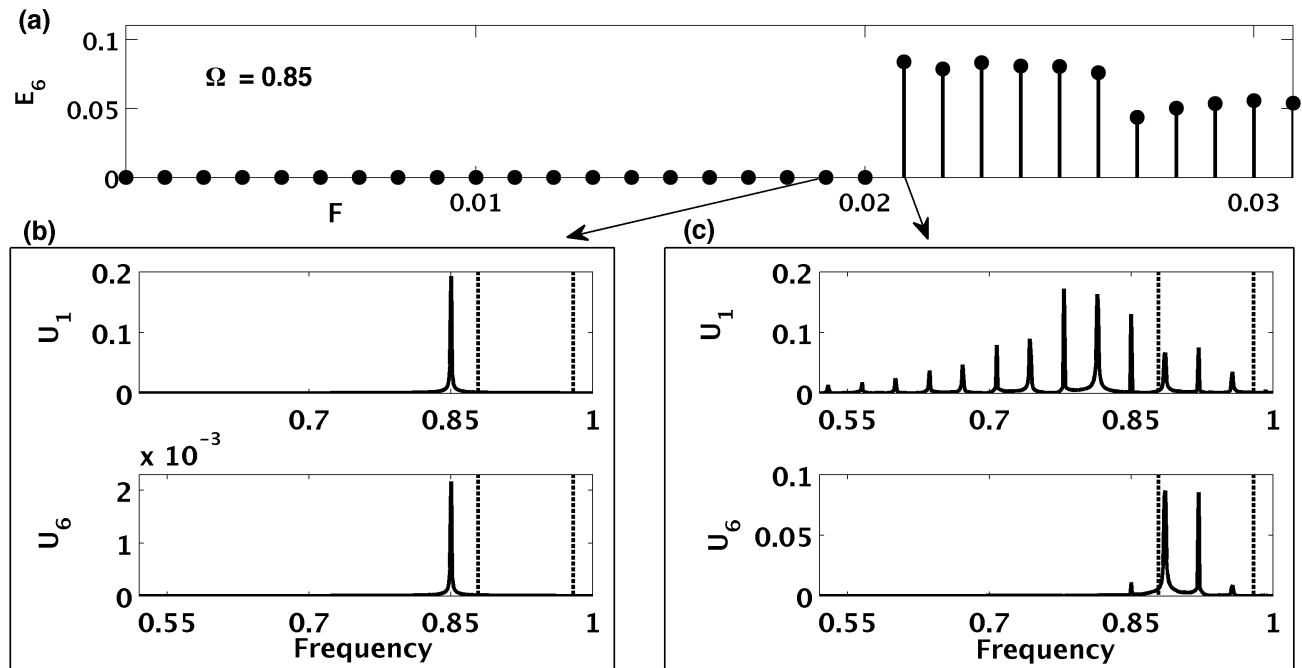


Figure 2: (a) Energy transmitted to the end of the structure, E_6 , as a function of the forcing amplitude, F . Energy is normalized to compensate for the increase in response amplitude, $u_6(t)$, due to increase in F . $E_6 = \int (u_6(t)/F)^2 dt$. (b) Frequency components of the first unit (U_1) and last unit (U_6) for case 1: $F = 0.19$, below the transmission threshold. The dashed vertical lines indicate the linear pass band of the structure. (c) Same as (b), but for case 2: $F = 0.21$, above the transmission threshold.

Viscous damping effect in laterally vibrating micro-resonator considering slip boundary conditions

Sahra Azma¹, Elnaz Alizadeh Haghighi^{1*}, Afsoon Vefagi and Ghader Rezazadeh¹

Mech Eng. Dept., Urmia University, Urmia, IRAN

*elnaz_ah.me20@yahoo.com

Abstract:

Laterally driven microstructures have played an important role in many micro-actuators and micro-sensors. In these devices, the damping level determines their amplitude response and stability, and therefore is a crucial parameter to their functionality. In contrast to vertically driven devices, in which squeeze film damping is the major source of energy dissipation, viscous drag of the ambient fluid is the dominant dissipative source in laterally driven structures.

Most of the studies on air damping conducted in the past have employed continuum models. These models are adequate for air in a device that has a minimum feature size on the order of microns or larger and is operated at around atmospheric pressure. Some examples for such devices are accelerometers and gyroscopes. However, there are cases in which continuum theory may fail to give a good prediction, for example, micro resonators operated in a low vacuum such as comb-drive resonators.

The parameter that determines the degree of rarefaction and the validity of the continuum model is Knudsen number (Kn) which is defined as the ratio of the mean free path of the gas molecule to the characteristic length of the flow. While $Kn \leq 0.01$ the regime is Continuum, and in situation of $0.01 \leq Kn \leq 0.1$ there is slip regime.

In the Continuum Regime, the Navier-Stokes equations with no-slip boundary conditions can be used to determine fluid flow behavior. For the Slip Regime, the Navier-Stokes equations can also be used, but slip boundary conditions are necessary since increment of the ratio of the mean free path to the characteristic length could result in difference between velocity of the fluid at the contact surface and the velocity of the surface itself, or there may be a delay in response of motion of the fluid to the motion of surface.

There are several researches that investigate air damping in continuum regime. However, air damping in slip regime has been seldom studied exclusively.

In this work, there is a tendency to study the air damping of laterally oscillating micro plate considering slip boundary conditions on the other hand the damping effect of the micro-plate with considerable gap size which resulted in Knudsen numbers less than 0.01 considering no slip boundary conditions has been investigated.

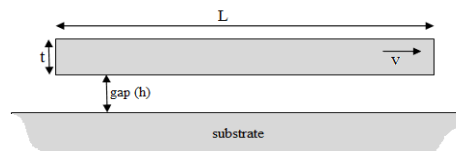
This paper deals with the analysis of viscous air damping of laterally moving plate. Logistic simplifications have been done on general Navier-Stokes equation in order to gain appropriate equation for the model. The oscillation of the structure has been presented in equation form with participation of fluid effects and slip boundary conditions. Thence the coupled governing partial differential equations of lateral vibration of the moving plate and fluid field have been derived. The obtained equations have been discretized over the beam's domain and fluid domains using a Galerkin based reduced order model. Eventually the effects of viscosity of the surrounding fluid and geometrical parameters of the oscillating structures such as length, thickness and gap size on the quality factor have been investigated.

It could be deduced from the investigation that increasing the gap size resulted in diminished damping ratio and high quality factor. It is because increasing the distance between micro-plate and fixed substrates results in smaller shear force acted on the micro-plate surface.

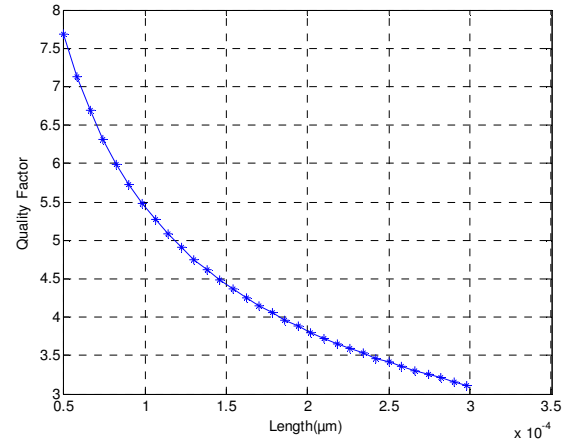
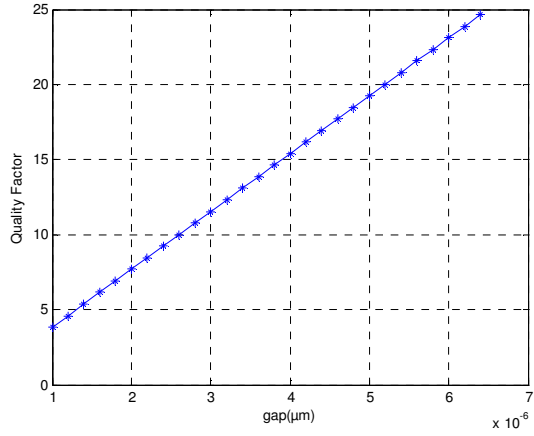
On the other hand the increment of the micro-beam thickness, due to growth of stiffness led to lower damping ratios resulted and high quality factors.

Since increasing temperature leads to higher viscosity of the surrounding fluid and greater amount of shear force, by rise in temperature values higher damping effects and lower quality factor observed.

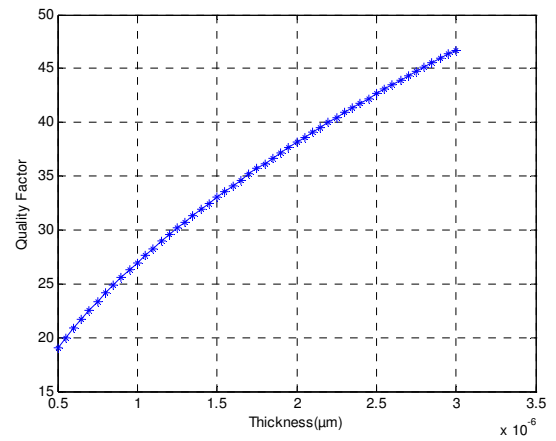
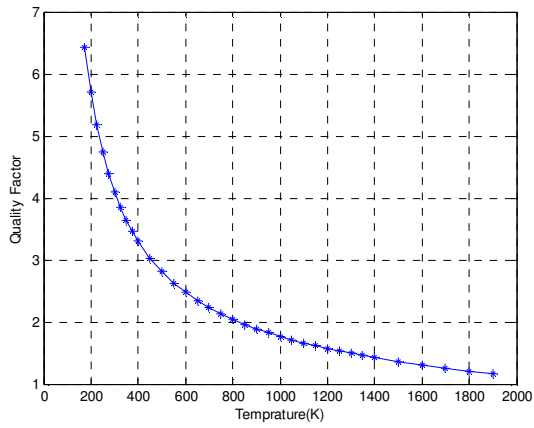
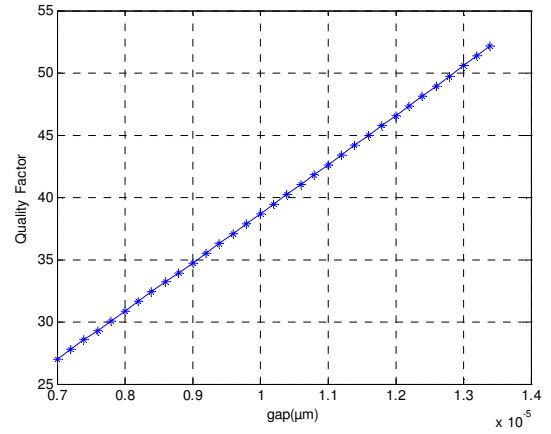
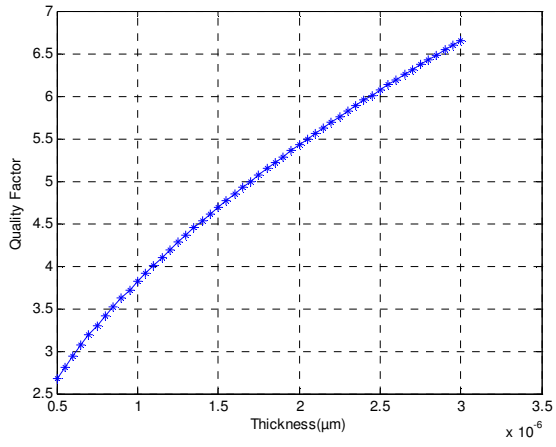
Also because of increased solid liquid interfaces which results in higher damping by increasing the length of the micro-plate the quality factor is decreased.

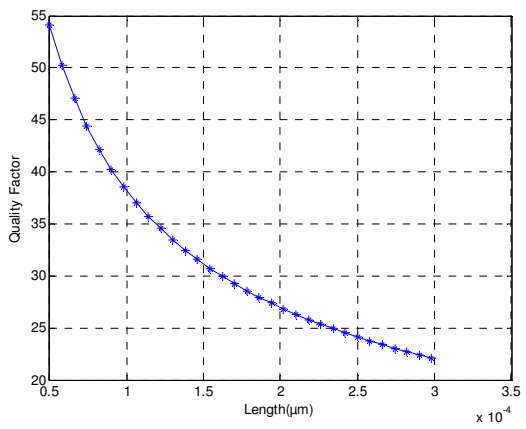
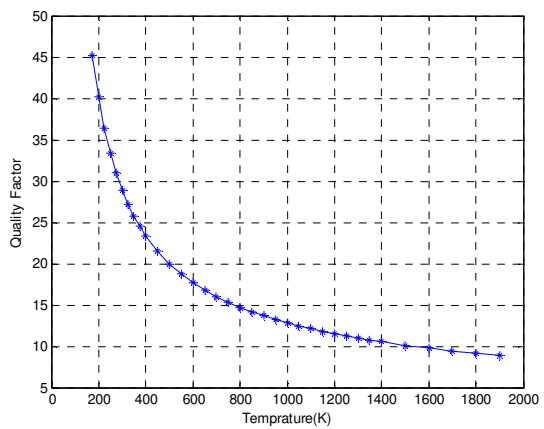


(a) slip boundary conditions



B) No slip boundary condition





Experimental Evaluation of Multiple Nonlinear Energy Sinks Coupled to a Large Nine-story Frame Structure for Seismic Hazard Mitigation

Nicholas Wierschem³, Sean Hubbard¹, Jie Luo³, D. Michael McFarland¹, Larry Fahnestock³,
Bill Spencer³, Dane Quinn⁴, Alexander Vakakis², and Lawrence Bergman¹

¹*Department of Aerospace Engineering*

²*Department of Mechanical Science and Engineering*

³*Department of Civil and Environmental Engineering*

*University of Illinois at Urbana – Champaign
Urbana, IL 61801*

⁴*Department of Mechanical Engineering
University of Akron – Akron, OH 44325*

We recently concluded an extensive project for the Defense Advanced Research Project Agency (DARPA), as part of their Structural Logic Program, demonstrating the feasibility of simultaneously and significantly increasing the stiffness and damping of an existing structure under various types of dynamic loading over a broad range of frequencies using fully passive, essentially nonlinear attachments; i.e., nonlinear energy sinks (NESs) [1]. The goal of the project was to develop a strategy to passively protect large-scale structures and systems from broadband transient loads applied directly to the structure or through ground motion; e.g., blasts, collisions, gusts, and other pulse-dominated loads. The addition of NESs to buildings had been proposed as a means to rapidly and passively dissipate the energy in a system subjected to impulsive loading. This rapid dissipation occurs because the essential nonlinearity of the NES allows it to resonate with one or more modes of the structure and engage in targeted energy transfer, the nearly one way transfer of energy to the NES where it is locally dissipated [2]. Additionally, the NES couples the modes of the structure and facilitates the transfer of energy from lower to higher modes of the structure where it can be dissipated at a faster time scale.

A large-scale 9-story steel structure, constructed specifically for the DARPA project, was employed as the test-bed for this work. This test structure, which is shown in Figure 1, is 5.13 m tall and has a mass of approximately 11,000 kg. The structure is composed of a steel base plate and nine 2.74 m by 1.22 m steel floor plates connected together by high strength steel columns. The top two floors of this structure have cutouts in them to accommodate a total of six NESs within the floors, making the resulting designs non-parasitic.

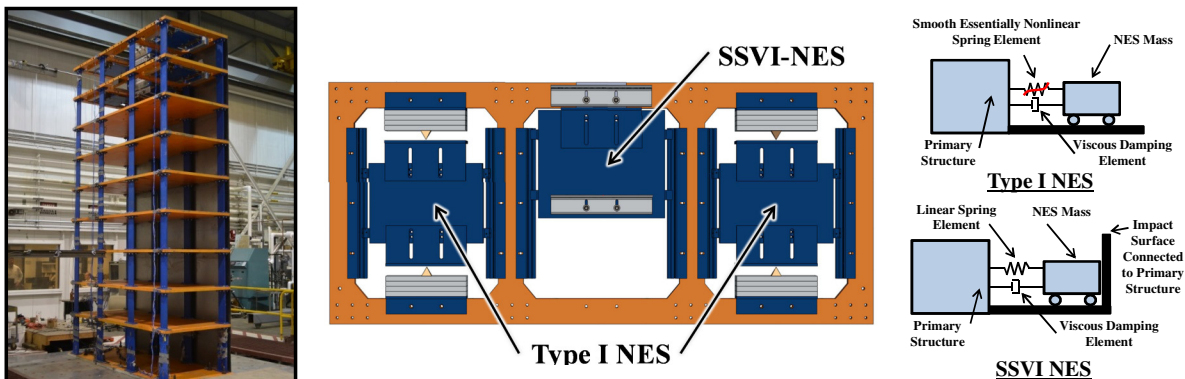


Figure 1. Base structure, NESs positioned in the floor plate, and conceptual models of the NES types employed

The system of NESs built into this large-scale structure consists of a combination of four Type-I NESs and two single-sided vibro-impact NESs (SSVI NESs). Conceptual models of these NESs are shown in Figure 1. The conceptual model of the Type I NES is composed of a mass connected to a primary structure through a viscous damping element and a smooth (no discontinuities in the

restoring force) essentially nonlinear spring element. This smooth essential nonlinearity allows this device to resonate with and participate in the transfer of energy with any mode or a sequence of modes of the primary structure. The conceptual model of the SSVI NES consists of a mass attached to a primary structure through a viscous damping element and a linear spring element; for this type of NES the relative displacement of the mass is limited on one side by an impact surface that is connected to the primary structure. Due to the discontinuity in restoring force, these impacts are broadband events, and because of them energy is scattered throughout the structure, principally to its higher modes [3]. The properties of these NESs were designed using computational simulations with the goal of mitigating the response of the structure when subjected to a shock-type blast loading.

While not the principal focus of the original project, the system of NESs was also evaluated, both computationally and experimentally, to assess its ability to mitigate the effects of earthquake loading. To accomplish this, the structure-NES system was assembled on a large scale hydraulic shaker located at the US Army Corps of Engineers Construction Engineering Research Laboratory in Champaign, Illinois and subsequently subjected to a series of historic seismic ground motions. Figure 2 provides an example of the results of this experimental work, showing the response of the structure with the system of NESs locked and unlocked to a scaled version of the JMA station record from the 1995 Kobe earthquake. The passive adaptivity of the NESs is evident in these results, as the performance of the protective system, which includes a significant reduction of the peak strain measured at the structure's first story columns, was outstanding when subjected to a loading it was not designed for. Figure 3 shows the resulting first mode effective damping [4] determined from the structural response to a range of scaled levels of the 1995 Kobe earthquake with the system of NESs locked, unlocked, and partially unlocked. The synergy between the types of NESs is demonstrated with all NESs unlocked, as in this case a high level of first mode effective damping is relatively consistent across all ground motion amplitudes considered.

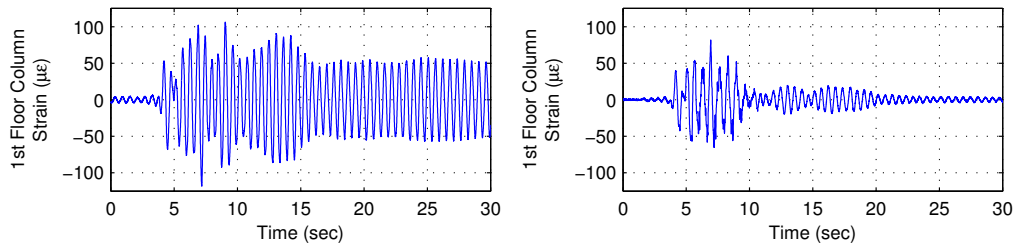


Figure 2. First floor column strain response to 1995 Kobe earthquake NESs locked (left) and NESs unlocked (right)

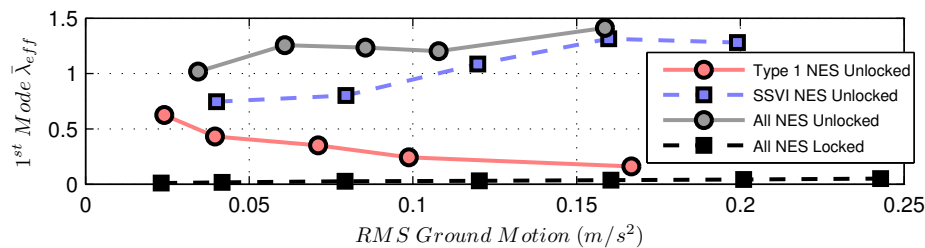


Figure 3. First mode effective damping

Acknowledgements

This research program is sponsored by the Defense Advanced Research Projects Agency through grant HR0011-10-1-0077; Dr. Aaron Lazarus is the program manager. The content of this paper does not necessarily reflect the position or the policy of the Government, and no official endorsement should be inferred. The assistance of James Wilcoski and Jonathan Trovillion during shake table testing at the U.S. Army Engineering Research and Development Center, Construction Engineering Research Laboratory is gratefully acknowledged.

References

- [1] N. E. Wierschem et al., “Structural Logic: Tailoring Stiffness and Damping of Large Scale Structures Via Passive Nonlinear Targeted Energy Transfer,” DARPA Strategic Technology Office (STO), Final Report: Grant No. HR0011-10-1-0077, 2013.
- [2] A. F. Vakakis, O. V. Gendelman, L. A. Bergman, D. M. McFarland, G. Kerschen, and Y. S. Lee, *Nonlinear Targeted Energy Transfer in Mechanical and Structural Systems*. Springer, 2008.
- [3] M. A. Al-Shudeifat, N. E. Wierschem, D. D. Quinn, A. F. Vakakis, L. A. Bergman, and B. F. Spencer, “Numerical and Experimental Investigation of a Highly Effective Single-Sided Vibro-Impact Nonlinear Energy Sink for Shock Mitigation,” *Int. J. Non-Linear Mech.*, vol. 52, pp. 96–109, 2013.
- [4] T. P. Sapsis, D. D. Quinn, A. F. Vakakis, and L. A. Bergman, “Effective Stiffening and Damping Enhancement of Structures With Strongly Nonlinear Local Attachments,” *J. Vib. Acoust.*, vol. 134, no. 1, pp. 011016–12, 2012.

Nonlinear Stiffening and Damping Effects of Non-contact Excitation System in Oberst Test Rig

Hasan Koruk^{1,a}, Mehmet Sait Ozer^{2,b}, Kenan Y. Sanliturk^{2,c}

¹MEF University, Mechanical Engineering Department, 34398 Istanbul, Turkey

²Istanbul Technical University, Mechanical Engineering Department, 34437 Istanbul, Turkey

^ahasan.koruk@mef.edu.tr, ^bozermehmet1@itu.edu.tr, ^csanliturk@itu.edu.tr

The stiffness effect of a non-contact excitation system in Oberst beam method has been investigated recently [1-3]. In this study, the stiffness effect of a non-contact excitation is studied for various types of samples including a few damped beams which are treated with two different viscoelastic materials (A and B). Furthermore, the damping effect of the non-contact excitation system is also investigated. Two ‘identical’ beams treated with material A are intentionally prepared to verify the results. The Oberst test rig is shown in Fig. 1 where L is beam length and Δ is the length of beam exposed to the electromagnetic field. Here, the electromagnetic effect is varied by changing the Δ parameter. In these tests, the transfer functions in mobility format, i.e. $\tilde{H}(\omega) = \tilde{V}(\omega) / \tilde{F}(\omega)$ are measured on samples where ‘ V ’ is the velocity, ‘ F ’ is the excitation force, ω is the excitation frequency and superscript \sim implies a complex valued quantity. The natural frequencies (f_r) and loss factors (η_r) of the samples are then identified using the so-called line-fit method.

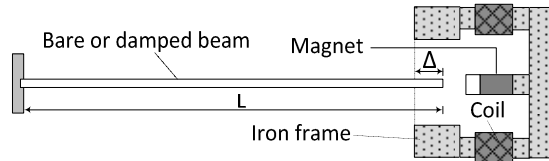


Fig. 1. The Oberst test rig including non-contact excitation system.

The identified first four natural frequencies of the test samples are presented in Fig. 2. It is seen that the stiffening effect of the excitation system is quite nonlinear though the stiffness effect of the excitation system has been modelled using a linear spring attached to the free end of the beam in Ref. [3].

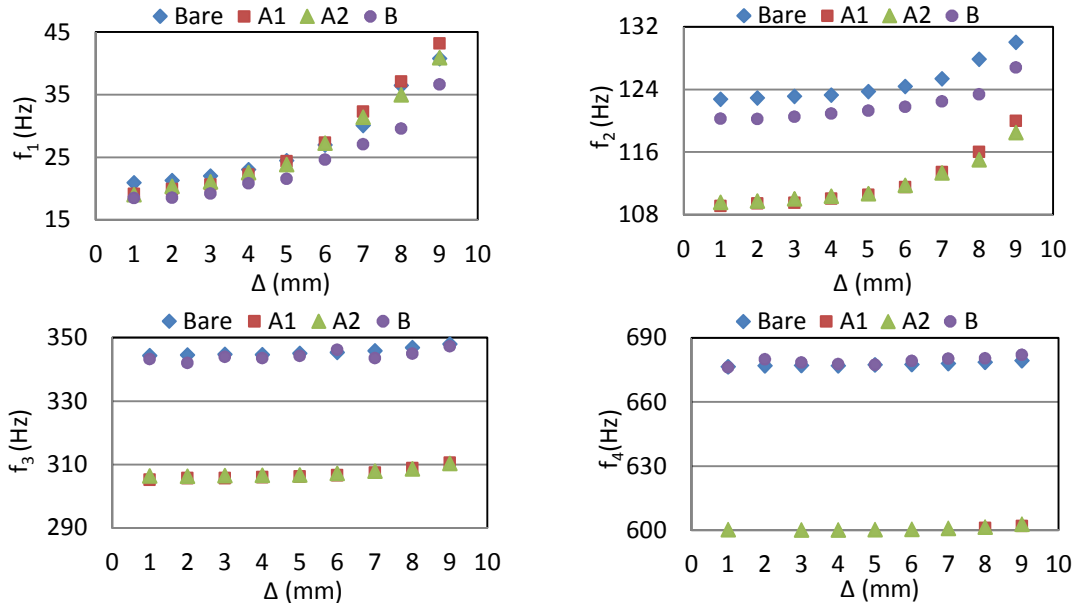


Fig. 2. The identified natural frequencies of the bare and the beams treated with damping materials A and B.

The identified first four modal loss factors for the test samples are presented in Fig. 3. Although the first modal loss factors are also included in Fig. 3, it should be noted that the first mode is not recommended to be used for identification of material properties. Therefore, the higher deviation in the first modal loss factor is expected due to the difficulties in identification of modal loss factor for this mode. In contrast to the trend observed for the identified natural frequencies, there is no consistent increase (or decrease) for the identified modal loss factors with respect to the Δ parameter. It can be said that the modal loss factors do not change significantly as electromagnetic field increases although there are some small variations due to the nature of damping, precision of line-fit method, the stiffening effect, etc. Overall, it can be said that the additional damping effect of the non-contact excitation system in the Oberst test rig is negligible.

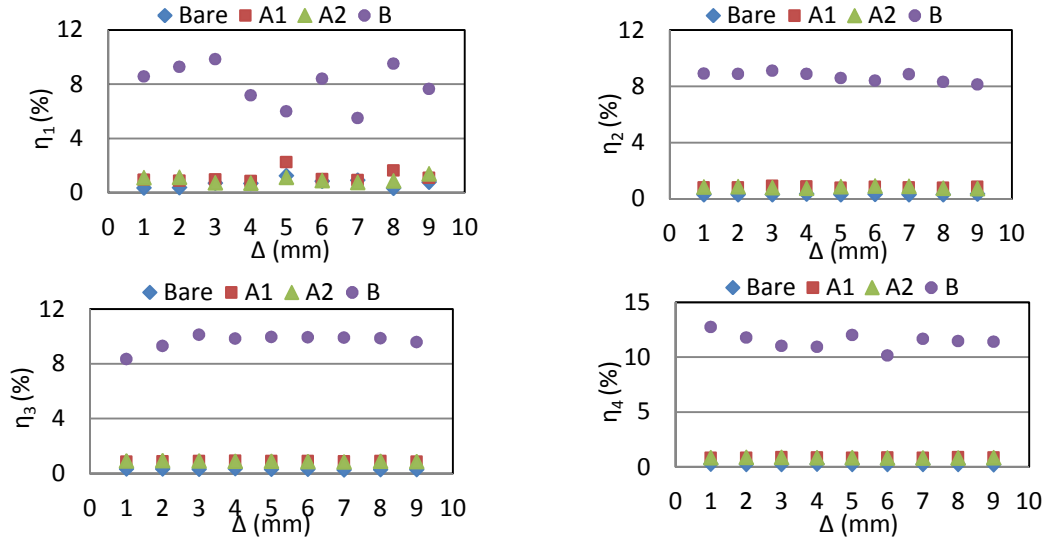


Fig. 3. The identified modal loss factors of the bare, the beams treated with damping materials A and B.

The variation of the first natural frequency as a function of the Δ parameter is approximated using a second order polynomial as $f_1 = 0.41\Delta^2 - 1.64\Delta + 22.65$ for the bare beam where $R^2 = 0.993$, $f_1 = 0.43\Delta^2 - 1.29\Delta + 20.40$ for the beam treated with damping material A where $R^2 = 0.999$ and $f_1 = 0.33\Delta^2 - 1.22\Delta + 19.65$ for the beam treated with damping material B where $R^2 = 0.985$. The fitted polynomials for the second natural frequencies for different beams are as $f_2 = 0.17\Delta^2 - 0.92\Delta + 123.88$ for the bare beam where $R^2 = 0.980$, $f_2 = 0.25\Delta^2 - 1.29\Delta + 110.67$ for the beam treated with damping material A where $R^2 = 0.983$ and $f_2 = 0.14\Delta^2 - 0.71\Delta + 121.09$ for the beam treated with damping material B where $R^2 = 0.936$. Similarly, the fitted polynomials for the third natural frequencies for different beams are: $f_3 = 0.076\Delta^2 - 0.36\Delta + 344.87$ for the bare beam where $R^2 = 0.980$ and $f_3 = 0.11\Delta^2 - 0.49\Delta + 305.98$ for the beam treated with damping material A where $R^2 = 0.972$. It is clearly seen that the contribution of the nonlinear term decreases as the mode number increases for all test samples considered here. One reason for this trend is that the natural frequencies of lower modes are more sensitive to the tip stiffness caused by electromagnetic effect. The other reason is due to the higher tip deflections of the beams at lower modes causing higher levels of stiffening effect for a nonlinear spring.

References

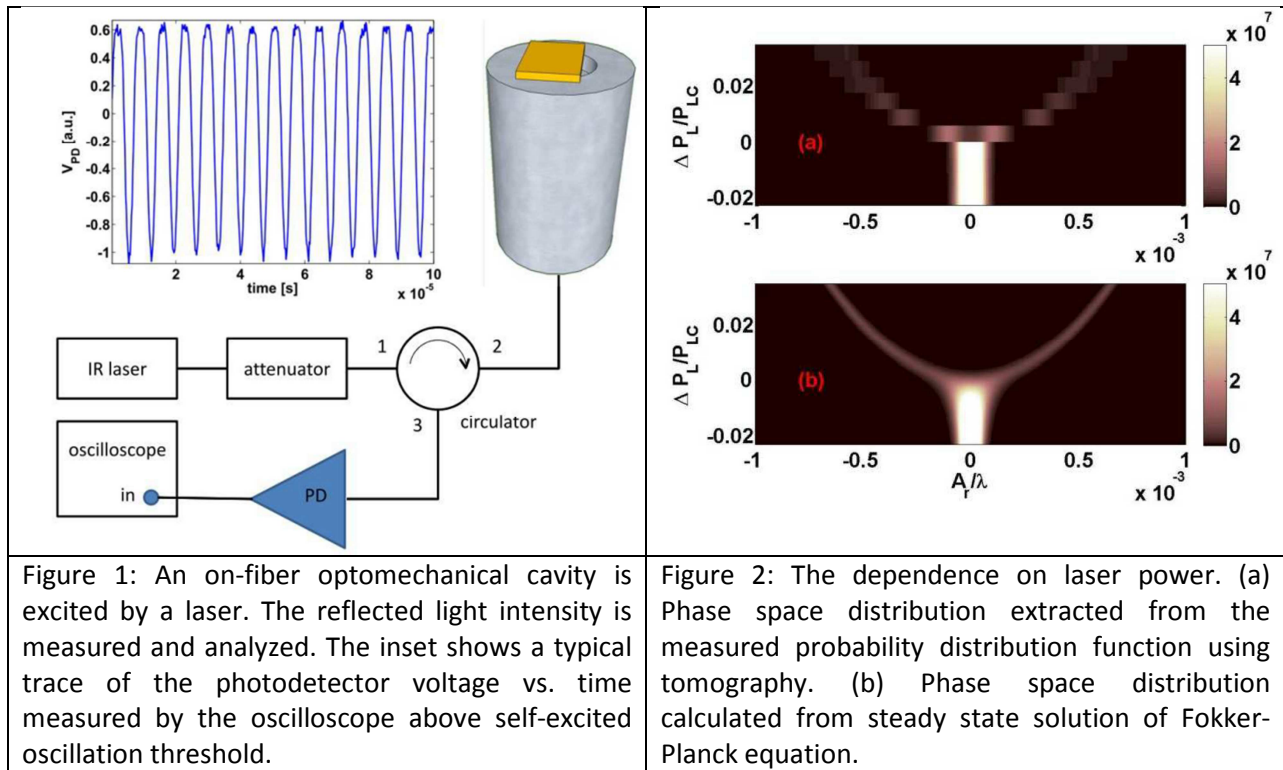
- [1] H. Koruk, K. Y. Sanliturk, "On measuring dynamic properties of damping materials using Oberst Beam Method", *ASME ESDA 2010*, Paper no: ESDA2010-24452, Istanbul, Turkey, 12-14 July 2010.
- [2] H. Koruk, K. Y. Sanliturk, "Identification and removal of adverse effects of non-contact electromagnetic excitation in Oberst Beam Test Method", *Mechanical Systems and Signal Processing* 30 (2012) 274-295.
- [3] H. Koruk, K. Y. Sanliturk, "Modelling electromagnetic effect of the non-contact excitation system in Oberst beam method", *Inter-Noise 2013*, Paper no: 1261, Innsbruck, Austria, 15-18 September, 2013.

Phase Space Distribution Near Self-Excited Oscillation Threshold

Yuvaraj Dhayalan, Ilya Baskin, Keren Shlomi and Eyal Buks

Department of Electrical Engineering, Technion, Haifa 32000 Israel

We study phase space distribution of an optomechanical cavity near the threshold of self-excited oscillation [1]. A fully on-fiber optomechanical cavity is fabricated by patterning a suspended metallic mirror on the tip of the fiber. Optically induced self-excited oscillation of the suspended mirror is observed above a threshold value of the injected laser power (see Fig. 1). A theoretical analysis based on Fokker-Planck equation evaluates the expected phase space distribution near threshold. A tomography technique is employed for extracting phase space distribution from the measured reflected optical power vs. time in steady state. Comparison between theory and experimental results allows the extraction of the device parameters (see Fig. 2).



[1] Yuvaraj Dhayalan, Ilya Baskin, Keren Shlomi and Eyal Buks, Phys. Rev. Lett. (in press), arXiv:1312.6372.

5th Conference on Nonlinear Vibrations, Localization and Energy Transfer
Istanbul, Turkey, July 2–4, 2014

SESSION 7

ON A NONLINEAR ENERGY SINK CONTROL (NES) APPROACH, APPLIED TO AN ELECTRO PENDULUM ARM, LIKE DEVICE

G. Füsün Alışverişçi⁽¹⁾, Hüseyin Bayıroğlu⁽¹⁾, Jorge Luis Palacios Felix⁽²⁾, José M. Balthazar⁽³⁾,
Reyolando Manoel Lopes Rebello da Fonseca Brasil⁽⁴⁾

⁽¹⁾*Yıldız Technical University, İstanbul, Turkey*

⁽²⁾*Universidade Federal do Pampa-UNIPAMPA, Alegrete, RS, Brasil*

⁽³⁾*Universidade Estadual Paulista-UNESP, Rio Claro, RS, Brasil*

⁽⁴⁾*Universidade Federal do ABC, Santo André, SP, Brasil*

This paper deals with a thin rod interdependent with a plate, on which electrical windings are applied. Connected to an electric circuit ([2]), its oscillations are due to the electromagnetic force, resulting from two identical and repulsive permanent magnets [1]. Also a NES (Nonlinear Energy Sink, [2], [3], [4], [5]) device is put on the free end of the pendulum. (Fig.1). This set-up is a system with three degrees of freedom: (i) the charge q of the nonlinear condenser (ii) the angular displacement θ of the pendulum, (iii) the displacement z of the M_{nes} (controlling the pendulum vibrations). We announced that the numerical results, obtained were showed, next: in the bifurcation diagram -Fig.2a, Poincare map in the Fig.2b and Lyapunov Exponents in the Fig.3. In Fig. 2, we can see that the action of the (NES) decreases the amplitude for $n=3$. In Fig. 2 and Fig.3, we can show that (NES) increased the nonlinear effect, for $n=3$.

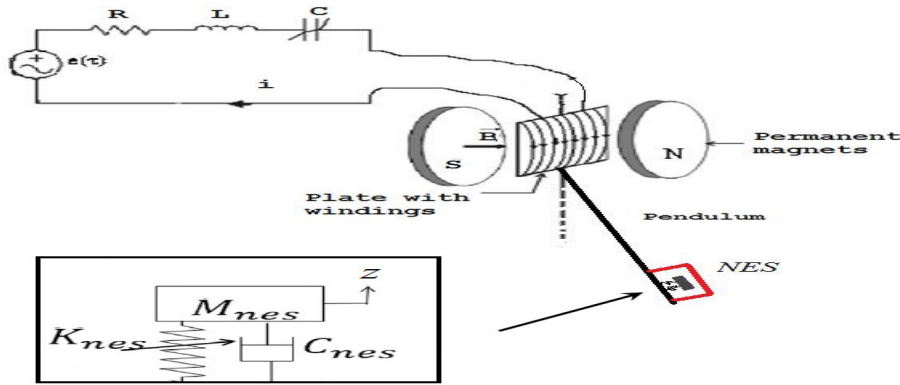
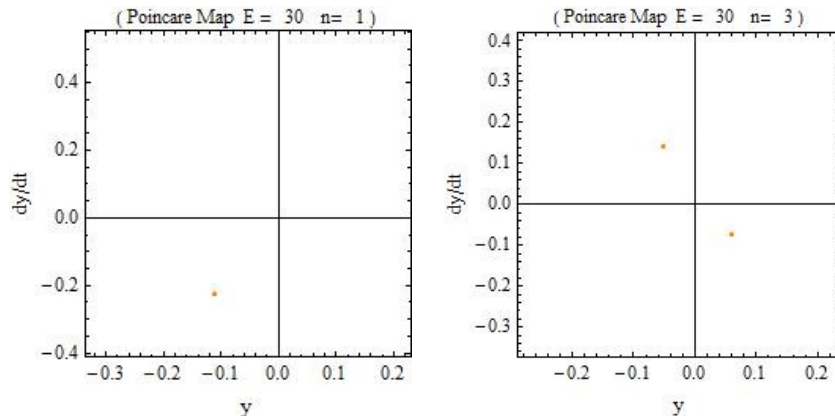


Figure 1. This is an idealization of a NES applied to a pendulum arm

The governing equations of motion ,will be of the form :

$$\begin{aligned}
 x + \mu \dot{x} + x + \alpha x^3 + \gamma_1 \dot{y} &= E \cos(\omega \tau) \\
 y + \mu_2 \dot{y} + \omega_2^2 \sin(y) - \gamma_2 \dot{x} + c_{nes} (\dot{y} - \dot{z}) + k_{nes} (y - z)^3 &= 0 \\
 \ddot{z} + c_{nes} (\dot{z} - \dot{y}) + k_{nes} (z - y)^3 &= 0
 \end{aligned}
 \tag{1}$$



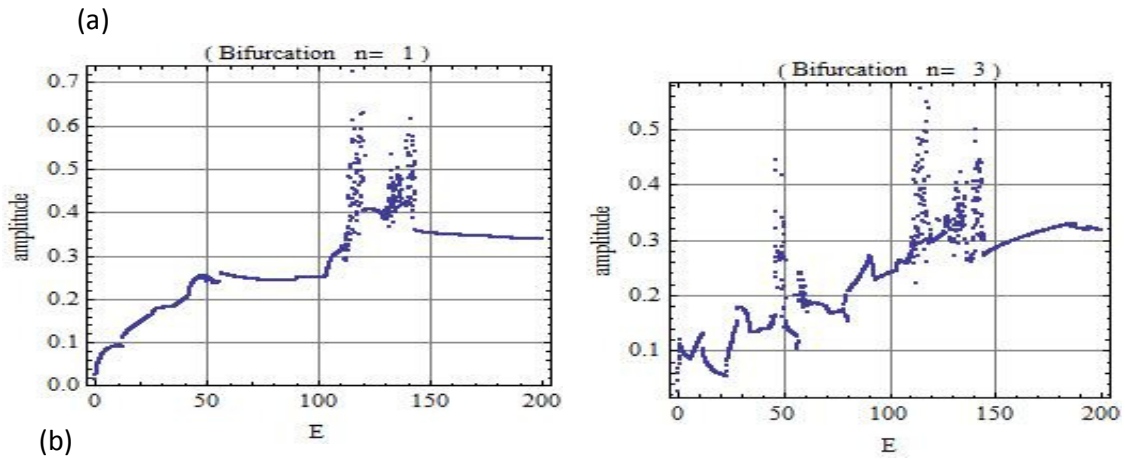


Figure 2: a) Poincare map for $n=1$ and $n=3$, b) Bifurcation diagram for $n=1$ and $n=3$

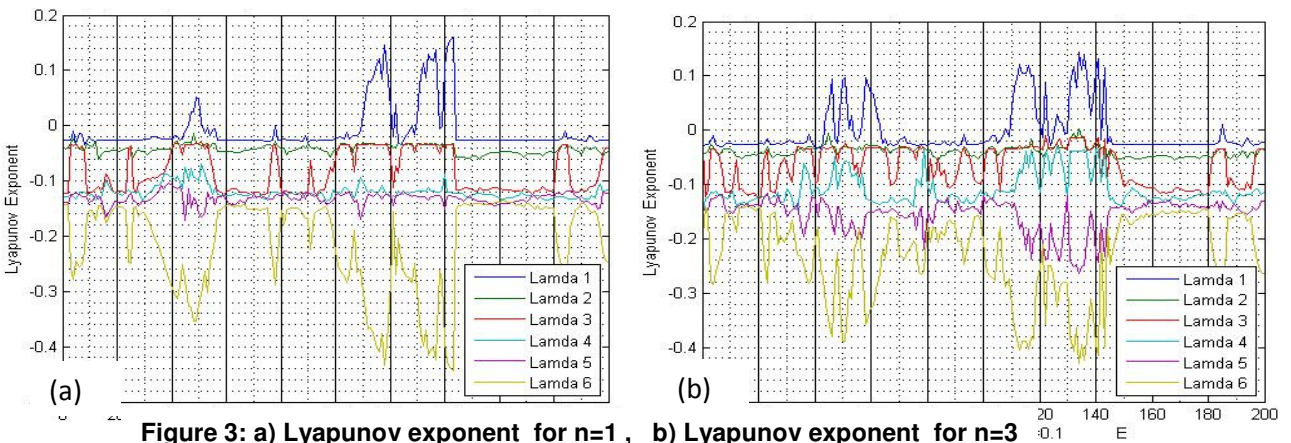


Figure 3: a) Lyapunov exponent for $n=1$, b) Lyapunov exponent for $n=3$

References

1. J.B.Mogo,P.Wofo,Dynamics of a Nonlinear Electromechanical Device With a Pendulum Arm.Journal of computational and nonlinear dynamics.DOI: 10.1115/1.2756080_
2. A. M. Tusset, Á. M. Bueno, D. Sado, J.M. Balthazar, D. Colón. SDRE control and sensibility analysis of a chaotic double pendulum arm excited by a RLC circuit based nonlinear shaker,Conference on Dynamical Systems Theory and Applications, December 2–5, 2013.Łódź, Poland, pp.195-204 (2013) and submitted (2014).
- 3.J.L.P.Felix and J.M. Balthazar,Comments on a Nonlinear and a Non-Ideal Electromechanical Damping Vibration Absorber, Sommerfeld Effect and Energy Transfer, Nonlinear Dynamics. Vol. 55, No. 1-2,pp. 1-11(2009).

4. J.L.P.Felix, Balthazar, J.M., Dantas, and M.J.H.: On energy pumping, synchronization and beat phenomenon in a non-ideal structure coupled to an essentially nonlinear oscillator. *Nonlinear Dynamics*. Volume 56, Numbers 1-2, 1-11 (2009).
5. A. F. Vakakis, O.V. Gendelman, L.A. Bergman, D.M. McFarland, G. Kerschen, Y.S. Lee, *Nonlinear Targeted Energy Transfer in Mechanical and Structural Systems*. *Solid Mechanics and Its Applications*. Springer, (2008).

VIBRATION MEASUREMENT ON A 1000 HP GAS TURBINE ENGINE TO TEST A NEWLY DESIGNED CASCADE COMPRESSOR MODULE

Sefa YILMAZTÜRK*, Samet ASLAN†, Tolga YASA‡
TUSAŞ Engine Industry, Eskişehir

ABSTRACT

Vibration-based condition monitoring and fault diagnosis is a most effective approach to maintain the safe and reliable operation of rotating machinery. Unfortunately, the vibration signal always exhibits non-linear and non-stationary characteristics, which makes vibration signal analysis and fault feature extraction very difficult. To extract the raw data Fourier transform is done to find out which component has the dominant vibration characteristic. The objective of this paper is to monitor the instantaneous vibrations for a 1000 HP engine which has a redesign highly loaded compressors. The test is conducted in three parts with different rotational speed levels namely; crank, idle and performance cycles. Order analysis is done to find out the cause of vibrations on the engine.

Keywords: *Vibration Monitoring, Order Analysis, Rotating Machinery.*

INTRODUCTION

The internal components of gas turbine engines operate under extreme conditions of high stress and temperatures. The main working surfaces inside the engine encountering these conditions are the multiple rotor and stator blade rows. In aero engines and other rotating machines, these components are influenced by dynamic effects of unbalance, misalignment, mechanical looseness, structural resonance and shaft bending [1].

When performing vibration testing, the instrumentation required depends on the application, location and purpose. For instance, eddy current proximity probes are used to measure the shaft vibrations in displacement relative to the bearing housing in mils [2]. Vibration data was measured to benchmark a 120 MW turbine generator to verify the peak responses on critical speeds with 90° eddy current probes [2]. This turbine generator was consisted of a high pressure rotor, a low pressure rotor and a generator rotor. The whole system was supported on six bearings. The vibration characteristics at partial load conditions on bearings were investigated. Velocity sensors are used to measure vibrations in velocity [m/s]. The vibration disturbance effect of a new 25 MW turbine-generator plant on a campus was investigated [3]. The measurements were taken at critical speeds with velocity sensors. According to the peak vibration locations, spring isolators and viscous dampers were designed. Piezoelectric accelerometers are used to measure vibration on the bearing houses and casings which measure the total vibration in g. They are capable of covering large frequency bandwidths, typically up to 10 kHz or higher, enabled by the typical resonant frequency of the accelerometers being on the order of 50 kHz [4]. A test rig was built for bearing and gears to identify diagnostics of rotating machinery in time domain and in order spectrum of the signal [5]. An accelerometer was mounted on the top surfaces of the housing of

* Rig Design Eng., E-mail: sefa.yilmazturk@tei.com.tr

† Test Eng., E-mail: samet.aslan@tei.com.tr

‡ Turbine Design Leader, E-mail: tolga.yasa@tei.com.tr

the cylindrical roller bearing. The sensor had a measurement band ranging from 0.5 Hz to 10 kHz. Order tracking method was used for vibration measurement that is a key step for bearing and gear diagnostics because it corrects the variability of speed due to fluctuations [6]. A new order tracking method was established for large speed variations. The measurements were taken with an accelerometer mounted on the bearing housing of the input shaft. The sampling frequency was 10 kHz during the experiment. This method is developed to estimate the instantaneous frequency of a certain harmonic of rotating frequency by extracting its waveform from overall signal.

In large rotating machines, it is difficult to make fault diagnosis process from overall vibration data. A new method has a single composite spectrum using all the measured vibration data [7]. A test rig was built up for three different faulty cases; misalignment, crack shaft and shaft rub. The test rig was excited by an instrumented hammer and vibration responses were measured by accelerometers along the length of the shafts. In another study a new transform method is developed to transform the time domain into order spectrum [8]. Three different test rig was used to obtain vibration data. First rig is designed for testing gears and bearings. Two identical accelerometers are mounted on the housing of the bearing and the tests are made at different shaft speeds. Second rig consists of three discs on a shaft that mounted on two bushings. Two proximity sensors are installed on bushing house to measure radial displacements. Final measurements are taken from a Kaplan turbine for hydrolic instabilities. Proximities are used for vibration measurements. With this new transform vibration levels of significant orders are obtained from overall vibrations. Order spectrogram analysis is done to understand the health diagnosis of rotating machines under different speed conditions [9]. Vibration signals are measured on two types of bearing; outer and inner raceway defect of a ball bearing. Measurements are taken from the bearing casing with an accelerometer. This type of analysis was %20-%30 more effective in investigating defects in the rolling bearing under varying speed conditions.

Torsional vibration on a blade disc with eight rectangular is investigated at healthy and fault conditions on a test rig [10]. The accelerometers were mounted on the bearing housing. The experiments were conducted at different shaft speeds. It is been found that healthy blade case gives a banded peak, however multiple peaks for cracked blade. External accelerometer on the casing of a gas turbine is used for blade vibration measurements. In a turbine test rig, it is assumed that the turbine casing vibration response could provide a means of blade condition monitoring [11]. It is believed that the high and low pressure forces excites the casing surface. The results obtained for measured casing vibrations is essentially the same as for the internal pressure signal, with the pressure force passing through the time. However in this case the measurement and interpretation of the pressure signal is less complex than the casing vibration response measurements. Conversely in practice, the ease of making pressure measurements is much less than for accelerometer measurements, since pressure transducers require perforation of the casing and operate in a much harsher environment.

When focusing on vibration response of rotating blades, it is easy to predict the resonance frequency; however difficulty remain in the prediction of vibrational stress [12, 13]. The dynamic stress caused by aerodynamic excitations in the rotating direction is measured with strain gage installations using a slip ring system [14]. This setup system is used to study blade vibrations using a remote sensing system via a set of strain gages bonded to one of the blades. An experimental investigation by means of holographic interferometry and telemetry involving the use of applied strain gages were carried out for impeller vibrations [15]. With this method it is possible to determine the mode shapes of a vibrating body. In contrast to the strain gage technique, this method provides information over the entire surface of the body under investigation, from which the amplitude distribution may be determined. This is especially advantageous in the case of the complex geometrical structures under investigation, as it is possible to identify a mode shape relatively quickly.

In vibration testing one of the main concerns in the measurement of the forced response of vibrating structures is the coupling between the test article and the exciter. When the structural behaviour of the structure is linear the resonant frequencies and mode shapes are obtained with a

hammer test [16]. Unfortunately, real applications of structures are connected with joints where the behaviour become nonlinear. These joints significantly change the dynamic behaviour of the engine. The dynamic responses of the components can be investigated in engine ground tests where the rotor is subjected to an excitation pattern where each blade is loaded with a series of pulses within a complete disk rotation. The number and the intensity of pulses depend on the components of the engine preceding the rotor (number of combustion chambers, stages, stator vanes) and the wide spectral content is usually characterized by several harmonic components whose excitation frequencies are mainly a multiple of the rotor angular speed. The harmonic index which defines the multiplicity is called engine order [17]. In this paper the newly designed high loaded compressor overall vibrations are monitored with time. Afterwards an order analysis is done and critical engine orders are investigated to find out the cause of the vibrations.

EXPERIMENTAL SETUP AND TEST CONDITIONS

The objective of this study is to monitor the vibration characteristics in real time on nine stage high loaded compressors in order to prevent the failure of engine and vibration analysis. The newly designed compressor is shown in Figure 1 below.

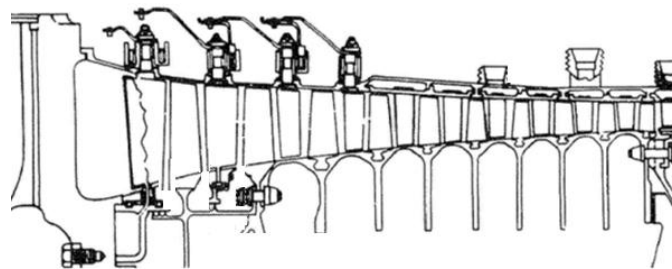


Figure 1 Nine Stage Compressor Module

The vibration measurements are performed by using accelerometers which are capable of measuring a range of up to 50 g at steady conditions and 500 g peak to peak variation. The maximum frequency limit is 36000 Hz $[(23365/60)*92]$. This limit meets with both frequency range and resonant frequency of the accelerometer.

A general view of the engine is shown in Figure 2. Accelerometers are placed on the engine considering four different places. One of the measurements is taken from the entrance of the compressor in radial direction. Two accelerometers are mounted on the combustor casing to measure from both radial and axial direction. The last measurement is taken from the entrance of the turbine in radial direction.

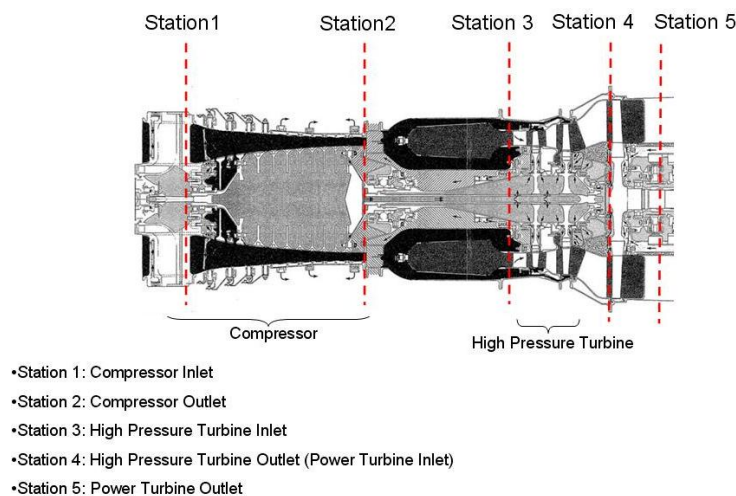


Figure 2 General View of the Engine

Overall vibration is monitored per one second during the tests. Two different RPM is measured from the compressor and power turbine. Order analysis is done in order to find out the source of

the vibration whether from power turbine or compressor. In Table 1 the blade passing frequencies in each compressor cascade is defined.

Table 1 Compressor Blade Passing Frequencies

Rotor Number	Frequency (kHz)
1	15
2	16
3	19
4	23
5	27
6	32
7	34
8	35
9	36

Bearing related vibrations are also taken into consideration. First three bearings mount the compressor. Fourth and fifth bearings mount the power turbine. In Table 2 the ball number of the bearings are shown. These numbers are important for order analysis.

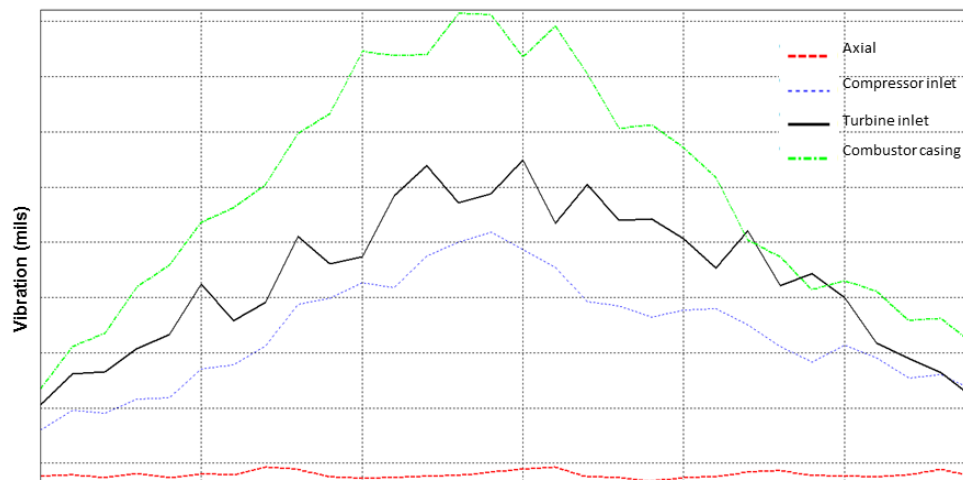
Table 2 Bearing Ball Numbers

Bearing Number	Ball Number
1	14
2	13
3	20
4	20
5	11

TEST RESULTS

Crank Test

In order to check the accuracy of the sensors and understand engine behavior characteristics, without combustion, rotor is started with an electric starter. As seen below in Figure 3, the instantaneous vibration indicates there is no sudden excitation that affects engine.



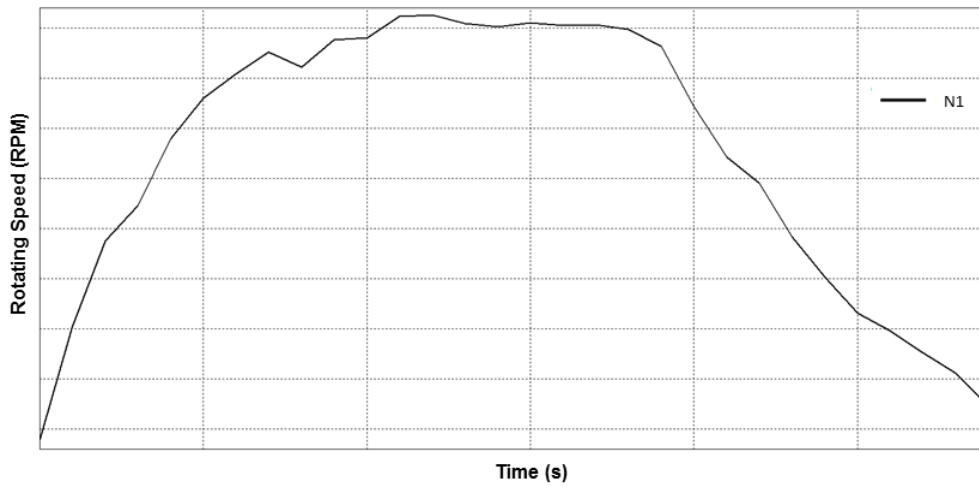


Figure 3 Crank Test Overall Vibrations

Idle Test

Idle test is where combustion takes places and power turbine reaches to its idle speed, N1 rpm, and works for some time. After the time period working at N1 rpm passes on N2 rpm and is ready for loading. In Figure 4 engine is operated at idle speed and overall vibration data are collected. It is seen that as the speed increases dominant vibration occurs at entrance of the turbine in radial direction.

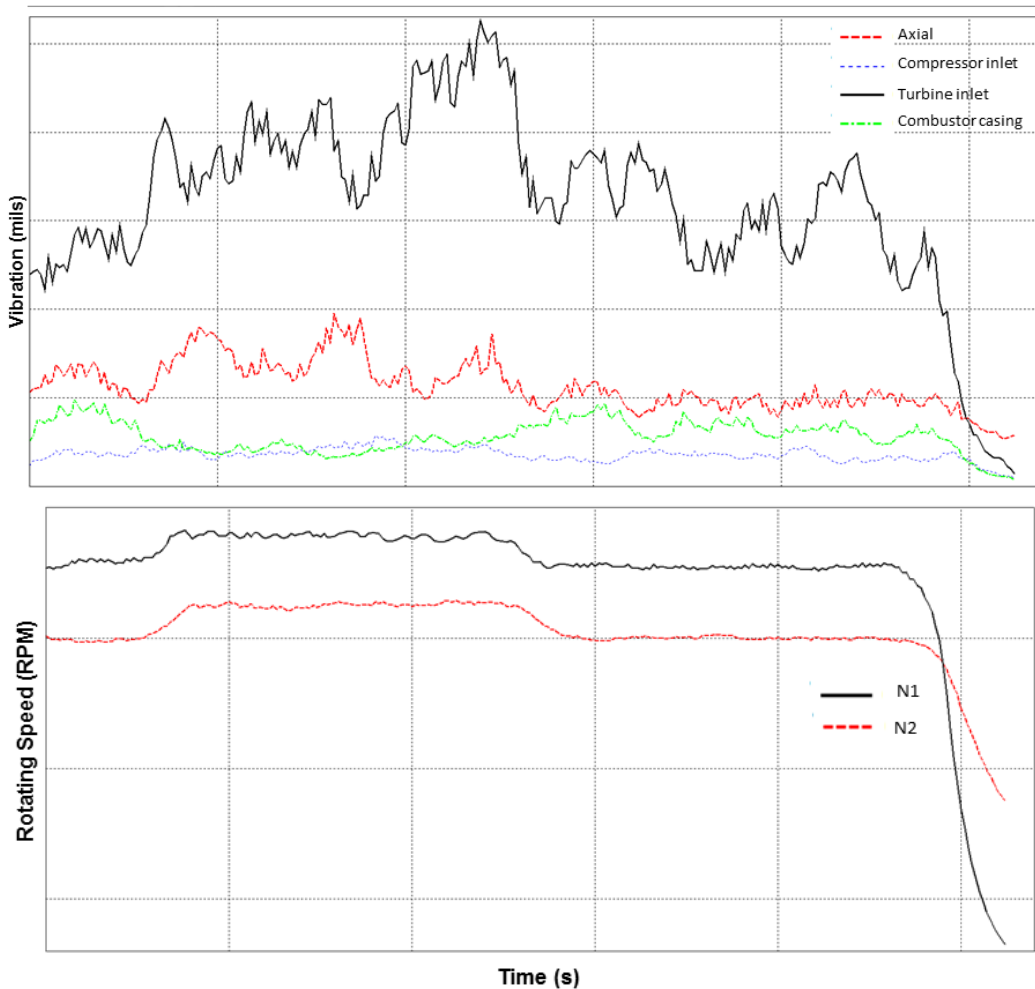


Figure 4 Idle Test Overall Vibrations

Performance Test

to determine the performance of the gas turbine the engine is loaded by using a electrical load unit at the level of 100-150-200-259 kW.

As seen in Figure 5, after the load is applied, combustor casing vibration is surpassed by compressor inlet vibrations. the compressor is mounted with three bearings so the speed increases, the temperature also increases on bearings. This effects the bearings and the vibration becomes dominant in this region.

Figure 5 shows that the lowest vibration comes from the compressor. The highest vibration comes from turbine. In order to understand which component causes the vibration order analysis is done for power turbine and the results are shown in Figure 6.

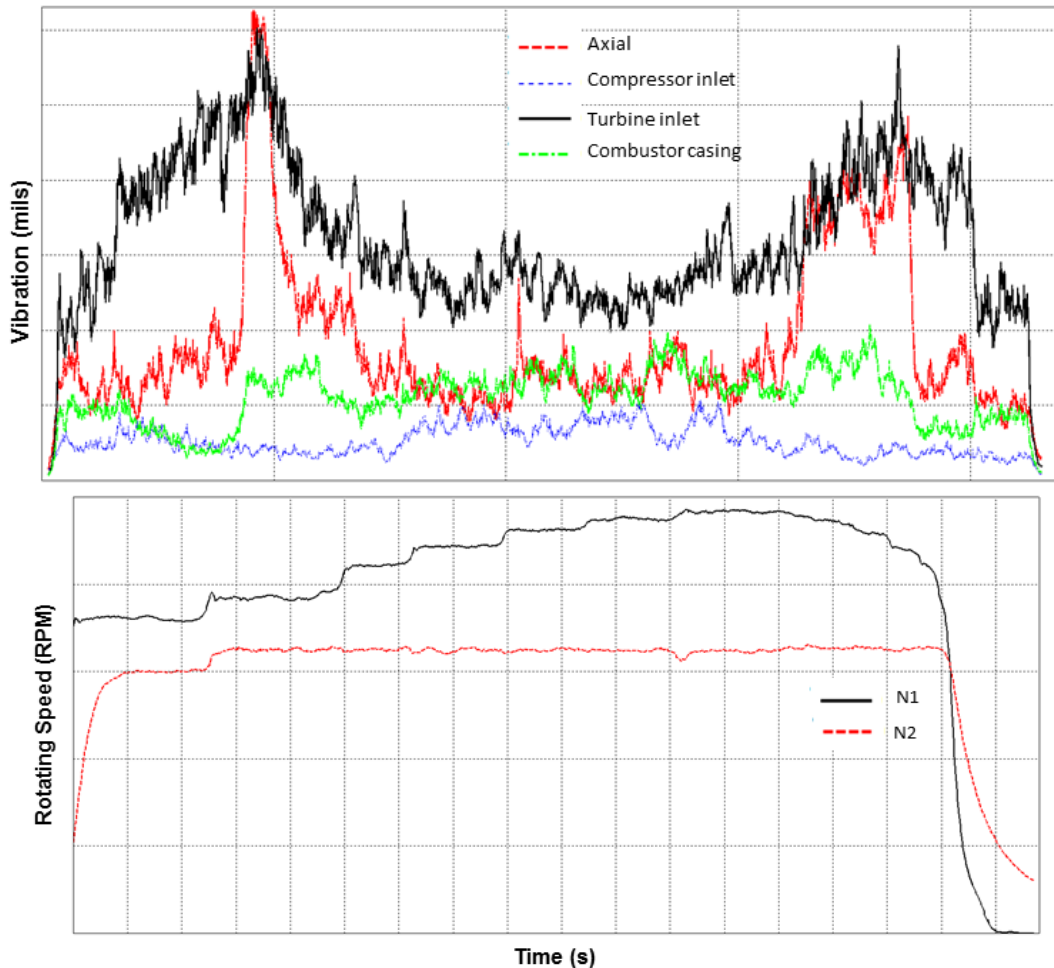


Figure 5 Performance Test Overall Vibrations

Figure 6 shows the critical components of the engine as described in Table 1 and Table 2. As expected from a rotating machine is that highest vibrations are occurred in the 1st engine order. The other components have no influence to vibration. 1st engine order describes unbalance. The figure also shows that bearings works well and vibrations is not at its critical point.

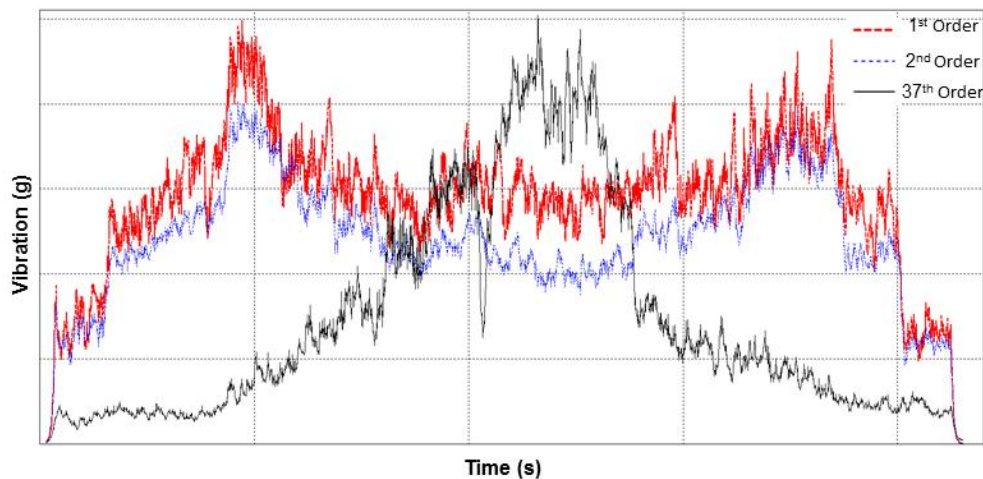


Figure 6 Order Analysis of the Measurement

1st

The most critical part is the first rotor of the engine as seen in Figure 6 at 37th order. Since the loading started, rotor vibrations increases in the first cascade. Rotor vibrations decreases when the loading is undone. Although the vibration limits are not exceeded, this incremental vibration may be a problem when to produce more power.

Kaynaklar

- [1] F. Al-Badour, M.Sunar, L.Cheded, *Vibration analysis of rotating machinery using time–frequency analysis and wavelet techniques*, Mechanical Systems and Signal Processing 25, 2011, 2083–2101.
- [2] D,R, Gruwell, F,Y, Zeidan, *Vibration and Eccentricity measurements combined with rotordynamic analysis on a six bearing turbine generator*, Proceedings of the 27th Turbomachinery Symposium, 1997.
- [3] J. B., Evans, *Vibration control for a new 15 MW steam turbine generator installation near academic teaching and research laboratories*, Twelfth International Congress on Sound and Vibration, 2005.
- [4] A. Jablonski, T.Barszcz, *Validation of vibration measurements for heavy duty machinery diagnostics*, Mechanical Systems and Signal Processing 38, 2013, 248–263.
- [5] P. Borghesani, P.Pennacchi, R.B.Randall, R.Ricci, *Order tracking for discrete-random separation in variable speed conditions*, Mechanical Systems and Signal Processing 30, 2012, 1–22.
- [6] M. Zhao, J. Lin, X. Wang, Y. Lei, J. Cao, *A tachometer-less order tracking technique for large speed variations*, Mechanical Systems and Signal Processing 40, 2013, 76–90.
- [7] K. Elbhah, J.Sinha *Vibration-based condition monitoring of rotating machines using a machine composite spectrum*, Journal of Sound and Vibration 332, 2013, 2831–2845.
- [8] P.Borghesani, P.Pennacchi, S.Chatterton, R.Ricci, *The velocity synchronous discrete Fourier transform for order tracking in the field of rotating machinery*, Mechanical Systems and Signal Processing 44, 2014, 118–133.
- [9] J. Wang, R.X.Gao, R. Yan *Multi-scale enveloping order spectrogram for rotating machine health diagnosis* Mechanical Systems and Signal Processing 46, 2014, 28–44.
- [10] A.A.Gubran, J..Sinha *Shaft instantaneous angular speed for blade vibration in rotating machine* Mechanical Systems and Signal Processing 44, 2014, 47–59.
- [11] G.L. Forbes, R. B. Randall, *Gas turbine casing vibrations under blade pressure excitation*, AIAC, 13th Australian International Aerospace Congress, 2009.

- [12] A.Higashio, H.Yamashita, M.Ota, *Dynamic Stress Measurement of Centrifugal Compressor Impeller and Study for Strenght Criteria Based on Correlation by unsteady CFD*, Proceedings of the 39th Turbomachinery Symposium, 2010.
- [13] F.Kushner, *Rotating Component modal analysis and resonance avodiance recommandations*, Proceedings of the 33th Turbomachinery Symposium, 2004
- [14] H.J. Bauer, A. Schulz, M. Schwitzke, *Aerodynamic excitation of blade vibrations in radial turbines*, MTZ, Volume 74, 2013.
- [15] H. Hasemann, D. Hagelstein, M. Rautenberg, *Coupled Vibration of Unshrouded Centrifugal Compressor Impellers. Part I: Experimental Investigation*, International Journal of Rotating Machinery, 2000, Vol. 6, No. 2, pp. 101-113.
- [16] S. Z. Rad, *Finite element, modal testing and modal Analysis of a radial flow impeller*, Iranian Journal of Science & Technology, Transaction B, Engineering, 2005, Vol. 29.
- [17] D.J. Ewins, *Control of vibration and resonance in aero engines and rotating machinery, An overview* International Journal of Pressure Vessels and Piping 87, 2010, 504-510.

Control of helicopter ground resonance by means of passive non-linear energy sink

B. Bergeot^a, S. Bellizzi^b, B. Cochelin^c

LMA, CNRS UPR7051, Aix-Marseille Univ., Centrale Marseille, F-13402 Marseille Cedex 20, France

^abaptiste.bergeot@centrale-marseille.fr

^bbellizzi@lma.cnrs-mrs.fr

^cbruno.cochelin@centrale-marseille.fr

Extended Abstract

Problem Statement. Helicopter Ground Resonance (HGR) [1, 2] is a dynamic instability involving the coupling of the blades motion in the rotational plane (i.e. the lag motion) and the motion of the fuselage. HGR can be very violent and can lead to the total destruction of the aircraft. The present work is a preliminary study of the capacity of a passive nonlinear absorber (or Nonlinear Energy Sink (NES)) to control an HGR.

Framework. In the domain of passive control vibration, it has been shown that the use of a NES can provide very interesting results. Under certain conditions an irreversible energy transfert from the primary system to the NES can occur. This phenomenon is called Targeted Energy Transfert (TET). In their seminal paper [3], Gendelman *et al.* analyze TET in term of resonance capture and nonlinear modes. More recent works show that the use of NES is also an interesting way to control dynamic instabilities. For instance, Lee *et al.* [4] show that a NES coupled to a wing in subsonic flow can partially or even completely suppress flutter instability by TET from the wing to the NES.

The simpler helicopter model that can describe HGR is well known. It involves only lag motion of the four blades and one direction of the fuselage motion. Linear stability of this model shows that HGR is due to a frequency coalescence between a lag mode and the fuselage mode and predicts the range of rotors speeds Ω for which this frequency coalescence occurs. In this work a NES is coupled to the fuselage in an ungrounded configuration (see Fig. 1). The differential equations which govern the time evolution of the fuselage displacement $y(t)$, the NES displacement $h(t)$ and the blades lagging angles $\delta_i(t)$ (with $i \in [1, 4]$) can be easily derived using Lagrange's equations. These equations of motion are:

$$\left\{ \begin{array}{l} (M + 4m_\delta) \ddot{y} + c_y \dot{y} + k_y y + \mu(\dot{y} - \dot{h}) + \alpha(y - h)^3 \\ + m_\delta \sum_{i=1}^4 \left\{ L \ddot{\delta}_i \cos(\psi_i + \delta_i) - L \left(\Omega + \dot{\delta}_i \right)^2 \sin(\psi_i + \delta_i) \right\} = 0 \end{array} \right. \quad (1a)$$

$$\left\{ \begin{array}{l} m_h \ddot{h} + \mu(\dot{h} - \dot{y}) + \alpha(h - y)^3 = 0. \end{array} \right. \quad (1b)$$

$$\left\{ \begin{array}{l} m_\delta L^2 \ddot{\delta}_i + c_\delta \dot{\delta}_i + k_\delta \delta_i + m_\delta L \ddot{y} \cos(\psi_i + \delta_i) = 0 \end{array} \right. \quad (1c)$$

$$\left\{ \begin{array}{l} \text{with } \psi_i = \Omega t - 2\pi \frac{i-1}{N}, \end{array} \right.$$

where $N = 4$ is number of blades, M is the mass of the fuselage, m_δ is the mass of one blade, m_h is the mass of the NES ($M > m_h$), c_y , c_δ and μ are damping coefficients, k_y and k_δ are linear stiffness coefficients and α is the cubic stiffness coefficient of the NES.

Results. Numerical parametric investigation of the system of equations (1) is performed. It consists to determine the possible regimes in the parameter space. We show that it is possible to partially or even completely suppress HGR by passively transferring energy from the fuselage to the NES. As in [4], three responses for the fuselage motion are highlighted: *strongly modulated response (SMR)*, *partial suppression* and *complete suppression* of the HGR. An example of SMR is depicted in Fig. 2.

We are currently working on the design of the NES. The aim is to know if the NES parameters leading to a good control of the HGR are compatible with industrial applications.

Acknowledgements. The authors wish to thank Mr. François Malburet for helpful discussions and suggestions. This research is done within the framework of the industrial chair "Dynamique des Systèmes Mécaniques Complexes (*Dynamics of complex mechanical systems*)" financed by the *Airbus Group Foundation*.

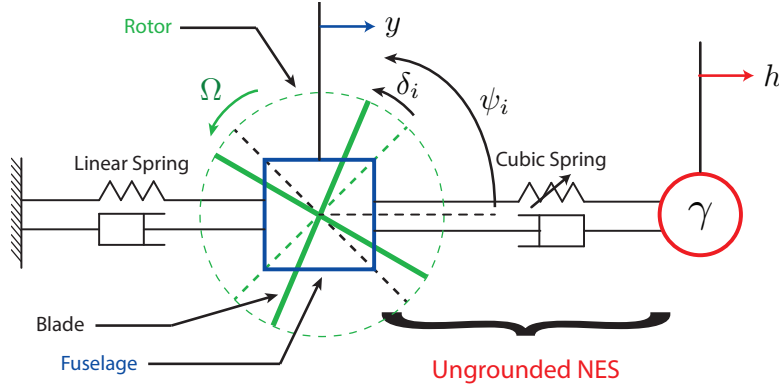


Figure 1: Schematic representation of the studied system.

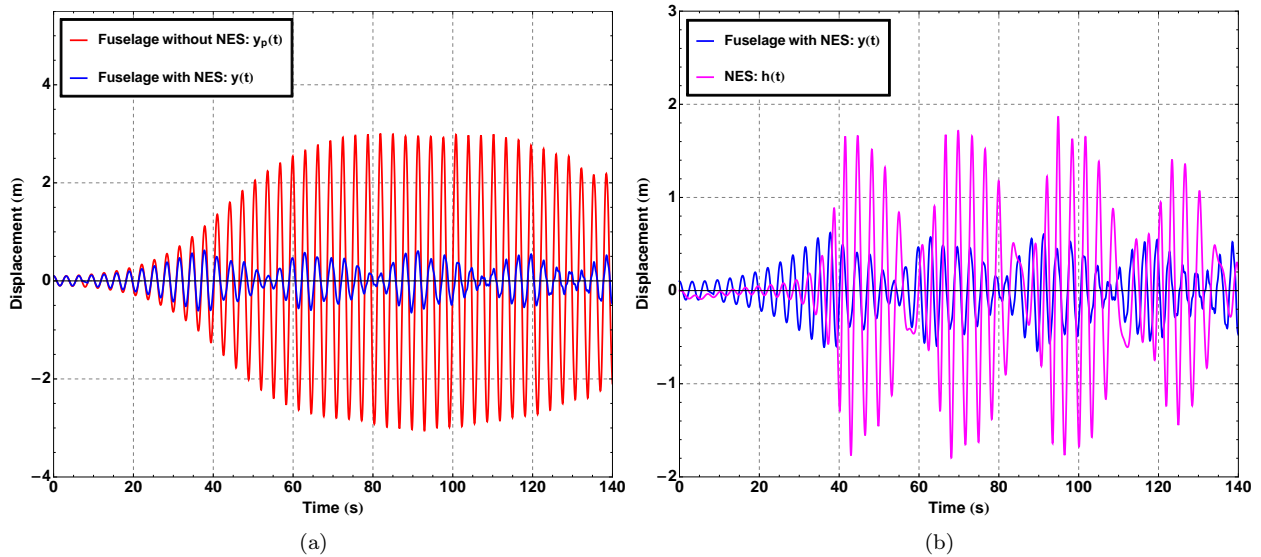


Figure 2: (a) Comparison between the fuselage motion without NES $y_p(t)$ (red line) and the fuselage motion with NES $y(t)$ (blue line). (b) Comparison between the NES motion $h(t)$ (magenta line) and the fuselage motion with NES $y(t)$ (blue line).

References

- [1] R.P. Coleman and A.M. Feingold. Theory of self excited mechanical oscillations of helicopter rotors with hinged blades. *NACA Report 1351*, 1958.
- [2] F. Malburet and Tomasz Kryszinski. *Instabilité mécanique: contrôle actif et passif*, chapter 2. Lavoisier, 2009.
- [3] O. Gendelman, L.I. Manevitch, a. F. Vakakis, and R. M'Closkey. Energy Pumping in Nonlinear Mechanical Oscillators: Part I—Dynamics of the Underlying Hamiltonian Systems. *Journal of Applied Mechanics*, 68(1):34, 2001.
- [4] Y.S. Lee, A.F. Vakakis, L.A. Bergman, D.M. McFarland, and G. Kerschen. Suppression Aeroelastic Instability Using Broadband Passive Targeted Energy Transfers, Part 1: Theory. *AIAA Journal*, 45(3):693–711, March 2007.

Collective dynamics of coupled nonlinear pendulums under simultaneous external and parametric excitations

Aymen Jallouli, Najib Kacem and Nouredine Bouhaddi

FEMTO-ST Institute, UMR 6174, Applied Mechanics Department, 24 chemin de l'Épitaphe, F-25000 Besançon, France

Summary. In order to investigate the collective nonlinear dynamics of an array of coupled pendulums under simultaneous external and parametric excitations, a computational model is developed while considering the main sources of nonlinearities. The equations of motion are solved using the harmonic balance method (HBM) coupled with the asymptotic numerical method (ANM). Numerical simulations are performed in the case of two coupled pendulums in order to investigate the complexity of the frequency responses in terms of bifurcation topologies and energy transfer.

Introduction

The sine-Gordon model and its discrete analog have attracted interest of people working in quite different fields. For instance, the collective dynamical behavior of an array of coupled pendulums with a small fraction of random long-range connection has been investigated under external excitation [1, 2]. Gavielides et al. [3] have investigated the effect of impurity introduced into a lattice and their ability to control the dynamic behavior of an array of coupled nonlinear chaotic oscillators, while Thakur et al. [4] have examined a pendulum array with harmonic coupling and horizontal sinusoidal driving. Hai-Qing et al. [5] and Alexeeva et al. [6] demonstrated the stabilizing effect of adding mass and length impurities on a chain of pendulums parametrically excited. In this context, a computational model for the nonlinear dynamics of a chain of coupled pendulums under simultaneous external and parametric excitations is developed. The principal goal is to track the collective dynamics of the considered system in terms of bifurcation topologies and energy transfer with respect to the excitation amplitudes.

Design and model

The considered system is depicted in Figure 1. It is composed of an horizontal axle A , of total length l , suspended at its ends by "frictionless" bearings. Along this axle, at equally spaced intervals, there are N equal pendulums. Each pendulum consists of a rigid rod, attached perpendicularly to the axle, with a mass at the end. At rest, all the pendulums point down the vertical, a is the distance of the center of mass from the central axis, g the gravity acceleration, θ_i is the angle between the i^{th} pendulum and the downward vertical, k_2 is the torque constant and k_4 is the coupling nonlinear stiffness. The pendulums have the same moment of inertia $I = ml^2$. The considered system is excited by two excitation forces at the drive frequency ω_e . The first one is an external force $F \cos(\omega_e t)$ applied on one or several pendulums, and a parametric excitation $4A_e \omega_e^2 \cos(2\omega_e t)$ due to the base excitation of the system. Hence, the equation of motion of the n^{th} pendulum can be written as:

$$ml^2 \frac{d^2 \theta_n}{dt^2} + \alpha l \frac{d \theta_n}{dt} + k_2 (2\theta_n - \theta_{n+1} - \theta_{n-1}) + k_4 \left((\theta_n - \theta_{n+1})^3 + (\theta_n - \theta_{n-1})^3 \right) + ml [g + 4A_e \omega_e^2 \cos(2\omega_e t)] \sin(\theta_n) = F \cos(\omega_e t) \quad (1)$$

The boundary conditions associated to Equation (1) are $\theta_0 = 0$ and $\theta_{N+1} = 0$. First, $\sin(\theta_n)$ is expanded in Taylor series up to the third order. Then, the resulting equation is numerically solved in the frequency domain using the harmonic balance method coupled with the asymptotic numerical continuation technique.

Numerical simulations

In order to investigate the effect of adding an external force, we plot numerically the frequency responses for an array of two coupled pendulums. In the case of a pure parametric excitation ($F = 0$), the two curves of θ_1 and θ_2 are identical due to the symmetry of the equations, as shown in Figure 2(a). Moreover, we notice that the resonant stable solution is limited to the frequency range $[10.29 \ 10.77] \text{ rad/s}$ while the trivial solution $\theta_n = 0$ is anywhere else. Figure 2(b) displays the frequency responses of the two pendulums under simultaneous external and parametric excitations. Remarkably, adding a

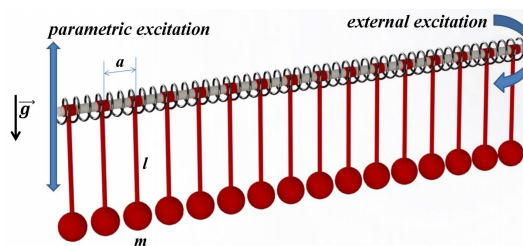


Figure 1: An array of coupled pendulums under simultaneous parametric and external excitations.

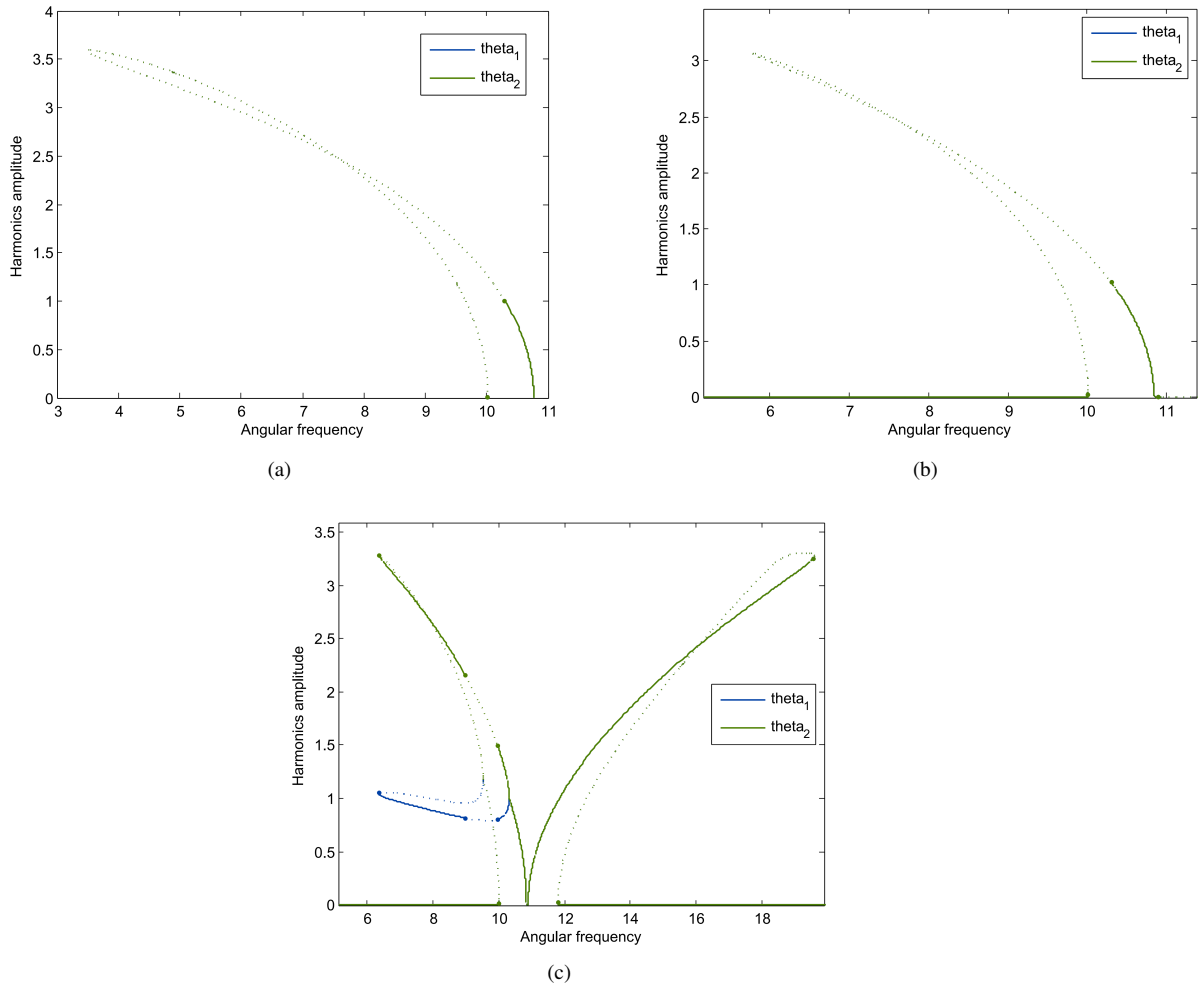


Figure 2: Forced frequency responses of the two coupled pendulums for the following set of parameters: $m = 0.1$, $l = 0.1$, $g = 9.81$, $A = 0.004$, $k_2 = 0.01$, $k_4 = 0.005$, $\alpha = 0.001$, $F = 10^{-6}$. (a): under pure parametric excitation ($F = 0$), (b): under simultaneous parametric and external excitations, and (c): the two pendulums are excited with the same parametric force while only the first pendulum is externally forced. Solid curves indicate stable solutions and dashed curves indicate unstable solutions.

small external force has an impact only on the unstable solution. Finally, we perform numerical simulations for the case of simultaneous excitations while the external one is localized on the first pendulum. Since the symmetry of the problem is broken, there are large differences between the two frequency responses as shown in Figure 2(c). For $\omega_e > 10.85 \text{ rad/s}$, a new branch is added providing a non-zero solution and compared to the two first cases, we can see the existence of new stable branches for $\omega_e < 10.85 \text{ rad/s}$.

Conclusions

A computational model for the nonlinear dynamics of an array of coupled pendulums under simultaneous parametric and external excitations has been developed. Particularly, it is shown that we can take advantage of the external force to stabilize the structure and increase the performances of the resulting collective dynamics.

Acknowledgments

This project has been performed in cooperation with the Labex ACTION program (contract ANR-11-LABX-01-01).

References

- [1] F. Qi, Z. Hou and H. Xin. *Ordering Chaos by Random Shortcuts*. Phys. Rev. Lett. **91** 6 (2003).
- [2] Y. Braiman, J. F. Lindner and W. L. Ditto. *Taming spatiotemporal chaos with disorder*. Nature **378** 30 (1995).
- [3] A. Gavrielides, T. Kottos, V. Kovanis and G. P. Tsironis. *Spatiotemporal organization of coupled nonlinear pendula through impurities*. Phys. Rev. E **58** 5 (1998).
- [4] R. B. Thakur, L. Q. English. *Driven Intrinsic Localized Modes in a Coupled Pendulum Array*. J. Phys. D: Appl. Phys. **41** 015503 (2008).
- [5] X. Hai-Qing, T. Yi. *Parametrically driven solitons in a chain of nonlinear coupled pendula with an impurity*. Chin. Phys. Lett. **23** 6 (2006).
- [6] N. V. Alexeeva, I. V. Barashenkov. *Impurity-induced stabilization of solitons in arrays of parametrically driven nonlinear oscillators*. Phys. Rev. Lett. **48** 14 (2000).

Stability of an inclined traveling heavy cable

Abhinav R. Dehadrai^{+,*}, Ishan Sharma⁺ and Shakti S. Gupta⁺

⁺Mechanics & Applied Mathematics Group, Department of Mechanical Engineering,
Indian Institute of Technology Kanpur, India.

Abstract

We analyse the stability of a heavy inextensible cable traveling at constant velocity at an angle against gravity. The governing equation for transverse in-plane vibrations are derived using Newton's second law or Hamilton's principle. Modal and transient solutions are obtained computationally at different velocities of operation and inclination angle. The margin of stability is identified from the critical values of the velocity. This margin will be validated with simple lab-scale experiments. Further, energy balance confirms that the system's energy in absence of dissipative forces is not constant; indicating that the system is nonconservative. Effects of external damping on the stability of the system is also analysed.

1 Introduction

TRAVELING CABLES are often used to drive mechanisms such as elevators in skyscrapers and mines (ground and under water), conveyor belts, automobile chain-drive, cableways, etc. These cables can be inclined at various angles to gravity. Understanding the dynamics of cables employed in these application is important to arrive at the critical speed of operation for designing proper control systems. Dynamics of horizontally traveling strings, or cables, and beams is well addressed in available literatures, [1]-[9]. We study the dynamics of a cable moving at constant velocity between fixed rollers and inclined with respect to the vertical. Such a system has been sparsely investigated before. We establish criterion for instability by looking for the system's critical velocity using computational modal and transient analyses. We are attempting to validate these critical points via simple experiments. Through energetics we justify that the system's stability, in presence or absence of damping, is not sufficiently characterized by its nonzero energy rate. Wickert and Mote [9] reached a similar conclusion for a horizontal system. Our basic model includes external loading, due to aerodynamic/hydrodynamic forces along with gravity.

2 Governing equation and numerical solution

A traveling heavy cable between two pairs of small, rigid and inertially fixed rollers is shown in Fig. 1. The inertially fixed Cartesian coordinate system is shown located between the base rollers. The distance between the centers of the rollers is L and the acceleration due to gravity acting vertically downwards is g . The cable has mass density ρ and its cross section is A_c . The tangential velocity of each material particle of the cable is v . Distributed external forces acting on the cable are also shown in Fig. 1. The transverse in-plane displacement of a generic material point of cable, located at a distance x along the X -axis, at time t , is taken as $y(x, t)$. The governing equation along with boundary condition derived using Newton's second law or Hamilton's principle is

$$\left(v^2 - \frac{T(x)}{\rho A_c} \right) \frac{\partial^2 y(x, t)}{\partial x^2} + 2v \frac{\partial^2 y(x, t)}{\partial x \partial t} + \frac{\partial^2 y(x, t)}{\partial t^2} + \left(\frac{V(x)}{\rho A_c} - g \right) \frac{\partial y(x, t)}{\partial x} = \frac{H(x)}{\rho A_c}, \text{ with } y(0, t) = y(L, t) = 0, \quad (1)$$

where $T(x) = T_0 + \rho A_c g x - \int_0^x V(x) dx$, and T_0 is the known tension at the cable's lower end. The Galerkin projection method [2] is employed for solving Eq. (1). Towards that end we assume $y(x, t) \approx \sum_{n=1}^N b_n(t) \psi_n(x)$ over

*email: abhinavd@iitk.ac.in

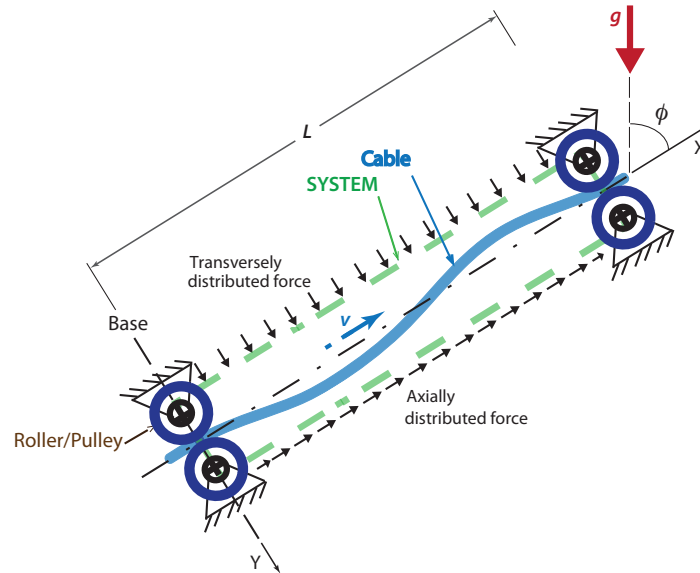


Figure 1: Obliquely traveling heavy cable, under external loading, between small fixed end-rollers.

the entire domain. Transient and modal solution are obtained by solving the discretized equations numerically at different values of velocity for various values of inclination ϕ . Note that the shape functions $\psi_n(x)$ are chosen as *sine* functions which satisfy the homogeneous boundary conditions. Values of the critical velocity for various ϕ are identified by the first occurrence of positive real part of any eigenvalue of system of equation. At this velocity the transient solution shows exponential growth – implying instability.

3 Energetics and experimental verification

Energy analysis of a vertical system (i.e. $\phi = 0$) shows that the rate of change of total energy of the system with time is *nonzero*. There is energy influx and efflux from the boundaries and power input by the gravity into the system. The latter contribution diminishes with increasing inclination. It is absent for a horizontal system [9] (i.e. $\phi = \pi/2$). In any case, the nonzero energy rate is an insufficient criterion to explain the instability of a traveling cable system.

We have built an experimental set-up, in which a bicycle chain is run between fixed sprockets. One of the these is driven by a motor whose speed is adjustable. The inclination of the system may also be set to any desired angle. We expect to see whether the critical velocity obtained from numerics matches with that observed through this experiment.

References

- [1] Barakat R, 1968, Transverse vibration of a moving thin rod, *J. Acoust. Soc. Am.*, 43, pp. 533-539.
- [2] Boyd, JP, 2013, *Chebyshev and Fourier spectral methods*, Courier Dover Publications.
- [3] Hagedorn P, DasGupta A, 2008, *Vibrations and Waves in Continuous Mechanical Systems*, Wiley, New York.
- [4] Miranker WL, 1960, The wave equation in a medium in motion, *IBM J. Res. Dev.*, 4(1), pp. 36-42.
- [5] Mote CD Jr., 1965, A study of band saw vibrations, *J. Frankl. Inst.*, 279, pp. 430-444.
- [6] Rogge T, 1972, Equations of motion for flexible cables, *J. Aircraft*, 9(11), pp. 799-800.
- [7] Sack R, 1954, Transverse oscillations in travelling strings, *Brit. J. Appl. Phys.*, 5, pp. 224-226.
- [8] Swope R, Ames W, 1963, Vibrations of a moving threadline, *J. Frankl. Inst.*, 1, pp. 36-55.
- [9] Wickert JA, Mote CD Jr., 1987, On the energetics of axially moving continua, *J. Acoust. Soc. Am.*, 85(3), pp. 1365-1368.